

12-2002

Torque Limit of a Mechanical Fastener in a Graphite/Epoxy Joint

Kristian M. Kostreva

Embry-Riddle Aeronautical University - Daytona Beach

Follow this and additional works at: <https://commons.erau.edu/db-theses>



Part of the [Aerospace Engineering Commons](#)

Scholarly Commons Citation

Kostreva, Kristian M., "Torque Limit of a Mechanical Fastener in a Graphite/Epoxy Joint" (2002). *Theses - Daytona Beach*. 105.

<https://commons.erau.edu/db-theses/105>

This thesis is brought to you for free and open access by Embry-Riddle Aeronautical University – Daytona Beach at ERAU Scholarly Commons. It has been accepted for inclusion in the Theses - Daytona Beach collection by an authorized administrator of ERAU Scholarly Commons. For more information, please contact commons@erau.edu.

TORQUE LIMIT OF A MECHANICAL FASTENER
IN A GRAPHITE/EPOXY JOINT

by

Kristian M. Kostreva

Embry–Riddle Aeronautical
University
December 2002

UMI Number: EP31896

INFORMATION TO USERS

The quality of this reproduction is dependent upon the quality of the copy submitted. Broken or indistinct print, colored or poor quality illustrations and photographs, print bleed-through, substandard margins, and improper alignment can adversely affect reproduction.

In the unlikely event that the author did not send a complete manuscript and there are missing pages, these will be noted. Also, if unauthorized copyright material had to be removed, a note will indicate the deletion.

UMI[®]

UMI Microform EP31896
Copyright 2011 by ProQuest LLC
All rights reserved. This microform edition is protected against
unauthorized copying under Title 17, United States Code.

ProQuest LLC
789 East Eisenhower Parkway
P.O. Box 1346
Ann Arbor, MI 48106-1346


**TORQUE LIMIT OF A MECHANICAL FASTENER
IN A GRAPHITE/EPOXY JOINT**

by


Kristian M. Kostreva

This thesis was prepared under the direction of the candidate's thesis committee chairman, Dr. Yi Zhao, Department of Aerospace Engineering, and has been approved by the members of this thesis committee. It was submitted to the Department of Aerospace Engineering and was accepted in partial fulfillment of the requirements for the degree of Master of Science in Aerospace Engineering.


THESIS COMMITTEE



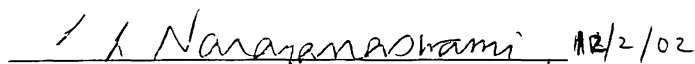
Dr. Yi Zhao
Chairman




Dr. Eric v. K. Hill
Member



Dr. Frank J. Radosta
Member



Graduate Program Coordinator, MSAE



Department Chair, Aerospace Engineering

2 DEC 2002
Date

ACKNOWLEDGMENTS

The author would first like to thank his advisor and thesis committee chair, Dr. Yi Zhao, for the opportunity to work on this project both at Embry-Riddle Aeronautical University and at the Marshall Space Flight Center. His drive towards seeking additional project support was a huge factor in the success of this thesis and the completion of the author's degree. His motivation and enthusiasm was inspirational, and his personal support and caring was monumental during those long work days. Enough thanks can never be extended to him for all the experience acquired.

Next, from his recommendation to Dr. Yi Zhao to his teachings and guidance in the discipline of acoustic emission nondestructive testing, the author would like to thank thesis committee member Dr. Eric Hill. He was the first to give me the chance to prove myself as a graduate student, and the experience acquired while under his advisement was priceless.

Great thanks is also extended to Dr. Frank Radosta for his wisdom and excellent instruction in many academic topics, not to mention the personal support he has offered by accepting a seat on the committee.

While at the Marshall Space Flight Center in the summer of 2002, the author had the opportunity to work with many fine individuals. Those most vital to the success of this work were Frank Thomas, Brett Smith, Dr. Wayne Gamwell and James Hodo; however, many others contributed time, knowledge, and support. There is not enough room on this page to thank each individually, so a general thanks is extended to those persons who in some way, even minor, helped with this project.

ABSTRACT

Author: Kristian M. Kostreva
Title: Torque Limit of a Mechanical Fastener in a Graphite/Epoxy Joint
Institution: Embry-Riddle Aeronautical University
Degree: Master of Science in Aerospace Engineering
Year: 2002

Presently there is a lack of confidence amongst engineers when specifying the preload of a mechanical fastener in a composite joint due to a lack of a fundamental knowledge base regarding the behavior of composites under fastener compressive load. As such, a novel experimental procedure was developed herein to determine the through-the-thickness compressive (TTTC) material properties. A total of 206 property tests were performed on four different graphite/epoxy material systems. The results confirmed that TTTC material properties vary with fiber orientation, laminate thickness, fiber volume fraction, and even laminate surface finish. Hence, the 'rule of mixtures' provides a poor estimate of the TTTC modulus in that it fails to account for any of these variables.

Finally, acoustic emission nondestructive testing, along with a modified approach to MSFC-STD-486B, Torque Limits for Standard Threaded Fastener, were used to determine the torque limit of a fastener in a single lap joint. The laminate configuration examined in these tests was manufactured in accordance with the MIL-HDBK-17 design code. The results demonstrated the inability of the fasteners employed to damage the one composite system investigated: fastener thread failure occurred first. Further study is necessary to confirm or refute these results for other composite systems and joint configurations.

TABLE OF CONTENTS

	Page
Signature Page.....	ii
Acknowledgements.....	iii
Abstract.....	iv
Table of Contents.....	v
List of Tables.....	vii
List of Figures.....	ix
CHAPTER 1. INTRODUCTION.....	1
1.1 Scope.....	1
1.2 Previous research.....	2
CHAPTER 2. THEORY AND BACKGROUND.....	5
2.1 Through-the-Thickness Material Properties.....	5
2.2 Acoustic Emission.....	9
2.3 Torque Limit of a Mechanical Fastener.....	10
CHAPTER 3. TEST MATERIALS AND PROCESSES.....	11
3.1 IM7 / 8552.....	11
3.2 AS4 / 3501-5a and AS4 / 3501-6.....	12
3.3 AS4 / 8552 8H Fabric.....	12
CHAPTER 4. EXPERIMENTATION.....	14
4.1 ASTM D3410-00 (90° Compression Tests).....	14
4.1.1 Coupon Specifications.....	14
4.1.2 Test Apparatus.....	14

4.2 Through-the-Thickness Compression Tests	15
4.2.1 Coupon Specifications	15
4.2.2 Test Apparatus	15
4.3 Torque-Tension Tests	16
CHAPTER 5. RESULTS	18
5.1 ASTM D3410-00 (90° Compression Tests)	18
5.2 Through-the-Thickness Compression Tests	19
5.2.1 IM7 / 8552.....	19
5.2.2 AS4 / 3501-5a	23
5.2.3 AS4 / 3501-6.....	26
5.2.4 AS4 / 8552 8H Fabric	30
5.3 Torque-Tension Tests	32
CHAPTER 6. CONCLUSIONS AND RECOMMENDATIONS	39
6.1 Conclusions.....	39
6.2 Recommendations.....	41
REFERENCES	43
Appendix A IM7 / 8552 TTTC Stress-Strain Data Plots.....	44
Appendix B AS4 / 3501-5a TTTC Stress-Strain Data Plots.....	55
Appendix C AS4 / 3501-6 TTTC Stress-Strain Data Plots	63
Appendix D AS4 / 8552 8H Fabric TTTC Stress-Strain Data Plots.....	71
Appendix E D3410-00 (90°) Stress-Strain Data Plots.....	76

LIST OF TABLES

	Page
Table 2.1 Displacement Measurement Tool Comparison.....	7
Table 5.1 IM7 / 8552 D3410 Results.....	18
Table 5.2 AS4 / 3501-5a D3410 Results	18
Table 5.3 AS4 / 3501-6 D3410 Results	18
Table 5.4 IM7 / 8552 [0] ₃₂ TTTC Results	19
Table 5.5 IM7 / 8552 [0, 90] _{6s} TTTC Results.....	19
Table 5.6 IM7 / 8552 [0, ±45, 90] _{3s} TTTC Results	20
Table 5.7 IM7 / 8552 [0, ±30, ±60, 90] _{2s} TTTC Results	20
Table 5.8 Thiokol Manufactured IM7 / 8552 [0, ±45, 90] _{3s} TTTC Results	20
Table 5.9 Thiokol Manufactured IM7 / 8552 [0, ±45, 90] _{4s} TTTC Results	21
Table 5.10 Thiokol Manufactured IM7 / 8552 [0, ±45, 90] _{5s} TTTC Results	21
Table 5.11 AS4 / 3501-5a [0] ₃₂ TTTC Results.....	23
Table 5.12 AS4 / 3501-5a [0, ±45, 90] _{2s} TTTC Results	23
Table 5.13 AS4 / 3501-5a [0, ±45, 90] _{3s} TTTC Results	24
Table 5.14 AS4 / 3501-5a [0, ±45, 90] _{4s} TTTC Results	24
Table 5.15 AS4 / 3501-5a [0, ±45, 90] _{5s} TTTC Results	24
Table 5.16 AS4 / 3501-6 [0] ₃₂ TTTC Results.....	26
Table 5.17 AS4 / 3501-6 [0, ±45, 90] _{2s} TTTC Results.....	27
Table 5.18 AS4 / 3501-6 [0, ±45, 90] _{3s} TTTC Results.....	27
Table 5.19 AS4 / 3501-6 [0, ±45, 90] _{4s} TTTC Results.....	27
Table 5.20 AS4 / 3501-6 [0, ±45, 90] _{5s} TTTC Results.....	28

Table 5.21 AS4 / 8552 8H Fabric – 9 Layers	30
Table 5.22 AS4 / 8552 8H Fabric – 12 Layers	31
Table 5.23 AS4 / 8552 8H Fabric – 15 Layers	31

LIST OF FIGURES

	Page
Figure 2.1 Prototypical TTTC Test Fixture with LDS and TTTC Coupon	7
Figure 2.2 TTTC Validity Concept.....	8
Figure 2.3 Acoustic Emission Signal Parameters	10
Figure 4.1 ASTM D3410 Test Fixture.....	14
Figure 4.2 220 Kip Test Machine at MSFC.....	15
Figure 4.3 Linear Displacement Sensor Calibration.....	16
Figure 4.4 33 Kip Test Machine at ERAU	16
Figure 4.5 486B Torque-Tension Test Set-up	17
Figure 5.1 Ratio of TTTC and D3410 Tests for IM7/8552 Modulus	21
Figure 5.2 Ratio of TTTC and D3410 Tests for IM7/8552 Ultimate Strengths	22
Figure 5.3 Thickness Effect on the IM7/8552 TTTC Properties	22
Figure 5.4 Ratio of TTTC and D3410 Tests for AS4/3501-5a Modulus.....	25
Figure 5.5 Ratio of TTTC and D3410 Tests for AS4/3501-5a Ultimate Strengths	25
Figure 5.6 Thickness Effect on the AS4/3501-5a TTTC Properties.....	26
Figure 5.7 Ratio of TTTC and D3410 Tests for AS4/3501-6 Modulus.....	28
Figure 5.8 Ratio of TTTC and D3410 Tests for AS4/3501-6 Ultimate Strengths.....	29
Figure 5.9 Thickness Effect on the AS4/3501-6 TTTC Properties	29
Figure 5.10 Thickness Effect on the AS4/8552 TTTC Properties.....	32
Figure 5.11 Acoustic Emission Hits for 0.5-in Bolt – Test 1	33
Figure 5.12 Acoustic Energy for 0.5-in Bolt – Test 1	33
Figure 5.13 Acoustic Emission Hits for 0.5-in Bolt – Test 2	34

Figure 5.14 Acoustic Energy for 0.5-in Bolt – Test 2	35
Figure 5.15 Acoustic Emission Hits for 0.5-in Bolt – Test 3	36
Figure 5.16 Acoustic Energy for 0.5-in Bolt – Test 3	36
Figure 5.17 Acoustic Emission Hits for 0.5-in Bolt – Test 4	37
Figure 5.18 Acoustic Emission Energy for 0.5-in Bolt – Test 4.....	37
Figure 5.19 Acoustic Emission Hits for 0.25-in Bolt – Test 1	38
Figure 5.20 Acoustic Energy for 0.25-in Bolt – Test 1	38

CHAPTER 1

INTRODUCTION

1.1 SCOPE

In modern aerospace/aeronautical engineering, fiber reinforced plastics (FRP) are increasingly being used in structural applications due to their high strength to weight ratios. For fiber/polymer matrix type composites, the strength of the composites comes from the fiber, while the matrix is primarily a bonding agent. It is for this reason that in-plane material properties have drawn much more attention than out-of-plane, or through-the-thickness (TTT) properties. In fact, there is neither a standard test for determining TTT properties, nor TTT data available in composite material data books. However, there are certain circumstances where TTT properties play a dominant role. One such example is the TTT bearing stress of composites caused by lateral compression of a mechanical fastener. It is therefore suggested that these material properties henceforth be known as through-the-thickness compression (TTTC) properties.

Since TTTC mechanical properties are critical in understanding the behavior of a mechanically fastened composite joint, a major portion of this work was expended in identifying the TTTC elastic modulus and the TTTC ultimate strength. A prototypical process to determine these properties is presented herein. There were 206 separate TTTC tests, which were performed on four different composite material systems. In order to

validate this new test procedure, standardized ASTM D3410-00 tests [1] were performed as a benchmark comparison for the TTTC tests.

There is great difficulty in determining the torque limit of a mechanical fastener in a composite joint because all modern approaches assume isotropic material behavior. One such method in practice by engineers at the Marshall Space Flight Center (NASA/MSFC) is to follow the specification MSFC-STD-486B [2] but use only half the experimentally determined torque value. The major concern, which initiated this conservative practice, is whether or not the composite members will be crushed as a result of the bolt preload. Presented herein is an approach which utilizes acoustic emission (AE) nondestructive evaluation during MSFC-STD-486B torque-tension testing of a graphite/epoxy lap joint to determine the onset of composite damage.

1.2 PREVIOUS RESEARCH

A major portion of the research to date concerning bolted composite joints has dealt with in-plane static load capacity [3]. These works helped spawn standards dealing with filled-hole static joint strength. Other investigations [4-6] have clearly shown that the torque load in the mechanical fastener significantly affects the joint strength in a beneficial manner by reducing the in-plane bearing strength dependence of the composite laminate. One study reported a maximum increase in joint strength of 28% [4]. This finding has helped to improve the reliability and efficiency of the joint in a composite structure. Therefore, the next step is to determine just how much preload can be applied.

Since the ability of the composite to withstand the bolt preload is directly related to the TTTC material properties, an in depth literature survey was performed.

Unfortunately, there are very few published works on this topic. One experimental study on TTT composite properties by Benzeggagh, et al. [7] attempted to determine indirectly the TTT tension strength and modulus of graphite/epoxy coupons made from a very thick 50 layer unidirectional plate. The limitation of this work was that the authors neither validated their work against known material properties, nor did they develop a test procedure that lends itself to testing realistic composite laminates.

Another work related to through-the-thickness composite properties by Avva, et al. [8] remarks that 3D braided composites may have TTT material property advantages over traditional laminated composites due their relatively low interlamina properties. Their work focused on experimentally comparing traditional composites, 2D braided composites, and 3D braided resin transfer molded (RTM) composites; however, the process in which the authors determined the material properties is highly complex. They used an indirect method of determining TTT properties; that is, they transformed data gathered from L-shaped curved-beam specimens under tension and four-point bending into through-the-thickness tensional and compressive material properties. Regardless of the approach, their results did show that the 2D textile composite TTT strength was lower than the unidirectional tape's (TTT strengths of the 3D braids could not be determined), and the through-the-thickness strength was found to decrease significantly with decreasing fiber volume fractions.

Finally, acoustic emission nondestructive testing has never been utilized in determining the torque limit of a mechanical fastener; yet, it was successfully applied by Hamada, et al. [9] to determine the in-plane bearing-failure modes of a mechanical

carbon/epoxy joint. Utilizing the measured acoustic energy, the investigators were able to accurately determine the start of in-plane failure of the composite.

CHAPTER 2

THEORY AND BACKGROUND

2.1 THROUGH-THE-THICKNESS MATERIAL PROPERTIES

Theoretically, the TTT compressive modulus of a composite, E_T , can be calculated from the following equations derived by Vinson [10]:

$$E_T = \frac{4K_T G_{23}}{K_T + mG_{23}},$$

where K_T is the plane strain bulk modulus,

$$\frac{1}{K_T} = \frac{K_f^{-1}V_f + \eta_K K_m^{-1}V_m}{V_f + \eta_K V_m},$$

G_{23} is the out-of-plane transverse shear modulus of a composite lamina,

$$\frac{1}{G_{23}} = \frac{G_f^{-1}V_f + \eta_4 G_m^{-1}V_m}{V_f + \eta_4 V_m}$$

and m is determined by

$$m = 1 + \frac{4K_T \nu_{12}^2}{E_{11}}.$$

V_f and V_m are the fiber and matrix volume fractions of the composite laminate, where $V_f + V_m = 1$. G_f and G_m are the shear modulus of the fiber and matrix, respectively. The Poisson's ratio of the laminate is ν_{12} , while E_{11} is the modulus of elasticity for the laminate in the fiber direction.

Also,

$$\begin{aligned}
 K_f &= \frac{E_f}{2(1-\nu_f)}, & K_m &= \frac{E_m}{2(1-\nu_m)}, \\
 E_{11} &= E_f V_f + E_m V_m, & \nu_{12} &= \nu_f V_f + \nu_m V_m, \\
 \eta_K &= \frac{1 + G_m/K_f}{2(1-\nu_m)}, & \eta_4 &= \frac{3 - 4\nu_m + G_m/G_f}{4(1-\nu_m)},
 \end{aligned}$$

with E_f and E_m being the elastic moduli of the fiber and matrix; likewise, ν_f and ν_m are the Poisson's ratio of the fiber and matrix. It is noteworthy that determination of E_T via Vinson's method is not possible for the materials presented in this work, since values for the shear modulus of the fiber, G_f , and the Poisson's ratio of the fiber and matrix, ν_f and ν_m , are not available. In fact, this theory does not lend itself to practical application because many of the required material constants are difficult to determine experimentally.

To determine the TTTC material properties of a composite laminate, an experimental approach was the only option. The major difficulty that arises when testing for TTTC properties is how to accurately measure the specimen's strain. The thickness of a composite laminate is often only a few thousands of an inch. This makes bonding a strain gage in the thickness dimension infeasible. In order to obtain strain measurements, an instrument capable of measuring extremely small displacements with great accuracy was required. Compiled in Table 2.1 are the most widely used displacement measurement devices with the critical features present for comparison.

Table 2.1 Displacement Measurement Tool Comparison

Measurement Tool	Features
LDS	$\leq 0.1\%$ full scale error No external conditioners 3.5 mV/V output Medium cost
LVDT	0.25% full scale error External conditioners required 4 mV/V output Low cost + conditioners
Extensometer	0.1-0.25% full scale error No external conditioners 3.5 mV/V output High cost

After careful consideration, the Linear Displacement Sensor (LDS) from Vishay with a full scale deflection of 0.25 inch was chosen because of its excellent full-scale error, acceptable cost, and ease of employment due to a four-arm active strain gage bridge. The next step was to design a compression fixture which would have the test coupon in proximity to the sensor, house the sensor to avoid any damaging coupon shrapnel, and allow for lead wire attachment to the data acquisition system. The initial design can be seen in Figure 2.1.

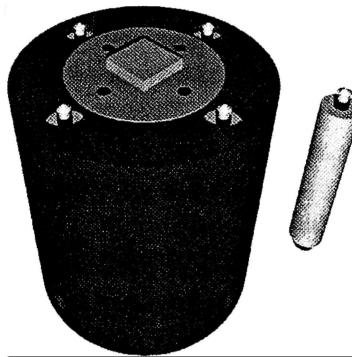


Figure 2.1 Prototypical TTTC Test Fixture with LDS and TTTC Coupon

Material selection for the TTTC test fixture was critical. The strength and stiffness requirements had to be as high as possible to prevent any significant error due to large deflections of the fixture during loading or damage due to a lack of strength. A medium carbon steel, AISI 4140, was selected. After machining, the fixture was normalized, quenched, and then tempered to a hardness of 50 RHC with a strength of approximately 220 ksi. The stiffness of steel is typically 29.7 Msi, approximately twenty-eight times greater than the highest TTTC stiffness of the coupons tested. During TTTC testing at Embry-Riddle Aeronautical University (ERAU), an upper compression head had to be machined from AISI 4140 and treated because of an inadequately strong compression head on the Tinius-Olsen (see Figure 4.4).

Validation of this new test procedure relied on the fact that the material properties for a unidirectional plate are theoretically equal in the y and z directions (Figure 2.2), i.e., $E_y = E_z$ and $\sigma_y = \sigma_z$. Therefore, the standardized ASTM D3410-00 90° compression test is performed to determine material properties in the y direction along with TTTC tests to determine z direction properties for comparison.

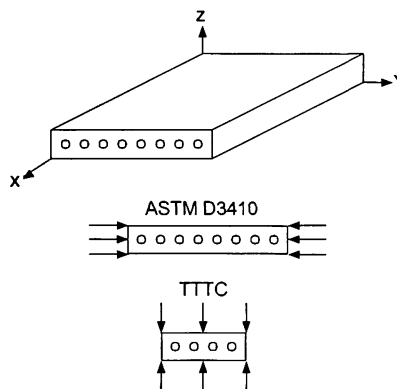


Figure 2.2 TTTC Validity Concept

Finally, there is the technical challenge of generating good data. Even the best laminate does not have a perfectly uniform thickness, and this presents difficulty when applying the load to the TTTC coupon during the beginning of the test. Lack of thickness uniformity means the upper compression head is not in complete contact with the TTTC coupon until the moving ram has achieved a certain displacement. This results in an effective stiffness much less than when the ram makes full contact. Resulting stress-strain data plots might have a slight nonlinearity at the beginning of the test until complete contact is achieved, at which point the actual coupon stiffness is seen in the stress-strain curves.

2.2 ACOUSTIC EMISSION

The textbook definition of acoustic emission is a transient elastic wave generated by the rapid release of energy from localized source within a material. AE is a passive, nondestructive technique requiring the structure or specimen to be under load in order to generate the failure mechanisms that produce the elastic waves. Piezoelectric sensors attached to the surface detect the stress waves that propagate throughout the material and output a voltage signal. A preamplifier is used to boost the voltage signal to a usable level, and a band-pass filter is used to remove unwanted noise. The voltage signal is then fed to a data acquisition system that extracts information about the signal and generates AE quantification parameters.

In the time domain, there are six AE parameters from which acoustic emission results are evaluated (Figure 2.2): amplitude, rise time, duration, energy, counts, and counts-to-peak. Amplitude (dB) is the peak amplitude of the voltage versus time signal.

Rise time (ms) is the time that it takes the signal to reach its maximum amplitude after the waveform first crosses a preset voltage threshold. Duration is the total length of the signal (ms) measured from the first to the last threshold crossing. Energy (V-s) is a measure of the area under the rectified waveform. Counts and counts-to-peak are measured by a digital counting circuit that is activated as the signal surpasses the threshold and deactivated once the signal falls below the threshold.

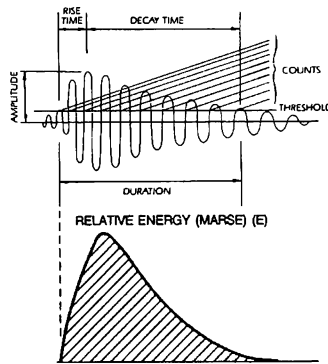


Figure 2.3 Acoustic Emission Signal Parameters

2.3 TORQUE LIMIT OF A MECHANICAL FASTENER

Currently the author only found one work attempting to predict the torque limit of a mechanical fastener in a composite joint. This work, by Zhao, et al. [11], describes the torque limit of a bolt as a function of bolt parameters and TTTC material properties of the composite laminate in the joint. Two models were derived in this work, one for maximum stress failure and the other for maximum strain failure. Validation of these models is beyond the scope of this work due to the inability to obtain a bolt and washer strong enough to fail the composite material tested.

CHAPTER 3

TEST MATERIALS AND PROCESSES

3.1 IM7 / 8552

The IM7/8552 prepreg tape is made from an intermediate modulus fiber that is encased in a mid-toughened, high strength, damage-resistant, 350°F cure, structural epoxy. The nominal cured ply thickness is 5.5 mils with a fiber volume fraction V_f of 60%. This system was used to manufacture six different laminate configurations: $[0]_{32}$, $[0, 90]_{6s}$, $[0, \pm 45, 90]_{3s}$, $[0, \pm 30, \pm 60, 90]_{2s}$, $[0, \pm 45, 90]_{3s}$, $[0, \pm 45, 90]_{4s}$, and $[0, \pm 45, 90]_{5s}$. The plates had nominal thicknesses of 0.176, 0.132, 0.132, 0.132, 0.132, 0.176, and 0.220 inches, respectively.

Lay-up of the plates involved a standard debulk procedure on the first and every successive fourth layer. The first four plate configurations were given a smooth/peel-ply finish, while the last three, manufactured by ATK Thiokol Propulsion, were given a smooth/smooth finish. All plates were cured in an autoclave according to the recommended Hexcel cure cycle. This specific IM7/8552 was donated by NASA/MSFC due to its expired shelf life; however, the material had never been opened from its sealed freezer bag and was in excellent working condition.

3.2 AS4 / 3501-5A AND AS4 / 3501-6

These two prepreg systems contain the AS4 fiber, an advanced strength carbon fiber. The 3501 systems are high strength, damage resistant, 350°F cure, structural epoxies with the -6 formula having a slightly higher glass transition temperature than the -5a formula (410°F dry versus 392°F dry, correspondingly). The nominal cured ply thickness and fiber volume fraction V_f are 5.2 mils and 62%, respectively.

Both the 3501-5a and 3501-6 prepreg systems were used to manufacture five plate configurations: $[0]_{32}$, $[0, \pm 45, 90]_{2s}$, $[0, \pm 45, 90]_{3s}$, $[0, \pm 45, 90]_{4s}$, and $[0, \pm 45, 90]_{5s}$. These plates had nominal thicknesses of 0.166, 0.083, 0.125, 0.166, and 0.208 inches, respectively. A standard debulk procedure was performed on the first and every consecutive fourth layer; in addition, an overnight debulk was done before curing. The cure process was performed to Hexcel specifications in an oven while under a 27 psig vacuum.

The AS4/3501-5a was purchased from Hexcel at less than a penny per linear foot and was not in the best working condition when received at ERAU, as it had been removed from the original seal bag. On the other hand, the AS4/3501-6 was purchased from Hexcel at overrun cost. This system was in excellent condition when received and was still sealed in the original freezer bag.

3.3 AS4 / 8552 8H FABRIC

The AS4/8552 8H fabric had the same fiber and epoxy properties mentioned in the previous two sections. The nominal fiber volume fraction V_f was 58% with a typical cure ply thickness of 13 mils. The weave of the fabric was an eight-harness satin; that is,

the fiber bundles that make up the fabric go over eight bundles and then under one. This weave makes the fabric very applicable to highly contoured lay-ups.

This prepreg fabric was used to manufacture three different plate thicknesses: 9, 12, and 15 layer laminates. Each layer of the plates had the same fabric orientation with fibers running at 0° and 90° with nominal thicknesses of 0.117, 0.156, and 0.195 inches, respectively. These plates were given a smooth/peel-ply finish and were cured in an autoclave according to specifications. No debulks were performed on these plates.

Tom Delay of ED23 at NASA/MSFC donated the AS4/8552 8H fabric. The material had exceeded its shelf life but had never been removed from the freezer and was in excellent working condition.

CHAPTER 4

EXPERIMENTATION

4.1 ASTM D3410-00 (90° COMPRESSION TESTS)

4.1.1 COUPON SPECIFICATIONS

The test specimens were wet cut to a nominal width and length of 0.25 inch by 5.5 inches from the IM7/8552, AS4/3501-5a, and AS4/3501-6 [0]₃₂ plates with a 320 grit diamond circular saw. Here the fibers were aligned 90° to the applied load. The surfaces were then wet sanded with 600 and 1000 grit emery paper to remove any saw marks.

4.1.2 TEST APPARATUS

A single 120 Ohm strain gage with a gage length of 32 mils was used to measure the specimen strain. Figure 4.1 shows the compression fixture used in these tests. An unsupported test section length of 1.0 inch was used in all ASTM D3410 tests performed.

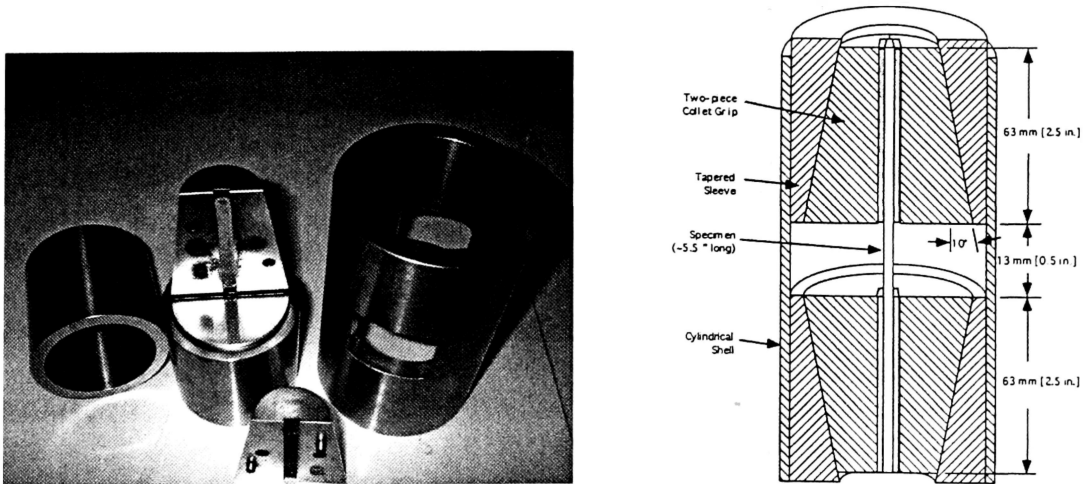


Figure 4.1 ASTM D3410 Test Fixture

4.2 THROUGH-THE-THICKNESS COMPRESSION TESTS

4.2.1 COUPON SPECIFICATIONS

IM7/8552 test specimens were wet cut using a 320 grit diamond circular saw to a nominal 0.5 inch length and 0.5 inch width. The cut edges of the coupons were then wet sanded with 600 and 1000 grit emery paper to remove any saw marks. TTTC test coupons were cut from the $[0]_{32}$, $[0, 90]_{6s}$, $[0, \pm 45, 90]_{3s}$, $[0, \pm 30, \pm 60, 90]_{2s}$, $[0, \pm 45, 90]_{3s}$, $[0, \pm 45, 90]_{4s}$, and $[0, \pm 45, 90]_{5s}$ IM7/8552 plates.

AS4/3501-5a, AS4/3501-6, and AS4/8552 test coupons were cut and sanded by the same means as the IM7/8552 coupons; however, the specimen's length and width were exactly twice the thickness of the plate they were cut from. Plates from which these TTTC coupons were cut are: $[0]_{32}$, $[0, \pm 45, 90]_{2s}$, $[0, \pm 45, 90]_{3s}$, $[0, \pm 45, 90]_{4s}$, $[0, \pm 45, 90]_{5s}$ (3501-5a & 3501-6), and 9, 12, and 15 layer (AS4/8552).

4.2.2 TEST APPARATUS

Through-the-thickness compression tests of the IM7/8552 were performed at NASA/MSFC on a 220 Kip MTS machine (Figure 4.2). A 50 mil full-scale calibration of the linear displacement sensor with a Mitutoyo calibrator can be seen in Figure 4.3.

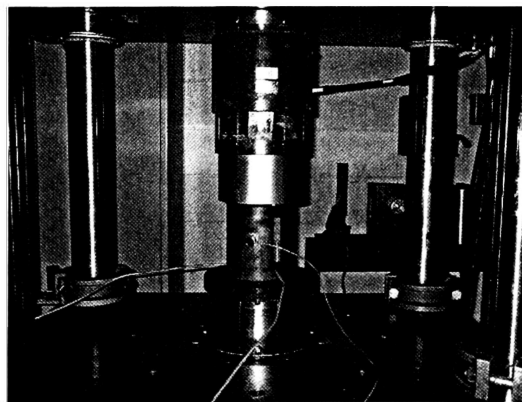


Figure 4.2 220 Kip Test Machine at MSFC

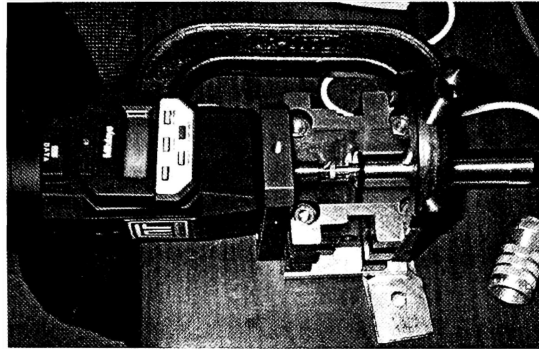


Figure 4.3 Linear Displacement Sensor Calibration

Through-the-thickness compression testing of the AS4/3501-5a, AS4/3501-6, and AS4/8552 coupons were performed at ERAU on the 33 Kip Tinius-Olsen (Figure 4.4). Linear displacement sensor calibration was performed in a similar manner to the calibration at the NASA/MSFC.



Figure 4.4 33 Kip Test Machine at ERAU

4.3 TORQUE-TENSION TESTS

ATK Thiokol Propulsion manufactured several IM7/8552 $[0, \pm 45, 90]_{3s}$ 5 inch by 5 inch coupons for testing. This specific laminate was chosen as MIL-HDBK-17

specifies this configuration when using a mechanical fastener to join a composite part. A 440 grit diamond embedded drill was used to drill the through-holes in the coupons. Two different 160 ksi bolts were intended for investigation, 0.25 inch and 0.5 inch diameters. The designations of the bolts were NAS1958C-32 (0.5 inch) and NAS1954C-32 (0.25 inch) with corresponding self-locking nuts. The 160 ksi washers used were NAS1587-8 ($d_o = 0.872$ inches and $d_i = 0.506$ inches) and NAS1587-4 ($d_o = 0.440$ inches and $d_i = 0.256$ inches), respectively. Seen in Figure 4.5 is the MSFC Standard 486B test fixture.

The AE system used was comprised of a R15 transducer (seen in Figure 4.5 coupled to the composite plate with hot glue) whose signal was amplified with a PAC 2/4/6 preamplifier set to 40 dB of gain. The test data presented herein were gathered with the PAC DSP-32 and MISTRAS software with all measurable time-domain parameters recorded. AE system settings included: preamp gain, 40 dB; system gain, 20 dB; threshold, 50 dB; peak definition time, 50 ms; hit definition time, 100 ms; and hit lockout time, 300 ms. An attenuation check with a mechanical pencil on the composite laminate showed no significant loss of signal for the worst case, the bolt hole between the signal source and AE transducer.

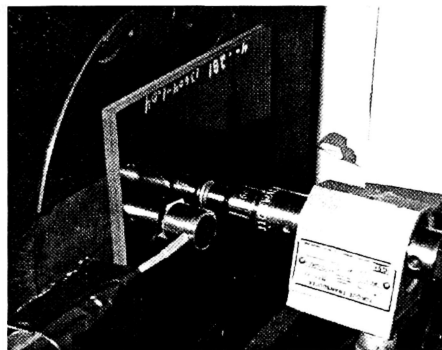


Figure 4.5 486B Torque-Tension Test Set-up

CHAPTER 5

RESULTS

5.1 ASTM D3410-00 (90° COMPRESSION TESTS)

The results of the D3410 90° compression tests are presented in Tables 5.1 – 5.3. Accompanying the results are the average and the percent variation, which is the standard deviation of the results divided by the average. The data plots from which these values were determined can be found in Appendix E.

Table 5.1 IM7 / 8552 D3410 Results

Specimen	Ultimate Strength (ksi)			Modulus (Msi)		
	Measured	Average	% Variation	Measured	Average	% Variation
1	35.8	37.0	4.4%	0.629	0.643	3.0%
2	38.1			0.656		

Table 5.2 AS4 / 3501-5a D3410 Results

Specimen	Ultimate Strength (ksi)			Modulus (Msi)		
	Measured	Average	% Variation	Measured	Average	% Variation
1	16.4	17.9	6.4%	0.573	0.553	4.8%
2	19.1			0.540		
3	18.4			0.577		
4	17.7			0.521		

Table 5.3 AS4 / 3501-6 D3410 Results

Specimen	Ultimate Strength (ksi)			Modulus (Msi)		
	Measured	Average	% Variation	Measured	Average	% Variation
1	27.6	26.5	2.7%	0.704	0.672	3.4%
2	26.2			0.654		
3	26.4			0.658		
4	26.0			0.671		

5.2 THROUGH-THE-THICKNESS COMPRESSION TESTS

5.2.1 IM7 / 8552

The results of the TTTC tests of the IM7/8552 coupons with the average and percent variation can be found in Tables 5.4 – 5.10. Refer to Appendix A for the data plots.

Table 5.4 IM7 / 8552 [0]₃₂ TTTC Results

Specimen	Ultimate Strength (ksi)			Modulus (Msi)		
	Measured	Average	% Variation	Measured	Average	% Variation
1	40.5	37.3	8.8%	0.740	0.662	18.5%
2	41.4			0.725		
3	37.8			0.748		
4	30.5			0.320		
5	34.5			0.691		
6	36.1			0.645		
7	36.8			0.650		
8	37.1			0.716		
9	36.0			0.681		
10	42.5			0.768		
11	35.5			0.711		
12	39.3			0.549		

Table 5.5 IM7 / 8552 [0, 90]_{6s} TTTC Results

Specimen	Ultimate Strength (ksi)			Modulus (Msi)		
	Measured	Average	% Variation	Measured	Average	% Variation
1	167.0	155.6	6.4%	1.320	1.295	1.6%
2	158.8			1.280		
3	165.0			1.280		
4	153.1			1.280		
5	159.6			1.280		
6	158.0			1.280		
7	140.6			1.270		
8	167.5			1.320		
9	151.1			1.330		
10	134.7			1.310		
11	156.6			1.300		
12	154.5			1.290		

Table 5.6 IM7 / 8552 [0, ±45, 90]_{3s} TTTC Results

Specimen	Ultimate Strength (ksi)			Modulus (Msi)		
	Measured	Average	% Variation	Measured	Average	% Variation
1	186.1	160.0	16.5%	1330	1361	2.2%
2	144.7			1390		
3	169.2			1340		
4	179.8			1310		
5	110.5			1330		
6	113.8			1410		
7	139.1			1370		
8	173.6			1350		
9	169.4			1370		
10	175.5			1390		
11	176.6			1370		
12	181.2			1370		

Table 5.7 IM7 / 8552 [0, ±30, ±60, 90]_{2s} TTTC Results

Specimen	Ultimate Strength (ksi)			Modulus (Msi)		
	Measured	Average	% Variation	Measured	Average	% Variation
1	176.6	178.3	1.3%	1310	1339	1.5%
2	177.1			1360		
3	182.4			1340		
4	180.3			1350		
5	182.2			1320		
6	175.8			1340		
7	178.7			1330		
8	178.6			1300		
9	177.4			1350		
10	178.8			1350		
11	176.2			1360		
12	175.8			1360		

Table 5.8 Thiokol Manufactured IM7 / 8552 [0, ±45, 90]_{3s} TTTC Results

Specimen	Ultimate Strength (ksi)			Modulus (Msi)		
	Measured	Average	% Variation	Measured	Average	% Variation
1	169.1	169.4	7.7%	1350	1370	1.8%
2	200.1			1410		
3	161.3			1340		
4	161.7			1340		
5	165.4			1350		
6	157.2			1390		
7	171.9			1380		
8	156.0			1370		
9	179.0			1390		
10	172.0			1380		

Table 5.9 Thiokol Manufactured IM7 / 8552 [0, ±45, 90]_{4s} TTTC Results

Specimen	Ultimate Strength (ksi)			Modulus (Msi)		
	Measured	Average	% Variation	Measured	Average	% Variation
1	177.7	171.4	3.8%	1.480	1.446	2.1%
2	172.1					
3	165.8					
4	164.2					
5	164.8					
6	177.6					
7	179.1					
8	171.6					
9	163.0					
10	177.9					

Table 5.10 Thiokol Manufactured IM7 / 8552 [0, ±45, 90]_{5s} TTTC Results

Specimen	Ultimate Strength (ksi)			Modulus (Msi)		
	Measured	Average	% Variation	Measured	Average	% Variation
1	178.5	170.8	5.2%	1.540	1.530	0.9%
2	180.0					
3	173.8					
4	161.7					
5	165.9					
6	169.4					
7	177.5					
8	181.7					
9	164.4					
10	155.3					

Figure 5.1 shows the comparison of the TTTC modulus and the ASTM D3410 90° compressive modulus. As expected, the results from the TTTC tests on the unidirectional plate, [0], match very closely to the D3410 results; however, the remaining three configurations have been found to be *twice as stiff* as the theory predicts.

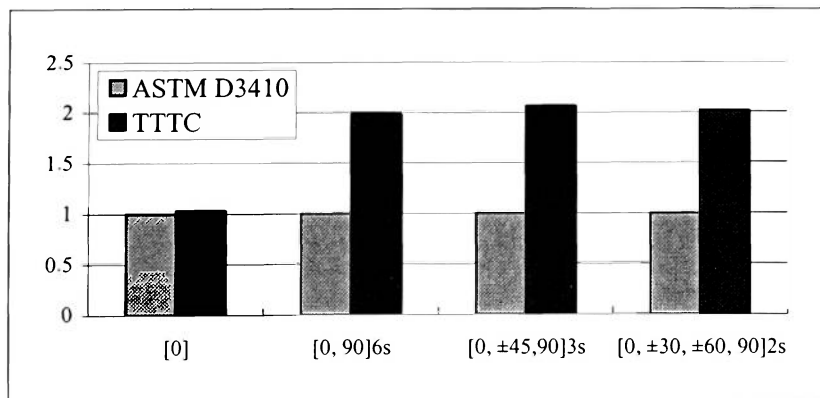


Figure 5.1 Ratio of TTTC and D3410 Tests for IM7/8552 Modulus

The TTTC ultimate strengths in Figure 5.2 compare very well with the D3410 ultimate strengths for the unidirectional plate, [0]. On the other hand, the cross-ply configuration is shown to be 4.2 times as strong, while the $[0, \pm 45, 90]_{3s}$ is 4.3 times the strength of the D3410 tests. The $[0, \pm 30, \pm 60, 90]_{2s}$ strength result is 4.525 times as strong as the D3410 result and 5.2% stronger than the $[0, \pm 45, 90]_{3s}$ laminate. *It is apparent from these results that the orientation of the fibers in the laminate plays an important role in the TTTC strengths.* Also, the $[0, \pm 45, 90]_{3s}$ plate with the smooth/smooth finish showed about a 10 ksi increase in the TTTC strength over the same plate with a smooth/peel-ply finish; whereas, no change in the modulus occurred.

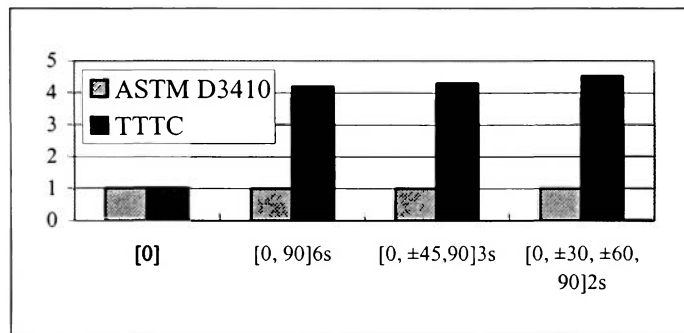


Figure 5.2 Ratio of TTTC and D3410 Tests for IM7/8552 Ultimate Strengths

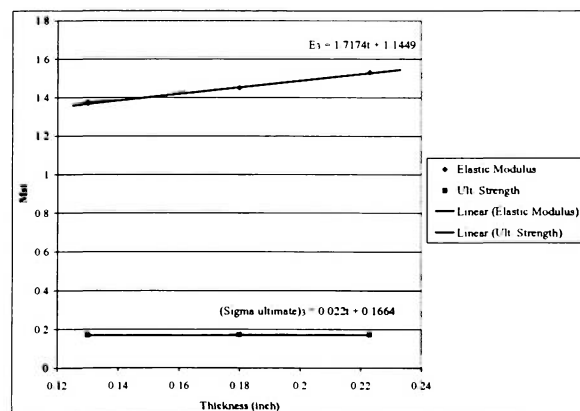


Figure 5.3 Thickness Effect on the IM7/8552 TTTC Properties

The results shown in Figure 5.3 are the averages taken from the ATK Thiokol Propulsion manufactured $[0, \pm 45, 90]_{3s}$, $[0, \pm 45, 90]_{4s}$, and $[0, \pm 45, 90]_{5s}$ plates, Tables 5.8 – 5.10. As can be seen from the linear regression equation having a nearly zero slope, there is no effect on the ultimate strengths as the thickness of the coupons increases; however, the elastic modulus seems to increase slightly as the coupons become thicker.

5.2.2 AS4 / 3501-5A

The results of the TTTC tests of the AS4/3501-5a coupons with the average and percent variation can be found in Tables 5.11 – 5.15. Refer to Appendix B for the data plots.

Table 5.11 AS4 / 3501-5a $[0]_{32}$ TTTC Results

Specimen	Ultimate Strength (ksi)			Modulus (Msi)		
	Measured	Average	% Variation	Measured	Average	% Variation
1	15.5	14.2	5.4%	0.537	0.525	8.0%
2	13.3			0.480		
3	14.6			0.518		
4	13.0			0.546		
5	13.7			0.498		
6	14.3			0.536		
7	14.9			0.451		
8	14.6			0.605		
9	14.0			0.531		
10	14.6			0.548		

Table 5.12 AS4 / 3501-5a $[0, \pm 45, 90]_{2s}$ TTTC Results

Specimen	Ultimate Strength (ksi)			Modulus (Msi)		
	Measured	Average	% Variation	Measured	Average	% Variation
1	125.9	125.7	3.7%	1.067	1.022	4.1%
2	119.4			1.051		
3	133.3			1.088		
4	125.4			1.000		
5	120.4			0.946		
6	127.3			0.985		
7	132.4			1.033		
8	126.9			1.002		
9	121.8			1.030		
10	124.6			1.023		

Table 5.13 AS4 / 3501-5a [0, ±45, 90]_{3s} TTTC Results

Specimen	Ultimate Strength (ksi)			Modulus (Msi)		
	Measured	Average	% Variation	Measured	Average	% Variation
1	119.2	121.3	6.7%	0.976	1.047	5.1%
2	116.4			0.996		
3	120.5			1.062		
4	120.5			1.081		
5	143.6			1.155		
6	115.4			1.088		
7	116.4			1.054		
8	121.1			1.031		
9	120.6			0.992		
10	119.8			1.040		

Table 5.14 AS4 / 3501-5a [0, ±45, 90]_{4s} TTTC Results

Specimen	Ultimate Strength (ksi)			Modulus (Msi)		
	Measured	Average	% Variation	Measured	Average	% Variation
1	113.1	119.5	3.7%	1.046	1.079	6.4%
2	121.3			1.028		
3	118.0			1.207		
4	115.1			1.039		
5	124.2			1.180		
6	123.1			1.050		
7	116.8			1.020		
8	115.6			1.007		
9	126.1			1.112		
10	121.9			1.103		

Table 5.15 AS4 / 3501-5a [0, ±45, 90]_{5s} TTTC Results

Specimen	Ultimate Strength (ksi)			Modulus (Msi)		
	Measured	Average	% Variation	Measured	Average	% Variation
1	135.5	130.1	2.5%	1.176	1.156	3.6%
2	132.2			1.133		
3	129.8			1.238		
4	129.3			1.192		
5	126.7			1.088		
6	128.3			1.128		
7	131.1			1.163		
8	129.0			1.119		
9	133.8			1.153		
10	124.8			1.165		

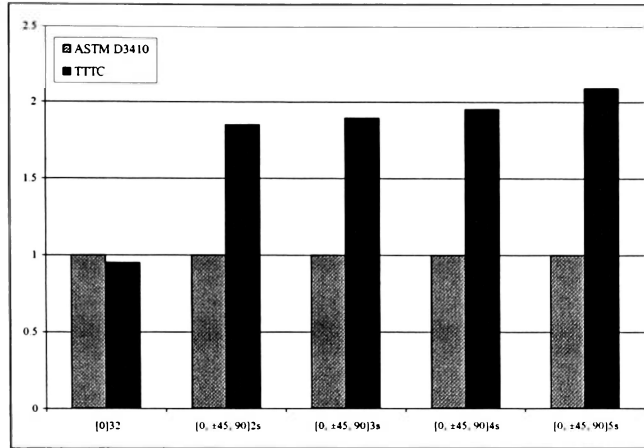


Figure 5.4 Ratio of TTTC and D3410 Tests for AS4/3501-5a Modulus

Shown in Figure 5.4 are comparisons of the TTTC modulus to the ASTM D3410 modulus for the AS4/3501-5a laminates. Like the IM7/8552 results, *there is nearly twice the stiffness increase when compared to current theory. Also, there is a dramatic increase in the TTTC ultimate strengths (Figure 5.5) of nearly seven times.*

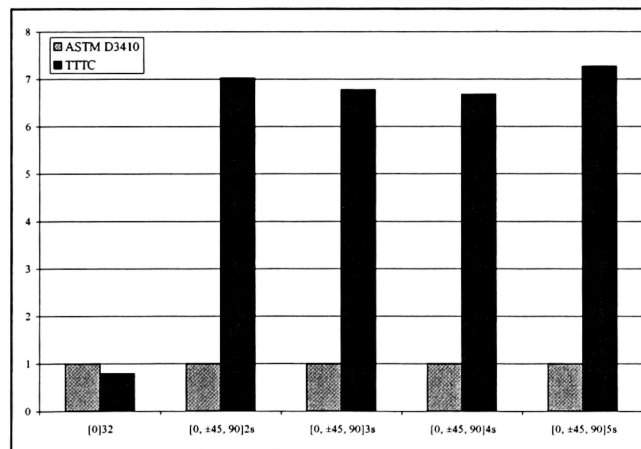


Figure 5.5 Ratio of TTTC and D3410 Tests for AS4/3501-5a Ultimate Strengths

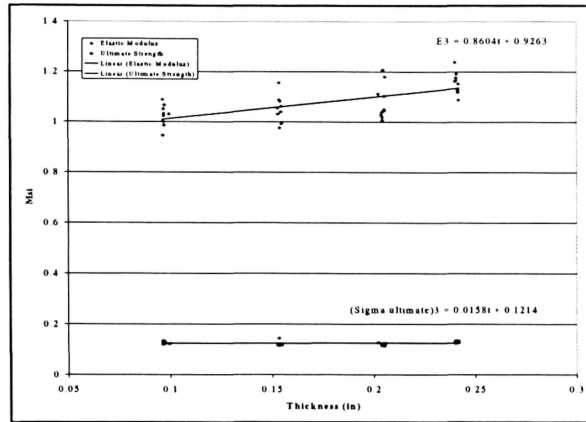


Figure 5.6 Thickness Effect on the AS4/3501-5a TTTC Properties

Unlike plotting just the average values in Figure 5.3, each coupon was plotted in Figure 5.6. Like the IM7/8552 results, there is no noticeable change in the ultimate strengths as the thickness of the laminate increases; conversely, there is again a slight increase in the elastic modulus of the laminate as the laminate thickness increases.

5.2.3 AS4 / 3501-6

Tables 5.16 – 5.20 contain the results of the TTTC tests on the AS4/3501-6. Refer to Appendix C for the test data plots. Specimens 4 and 10 were removed from Table 5.16 since they were found to be outliers.

Table 5.16 AS4 / 3501-6 [0]₃₂ TTTC Results

Specimen	Ultimate Strength (ksi)			Modulus (Msi)		
	Measured	Average	% Variation	Measured	Average	% Variation
1	25.8	28.4	5.7%	0.838	0.772	11.5%
2	28.2			0.803		
3	27.9			0.769		
4						
5	31.1			0.586		
6	30.0			0.763		
7	27.9			0.720		
8	27.3			0.825		
9	28.7			0.869		
10						

Table 5.17 AS4 / 3501-6 [0, ±45, 90]_{2s} TTTC Results

Specimen	Ultimate Strength (ksi)			Modulus (Msi)		
	Measured	Average	% Variation	Measured	Average	% Variation
1	165 0	156 0	5 4%	1 066	1 058	4 1%
2	160 8			1 046		
3	147 2			1 024		
4	163 2			1 127		
5	156 1			1 056		
6	155 6			1 030		
7	154 5			1 010		
8	162 9			1 143		
9	137 5			1 042		
10	156 9			1 036		

Table 5.18 AS4 / 3501-6 [0, ±45, 90]_{3s} TTTC Results

Specimen	Ultimate Strength (ksi)			Modulus (Msi)		
	Measured	Average	% Variation	Measured	Average	% Variation
1	147 2	153 6	2 5%	1 122	1 099	1 9%
2	150 1			1 105		
3	151 9			1 095		
4	154 3			1 117		
5	150 5			1 070		
6	157 8			1 132		
7	157 2			1 077		
8	156 6			1 098		
9	158 3			1 090		
10	152 2			1 079		

Table 5.19 AS4 / 3501-6 [0, ±45, 90]_{4s} TTTC Results

Specimen	Ultimate Strength (ksi)			Modulus (Msi)		
	Measured	Average	% Variation	Measured	Average	% Variation
1	132 5	138 5	4 1%	1 170	1 249	4 0%
2	144 2			1 255		
3	143 8			1 212		
4						
5	130 6			1 272		
6	134 5			1 271		
7	135 6			1 205		
8	137 2			1 301		
9	143 2			1 225		
10	145 2			1 327		

Table 5.20 AS4 / 3501-6 [0, ±45, 90]_{5s} TTTC Results

Specimen	Ultimate Strength (ksi)			Modulus (Msi)		
	Measured	Average	% Variation	Measured	Average	% Variation
1	143.4	152.8	5.8%	1.269	1.360	3.4%
2	156.3			1.411		
3	174.4			1.406		
4	154.6			1.301		
5	149.2			1.375		
6	147.0			1.376		
7	144.1			1.353		
8	155.7			1.352		
9	154.0			1.347		
10	149.7			1.409		

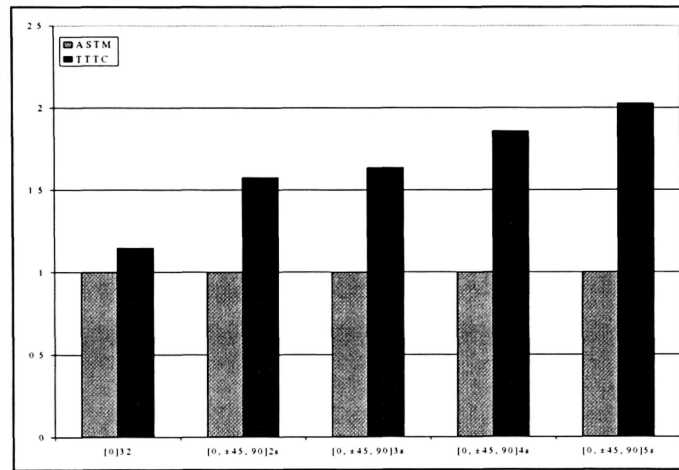


Figure 5.7 Ratio of TTTC and D3410 Tests for AS4/3501-6 Modulus

Examining Figure 5.7, again it can be seen that the TTTC modulus of the AS4/3501-6 is higher than what was predicted by D3410. Also, there is poor correlation between the [0] TTTC tests and the ASTM tests. There is evidence, given to the 11.5% variation in the modulus results of the [0] TTTC tests, that perhaps outliers exist in the results, causing the average to be higher than was expected.

Unlike the modulus results, the [0] TTTC strengths of the AS4/3501-6 match closely with the ASTM tests, Figure 5.8. Like the IM7/8552 and AS4/3501-5a results, *the TTTC strengths of the quasi-isotropic laminates are significantly higher than theory*

would suggest. However, the average TTTC strength of the $[0, \pm 45, 90]_{4s}$ laminate is less than the others. Previous results have shown a closer equivalence in TTTC strengths regardless of thickness.

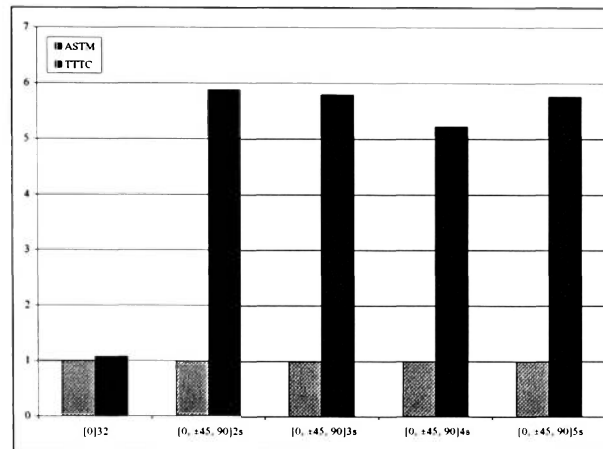


Figure 5.8 Ratio of TTTC and D3410 Tests for AS4/3501-6 Ultimate Strengths

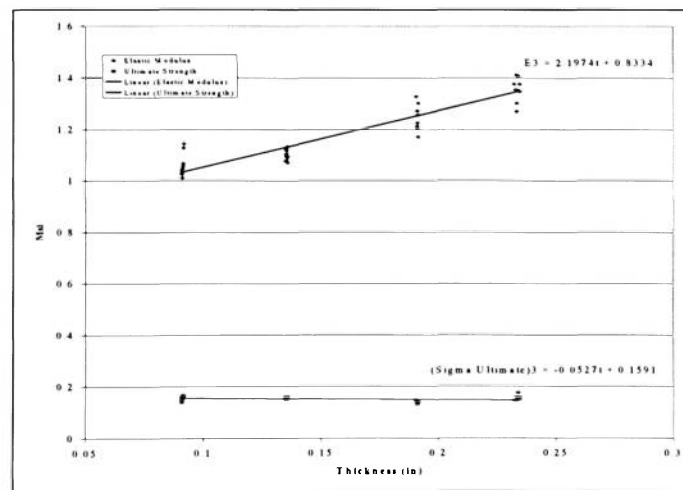


Figure 5.9 Thickness Effect on the AS4/3501-6 TTTC Properties

Like the IM7/8552 and AS4/3501-5a, there is no noticeable change in the ultimate strengths as the thickness of the laminate increases (Figure 5.9); however, disparate to

the IM7/8552 and AS4/3501-5a, there is a more dramatic increase in the elastic modulus of the laminate as the thickness increases.

Due to the poor condition of the AS4/3501-5a prepreg, the flow of the resin during the cure process was reduced. According to Hexcel specifications, 3501-5a TTTC coupons should have had the same nominal thickness as the 3501-6; however, all 3501-5a coupons were slightly thicker when compared to the same 3501-6 coupon. This suggests that, the 3501-5a coupons had a slightly higher resin content due to the poor flow qualities. The results are a reduction in TTTC strength, while the TTTC modulus remained approximately the same.

5.2.4 AS4 / 8552 8H FABRIC

Compiled in Tables 5.21 – 5.23 are the AS4/8552 TTTC test results, whose data plots are found in Appendix D.

Table 5.21 AS4 / 8552 8H Fabric – 9 Layers

Specimen	Ultimate Strength (ksi)			Modulus (Msi)		
	Measured	Average	% Variation	Measured	Average	% Variation
1	150.4	158.9	5.0%	1320	1367	3.1%
2	164.4			1346		
3	159.5			1398		
4	160.5			1390		
5	161.6			1436		
6	156.2			1413		
7	173.0			1360		
8	149.9			1332		
9	165.6			1368		
10	147.8			1302		

Table 5.22 AS4 / 8552 8H Fabric – 12 Layers

Specimen	Ultimate Strength (ksi)			Modulus (Msi)		
	Measured	Average	% Variation	Measured	Average	% Variation
1	162.2	160.2	4.5%	1.317	1.389	3.5%
2	155.1			1.349		
3	148.5			1.385		
4	155.8			1.320		
5	168.3			1.419		
6	156.9			1.446		
7	166.4			1.364		
8	161.1			1.426		
9	171.9			1.440		
10	155.6			1.428		

Table 5.23 AS4 / 8552 8H Fabric – 15 Layers

Specimen	Ultimate Strength (ksi)			Modulus (Msi)		
	Measured	Average	% Variation	Measured	Average	% Variation
1	151.0	159.9	3.7%	1.344	1.362	2.7%
2	157.0			1.302		
3	164.4			1.372		
4	173.1			1.394		
5	154.5			1.368		
6	159.2			1.337		
7	158.4			1.358		
8	160.2			1.324		
9	159.6			1.414		
10	161.9			1.405		

Unlike the laminates constructed from unidirectional tape, the TTTC modulus results of the AS4/8552 fabric do not show the same trend (Figure 5.10). *There appears to be no increase in the TTTC modulus as the thickness of the laminate increases, and similar to the other TTTC strength results, there is no increase in the ultimate strength as the thickness increases.*

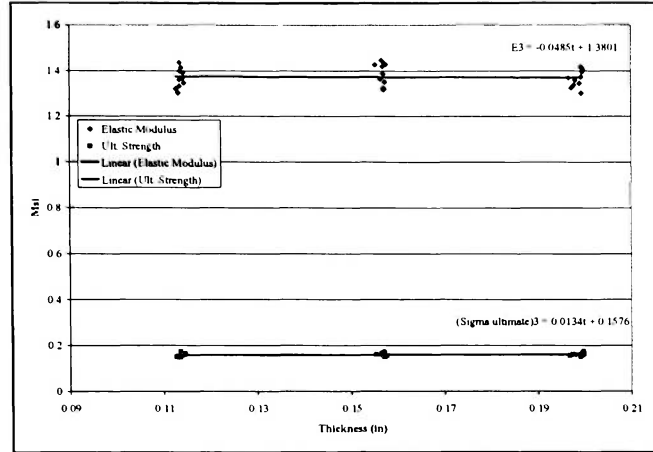


Figure 5.10 Thickness Effect on the AS4/8552 TTTC Properties

5.3 TORQUE-TENSION TESTS

Figures 5.11 – 5.12 show the torque-tension data for the 0.5 inch diameter bolt superimposed over the acoustic emission hits and acoustic emission energy, respectively. From Figure 5.11, it is difficult to distinguish the AE activity associated with either bolt or plate failure. Many of the hits in this figure are in fact from the frictional noise generated from the bolt-nut interface during the loading of the bolt. However, when examining the acoustic emission energy, (Figure 5.12), it is clear by the sudden increase in the acoustic emission energy right before thread rupture that the AE data shows bolt failure. Examination of the composite plates with a micrometer showed no measurable change in plate thickness in the washer region. A visual inspection of the bolt-hole revealed no interlamina failure. In fact, performing a simple calculation by dividing the maximum bolt load, 20 kips, by the area of the washer, 0.3956 in^2 , a reasonable estimate of the stress level in the plates was found to be 50.5 ksi, not even one-third the average TTTC ultimate strength of the Thiokol IM7/8552 $[0, \pm 45, 90]_{3s}$ laminate. If matrix

cracking or interlaminar shear failures occurred, they were drowned out by the friction noise AE detected.

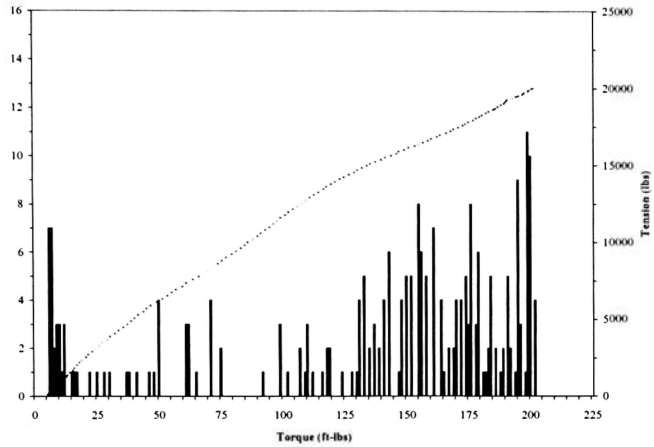


Figure 5.11 Acoustic Emission Hits for 0.5-in Bolt – Test 1

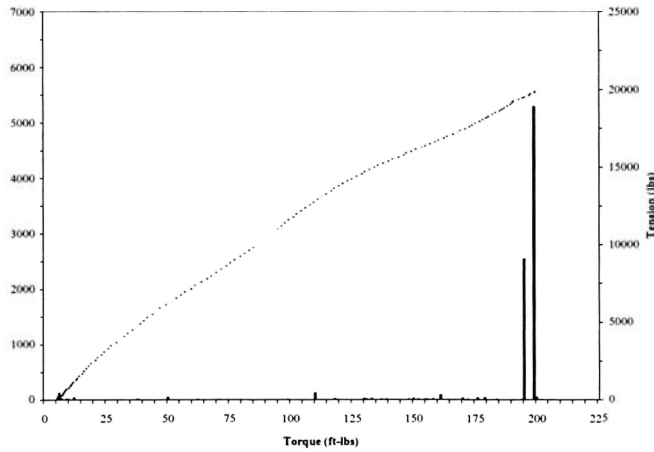


Figure 5.12 Acoustic Energy for 0.5-in Bolt – Test 1

For the second test involving a 0.5 inch bolt, calcium grease was applied in between the bolt-thread and nut-thread interface to hopefully eliminate friction. This did not work as well as expected. Instead, it was observed that the washer would periodically

slip and then spin against the composite plate. This is evident in the large amount of acoustic energy detected at approximately 100 and 185 ft-lbs of torque in Figure 5.14. Also, due to the differential movement between the washer and the spinning nut, unwanted signals were detected by the AE system throughout the test (Figure 5.13). Again the AE data collected during this test is ambiguous due to frictional sources. However, the AE data did become critically active during the sudden increase in the curve at the end of the test, indicating bolt thread failure. Visual and micrometer examinations of the laminate in the washer region showed no signs of any failure. A quick calculation of the stress levels in the plate at the time of failure equate to 82.1 ksi, half of the expected failure stress seen during the TTTC tests. All of this indicated that the laminate did not experience matrix cracking or interlaminar shear failure during the torque test.

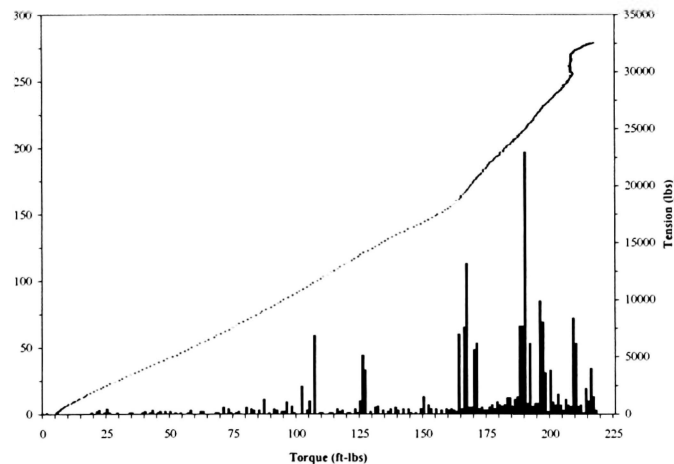


Figure 5.13 Acoustic Emission Hits for 0.5-in Bolt – Test 2

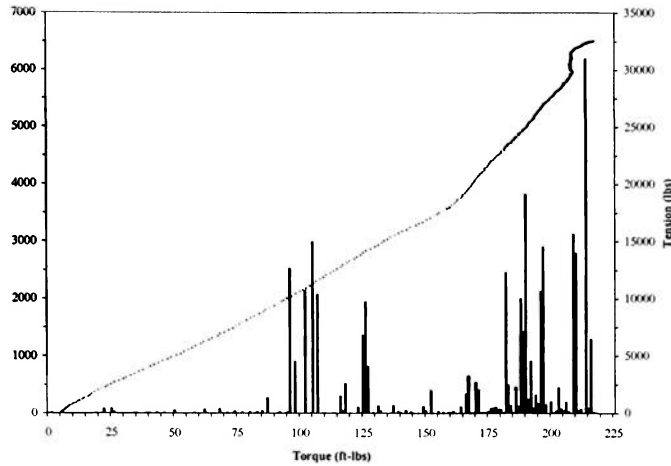


Figure 5.14 Acoustic Energy for 0.5-in Bolt – Test 2

For the third test of the 0.5 inch bolt, calcium grease was employed in the bolt-nut interface and the nut-washer interface to prevent the nut from spinning the washer against the composite plate. Again there were small amounts of AE activity throughout the test (Figure 5.15), which says that there is still a source of AE signals as the torque is increased. However, when examining Figure 5.16, the acoustic energy, it is seen that the noise from the frictional source was practically eliminated. There was a noticeable amount of energy at 200 ft-lbs of torque that could be either matrix cracking, interlamina shear failure, or thread failure, but the source of this AE is unidentified. Despite this, thread failure in the bolt is clearly identified by the AE data at 262 ft-lbs of torque. The composite plate was examined by the same means as before and showed no signs of any failure. The stress levels in the composite plates at bolt failure were approximately the same as test 2.

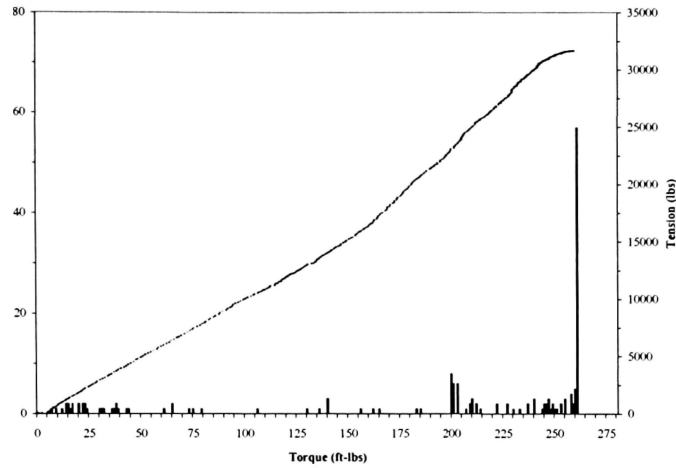


Figure 5.15 Acoustic Emission Hits for 0.5-in Bolt – Test 3

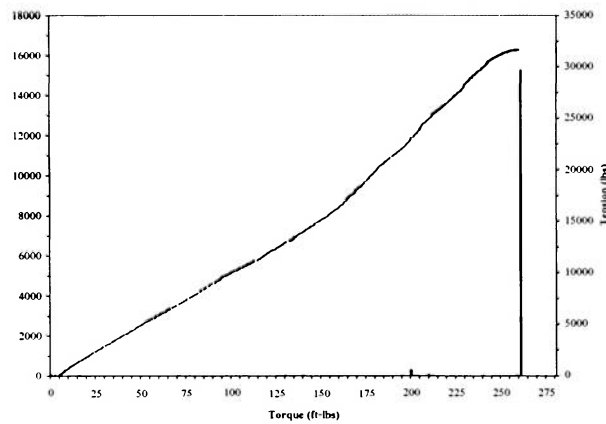


Figure 5.16 Acoustic Energy for 0.5-in Bolt – Test 3

The fourth and final test of the 0.5 inch bolt was lubricated in the same way as test 3. There is a large amount of AE activity at the beginning of the test (Figure 5.17), most likely due to friction sources. The AE energy detected, Figure 5.18, increased noticeably around 200 ft-lbs but was nearly equivalent to the energy detected at the beginning of the test. It is apparent that these sources are not from the composite plates experiencing

failure but rather from friction between the plates and washer. Bolt failure was again evidenced by the critical AE activity near thread rupture.

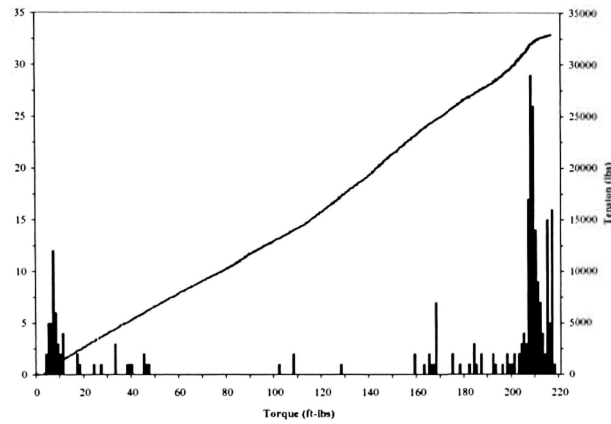


Figure 5.17 Acoustic Emission Hits for 0.5-in Bolt – Test 4

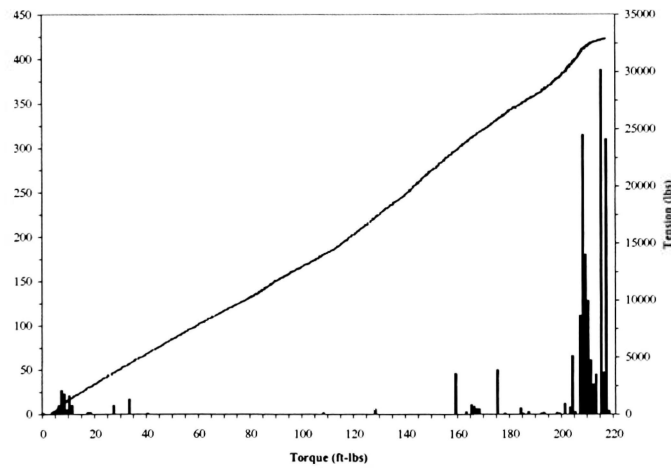


Figure 5.18 Acoustic Emission Energy for 0.5-in Bolt – Test 4

Since plate failure did not occur using the 0.5 inch diameter bolts, there was no chance that the 0.25 inch diameter bolt would fail the plates. One test was performed to both verify this and hopefully eliminate the ambiguous AE signals. As such, calcium

grease was applied to all interfaces, including the plate-washer interface, which had not been done for the 0.5 inch diameter bolt tests. Unfortunately, this did not eradicate the AE detected at the very beginning of the test, as can be seen in Figure 5.19. However, the measured energy levels of these sources were very nearly zero, (Figure 5.20). In fact, the only significant AE energy that was detected occurred at the failure of the bolt threads. The waviness seen in the tension versus torque curve was produced by slippage in the test stand.

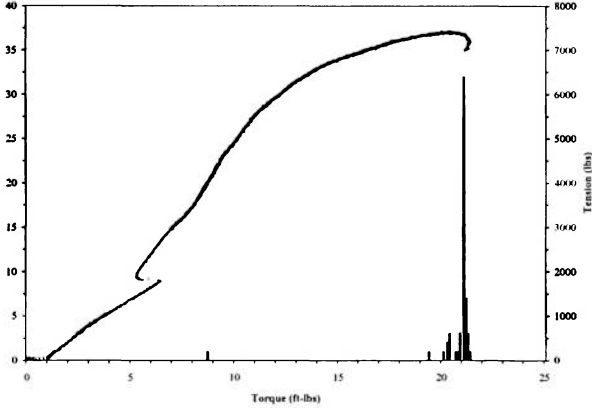


Figure 5.19 Acoustic Emission Hits for 0.25-in Bolt – Test 1

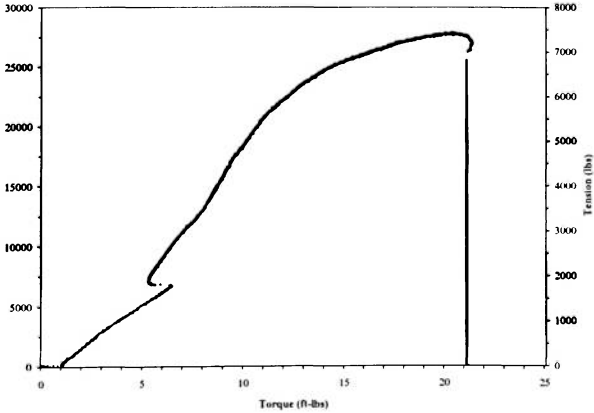


Figure 5.20 Acoustic Energy for 0.25-in Bolt – Test 1

CHAPTER 6

CONCLUSIONS AND RECOMMENDATIONS

6.1 CONCLUSIONS

- The process for determining TTTC material properties using a linear displacement sensor has proven successful for both traditional laminates and 2D fabric laminates. TTTC testing compares favorably to the standard ASTM D3410-00 90° compression test for a unidirectional plate. A TTTC coupon ratio of width or length to thickness equal to or greater than two produced consistent results without buckling. Coupons from 0.090 inch to 0.250 inch thick were successfully tested.
- Since all the composite systems examined were beyond their shelf life, the actual TTTC values were not as significant as the trends in the data.
- The matrix is the dominant factor in the TTTC modulus; however, fiber configurations from cross-ply to quasi-isotropic on average tended to double the stiffness for the three commonly used composite systems tested.
- The fiber configuration of the laminate plays a dominant role in the TTTC strength. This was seen through an increase in TTTC strengths for each successive configuration: [0], [0, 90], [0, ±45, 90], and [0, ±30, ±60, 90]. Therefore, it is believed that the role of the fibers in TTTC strengths is the constraint against the transverse Poisson effect, applying a lateral compressive load, resulting in in-plane deflection.

- The thickness of the composite seems to slightly influence the TTTC modulus of the laminate when the configurations are the same; yet, the TTTC strengths are unaffected by this. This phenomenon was shown to exist for three composite systems from three to four thicknesses. This was shown to be invalid for the fabric.
- The ‘rule of mixtures’ does not give a good estimation of the TTTC modulus because fiber orientation is not taken into account.
- The surface finish of the laminate plays a role in the TTTC strength by increasing it, but does not affect the TTTC modulus: the smoother the finish, the greater the TTTC strength.
- A major loss in TTTC strength can be expected when the fiber volume fraction is slightly reduced (this concurs with the result of Avva, et al. [8]); on the other hand, the TTTC modulus does not seem to be reduced in the same degree.
- The TTTC work took place on two different set-ups, and the plates were manufactured by two different people. The 3501 plates used in the TTTC tests were cured two plates at a time under conditions that were out of specifications. It is highly possible that this variability in the manufacturing processes affected the results. It is definitive to note that with such bad input to the tests, the trends in the results were not significantly disrupted.
- The results of the 486B tests showed that the composite plates under investigation did not experience major failure before the bolt failed. Both acoustic emission and visual examination confirmed this; however, the friction noise presented a difficult problem in performing acoustic emission inspection. The current practice of reducing by half the fastener preload specified by 486B is a very conservative approach when using a

0.5 inch diameter bolt (or less) on the IM7/8552 composite configured according to MIL-17 design criteria. A direct implication of using fewer bolts with higher preloads to achieve the same static strength is a major improvement on the efficiency of joints configured in this manner.

6.2 RECOMMENDATIONS

- Design and manufacture an upper compression ram that can adjust to a TTTC coupon that does not have a completely uniform thickness. Such a design schematic exists within ASTM C695, Standard Test Method for Compressive Strength of Carbon and Graphite. This improvement in the test apparatus would reduce, or possibly even eliminate, the nonlinearity at the beginning of the load ramp.
- Perform TTTC testing on at least four nondiscrepant autoclave cured composite systems, holding either the matrix the same or the reinforcement the same to better examine the role that each of these plays in the TTTC properties. Since the matrix is a key player in TTTC properties, nondiscrepant materials would remove many uncertainties.
- Find a bolt and washer assembly stronger than 160 ksi. This would allow for a better test set-up to determine exactly at what bolt torque the composites are failing. This would also allow for verification of the models proposed by Zhao et al. [11] without having the bolt fail.
- Due to the difficulty in sorting the frictional acoustic emission from the composite AE, a neural network might be an excellent tool to utilize. Also, using a wideband

AE transducer rather than a resonant one, would allow for frequency analysis in determining which detected AE sources are extraneous.

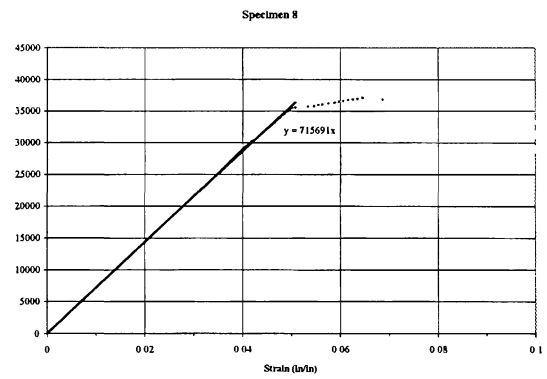
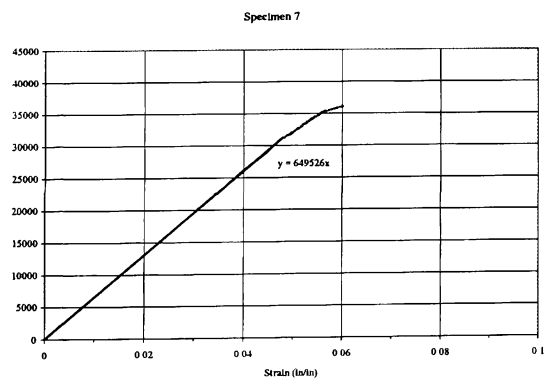
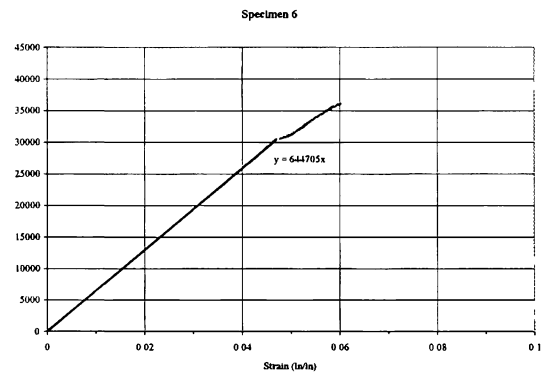
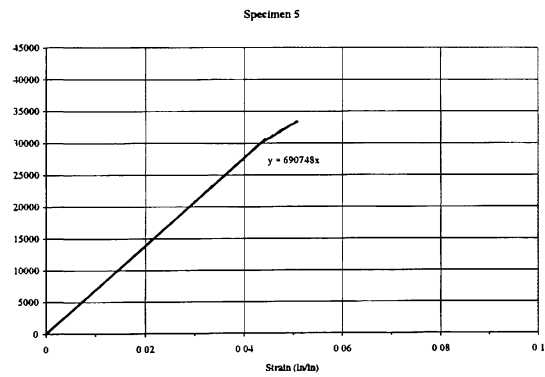
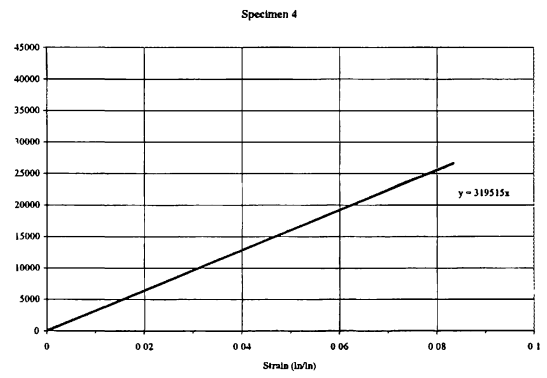
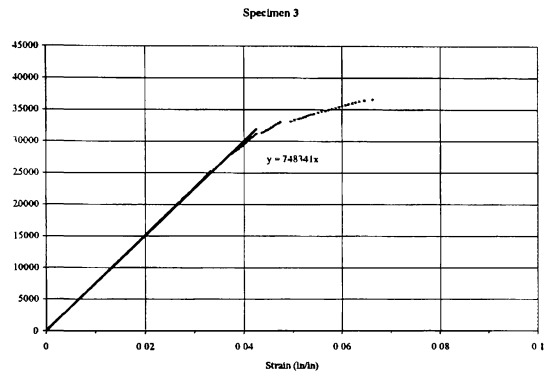
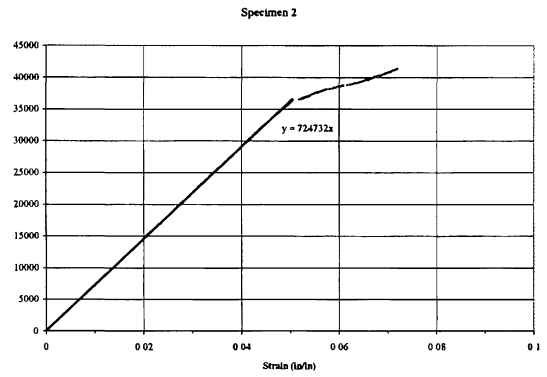
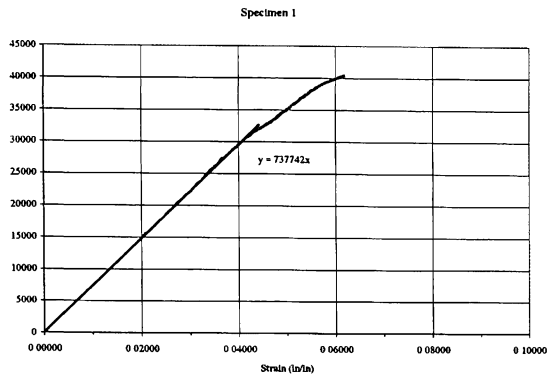
REFERENCES

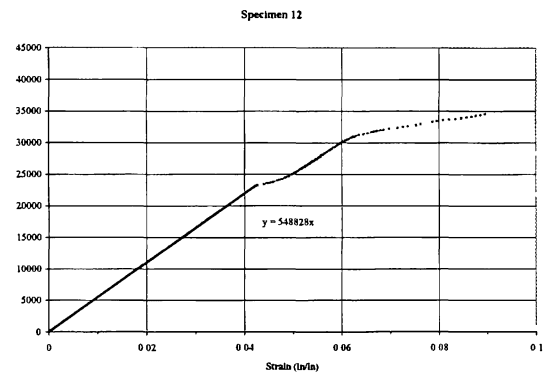
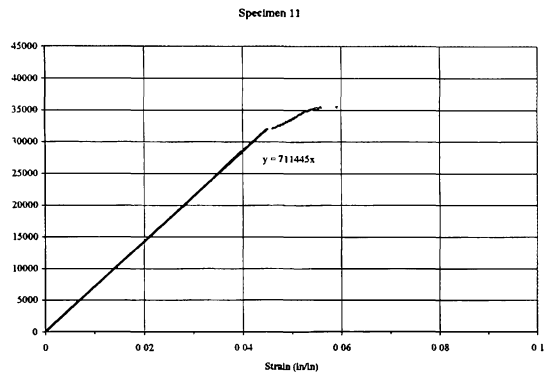
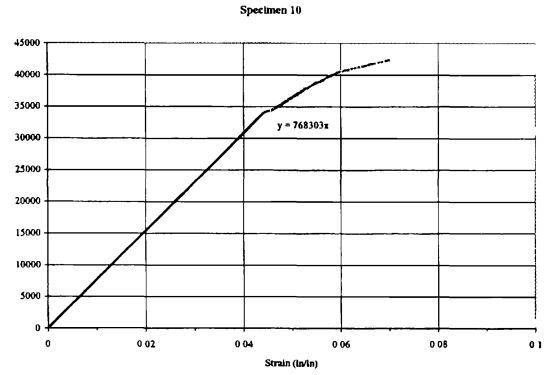
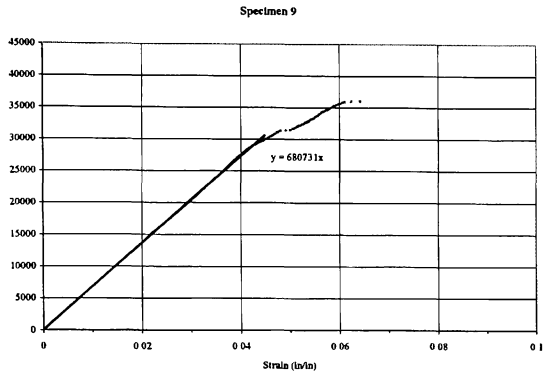
1. ASTM D3410-00, "Standard Test Method for Compressive Properties of Polymer Matrix Composite Materials with Unsupported Gage Section by Shear Loading," American Society for Testing and Materials, Conshohocken, PA, 2000.
2. Torque Limits for Standard, Threaded Fasteners, MSFC-STD-486B, November 1992.
3. Hart-Smith, L. J., "Bolted Joints in Graphite-Epoxy Composites," NASA CR-144899, June 1976.
4. Horn, W. J., and Schmitt, R. R., "Influence of Clamp-up Force on the Strength of Bolted Composite Joints," *AIAA Journal*, Vol. 32, No. 3, 1993, pp. 665-667.
5. Sun, H.-T., Chang, F.-K., and Qing, X., "The Response of Composite Joints with Bolt-Clamping Loads, Part I: Model Development," *Journal of Composite Materials*, Vol. 36, No. 1, 2002, pp. 47-67.
6. Sun, H.-T., Chang, F.-K., and Qing, X., "The Response of Composite Joints with Bolt-Clamping Loads, Part II: Model Verification," *Journal of Composite Materials*, Vol. 36, No. 1, 2002, pp. 69-92.
7. Benzeggagh, M. L., Khellil, K., and Chotard, T., "Experimental Determination of Tsai Failure Tensorial Terms F_{ij} for Unidirectional Composite Materials," *Composite Science and Technology*, Vol. 55, No. 2, 1995, pp. 145-156.
8. Avva V. S., H.G. Allen, and K.N. Shivakumar, "Through-the-Thickness Tension Strength of 3-D Braided Composites," *Journal of Composite Materials*, Vol. 30, No. 1, 1996.
9. Hamada, H., Haruna, K., and Maekawa, Z.-L., "Effects of Stacking Sequences on Mechanically Fastened Joint Strength in Quasi-Isotropic Carbon-Epoxy Laminates," *Journal of Composites Technology & Research*, Vol. 17, No. 3, July 1995, pp. 249-259.
10. Vinson, J. R., and Sierakowski, R. L., The Behavior of Structures Composed of Composite Materials, Martinus Nijhoff Publishers, Dordrecht, The Netherlands, 1986.
11. Y. Zhao, D. Ford, and S. Richardson, "Torque Limit for Fasteners in Composites," Technical Report, NASA/MSFC ED23, August 2001.

APPENDIX A

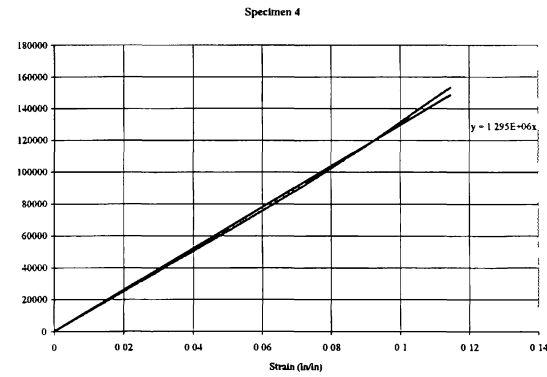
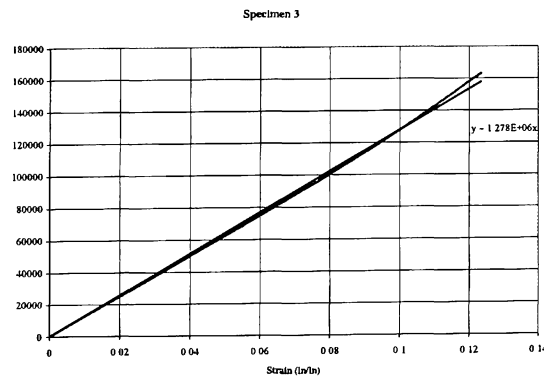
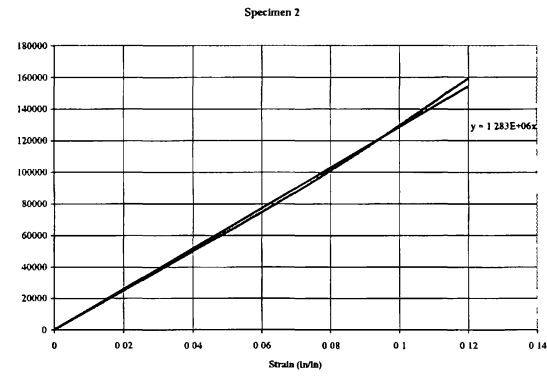
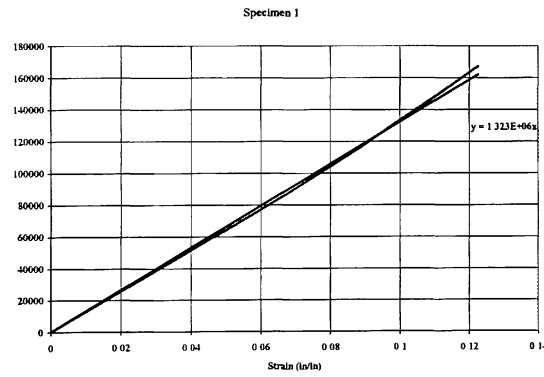
IM7 / 8552 TTTC STRESS-STRAIN DATA PLOTS

[0]₃₂

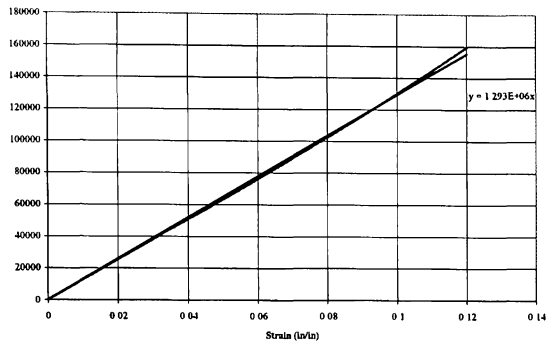




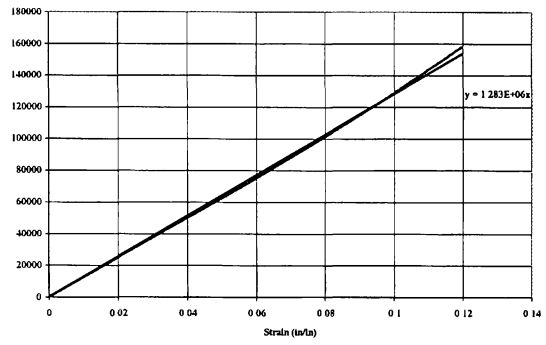
[0, 90]₆S



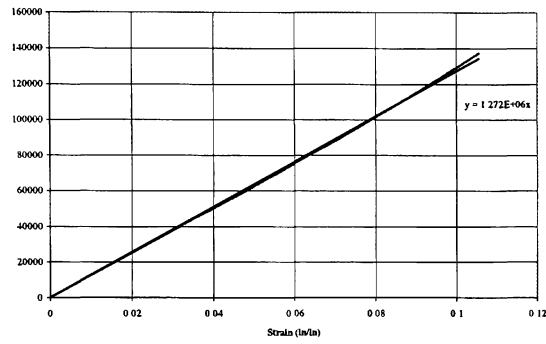
Specimen 5



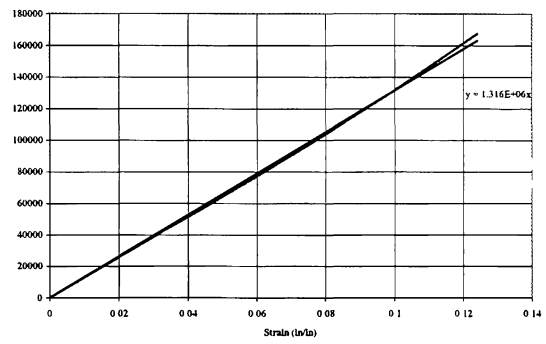
Specimen 6



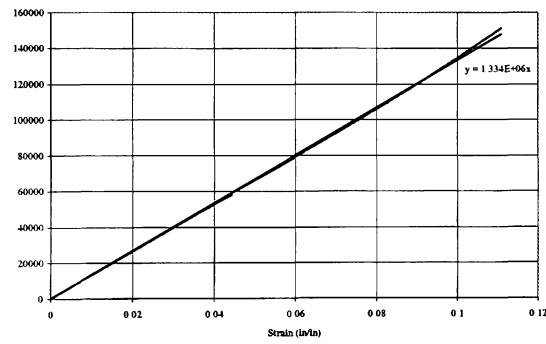
Specimen 7



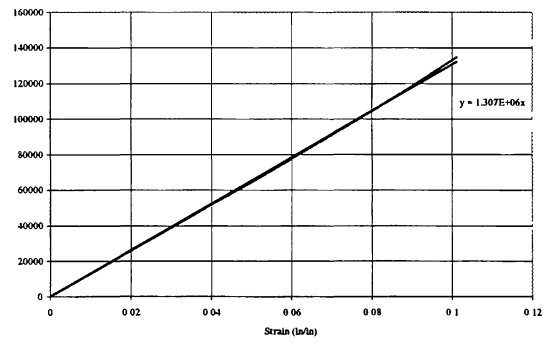
Specimen 8



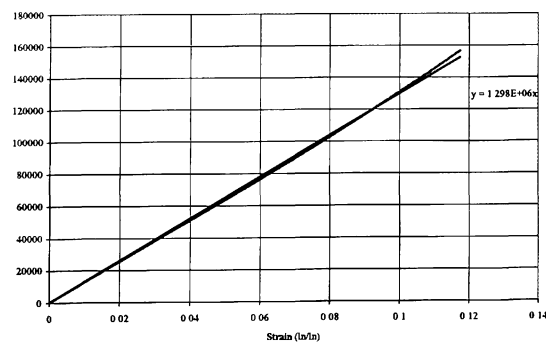
Specimen 9



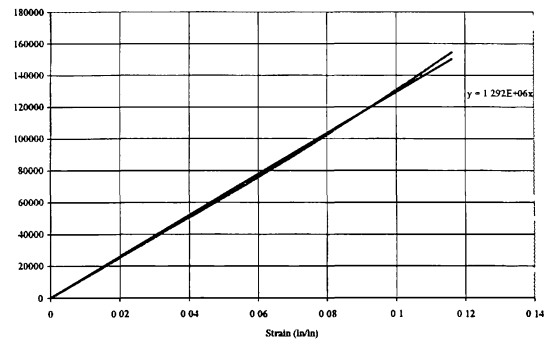
Specimen 10



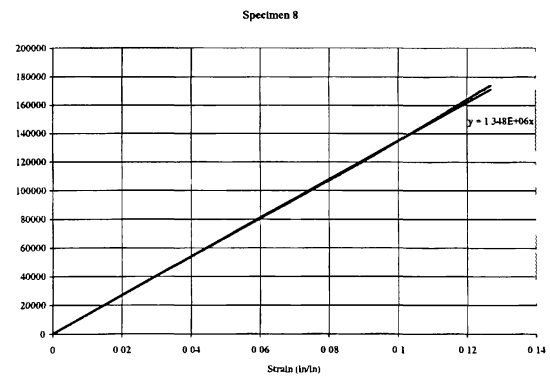
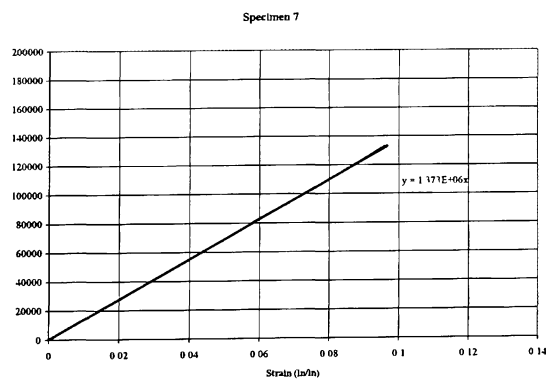
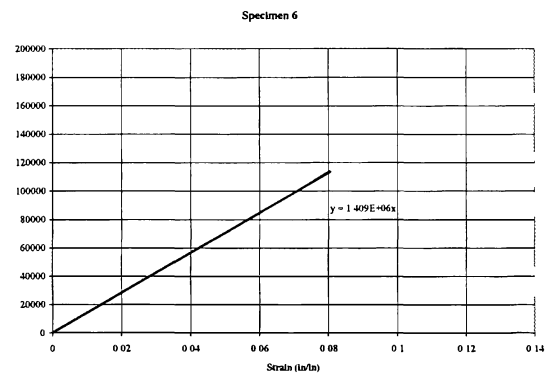
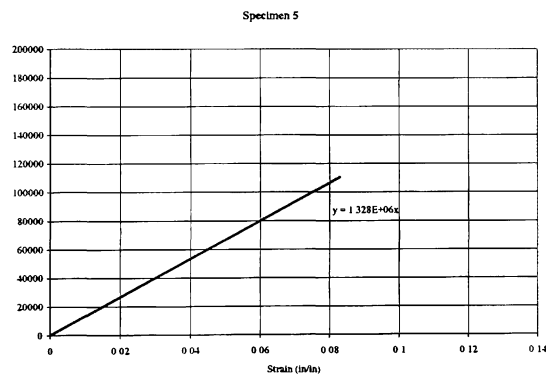
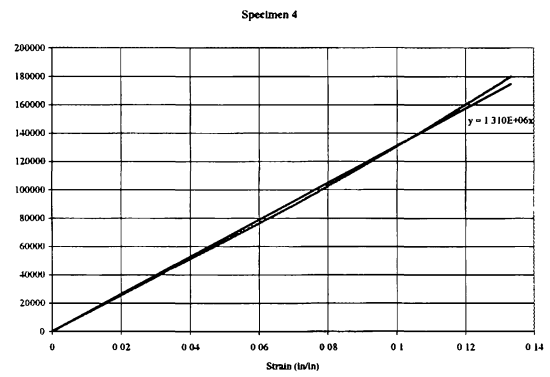
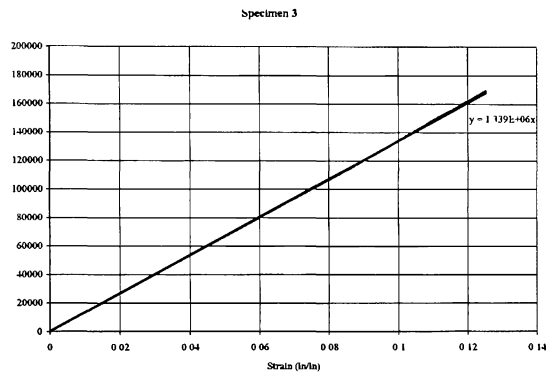
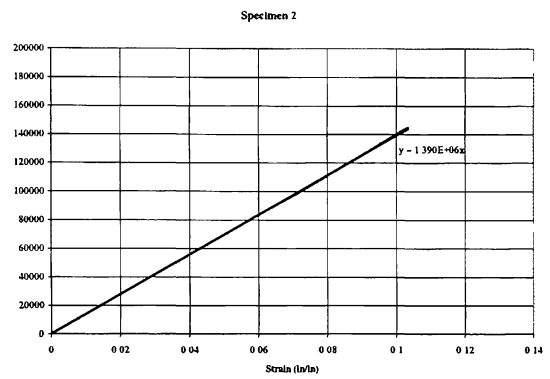
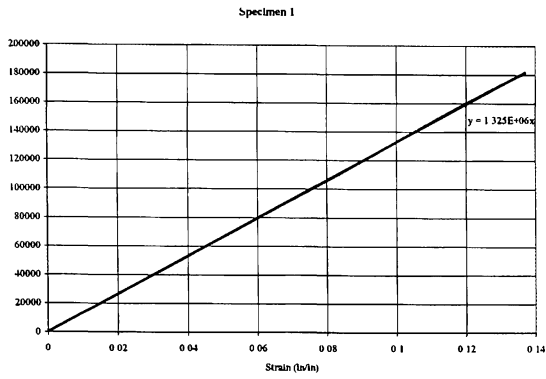
Specimen 11

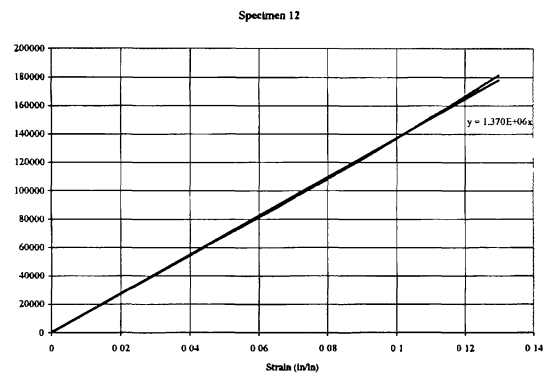
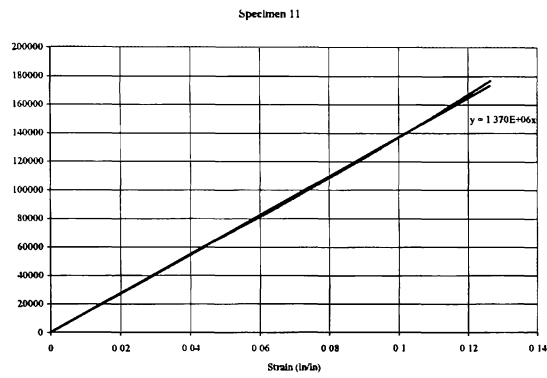
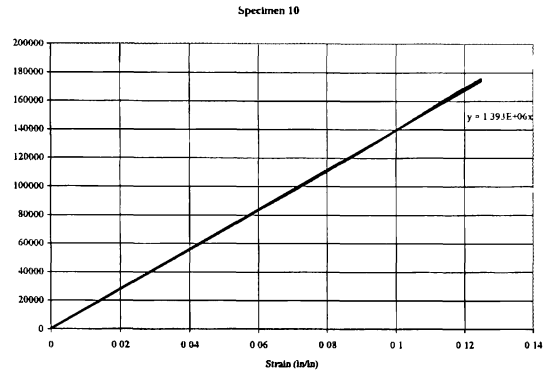
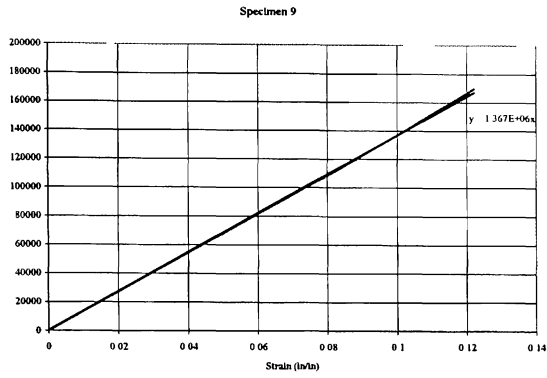


Specimen 12

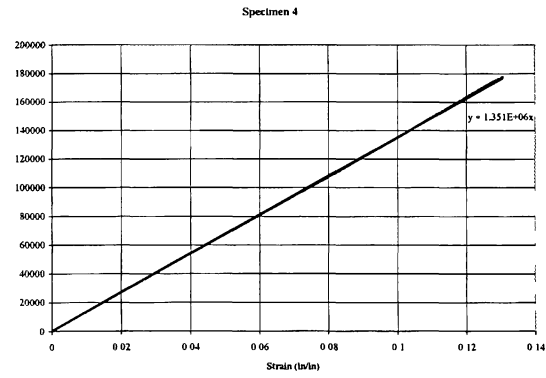
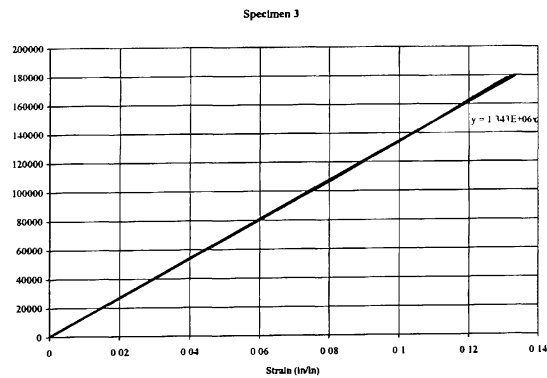
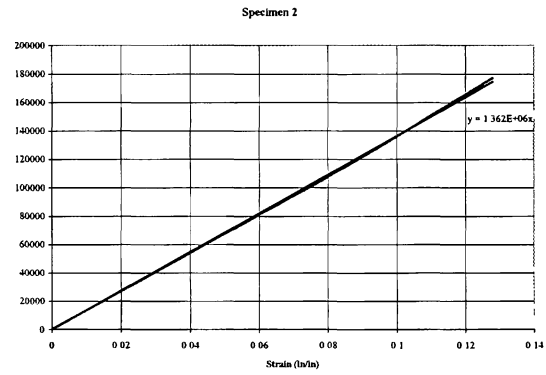
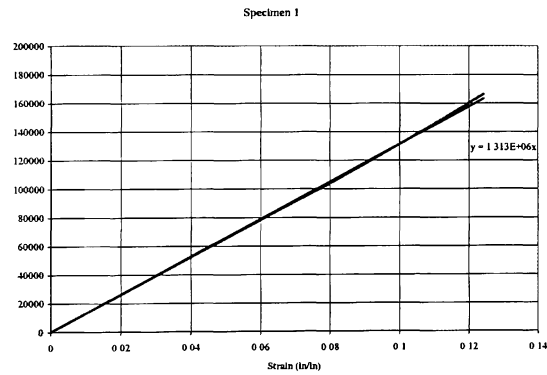


[0, ±45, 90]3S

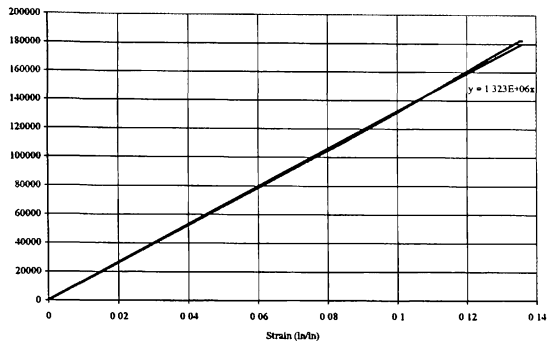




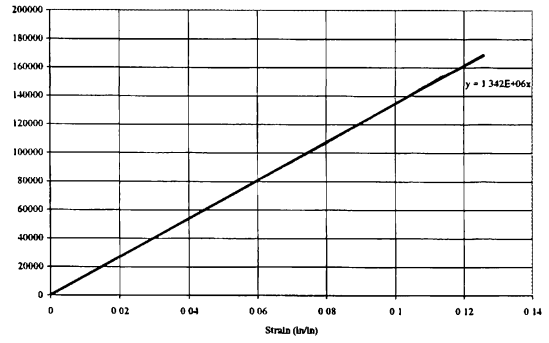
$[0, \pm 30, \pm 60, 90]_{2S}$



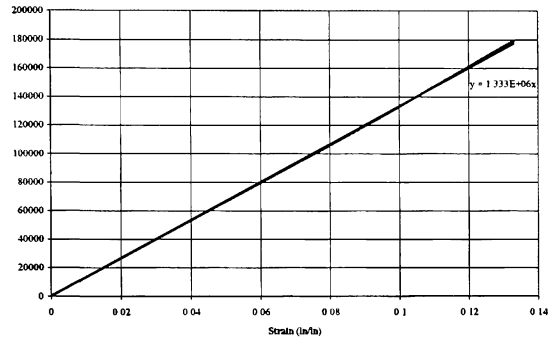
Specimen 5



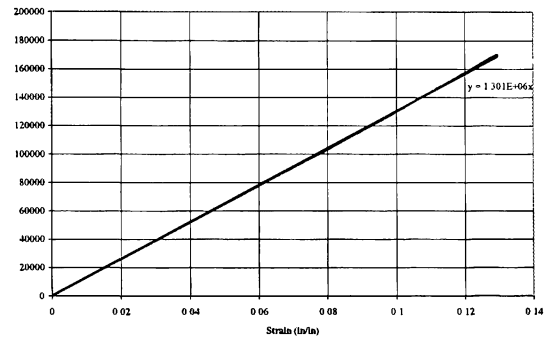
Specimen 6



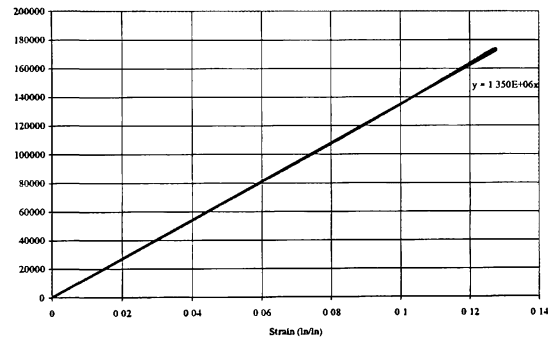
Specimen 7



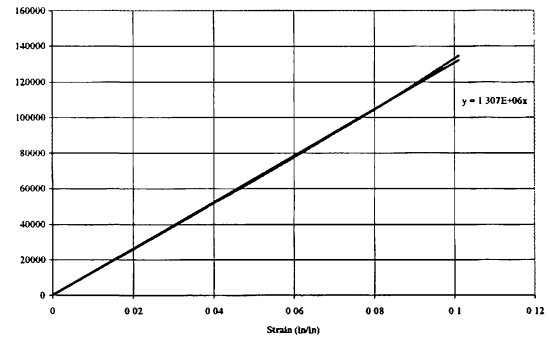
Specimen 8



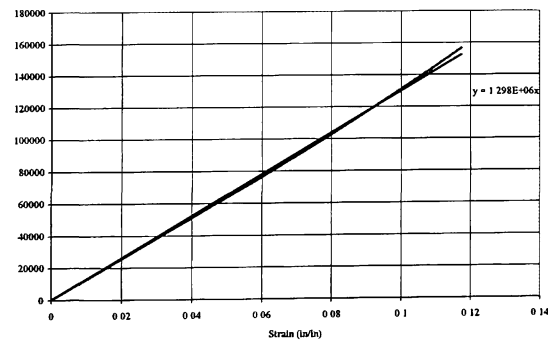
Specimen 9



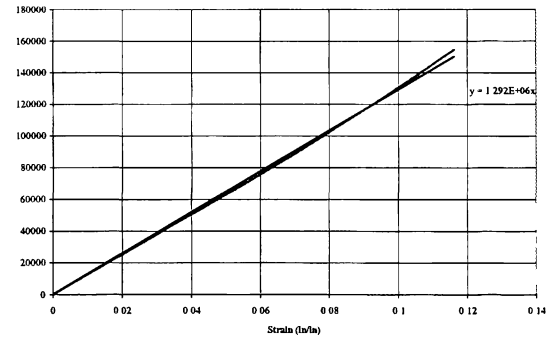
Specimen 10



Specimen 11

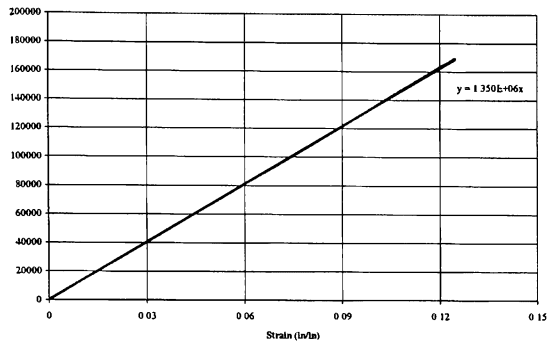


Specimen 12

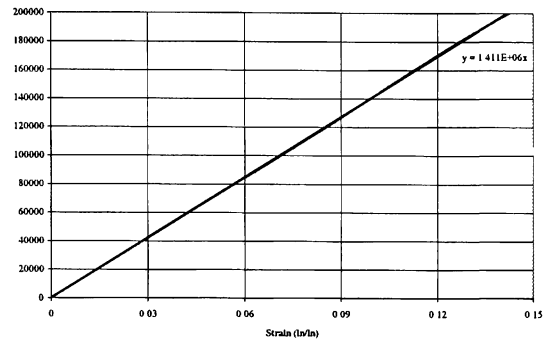


Thiokol [0, ±45, 90]3S

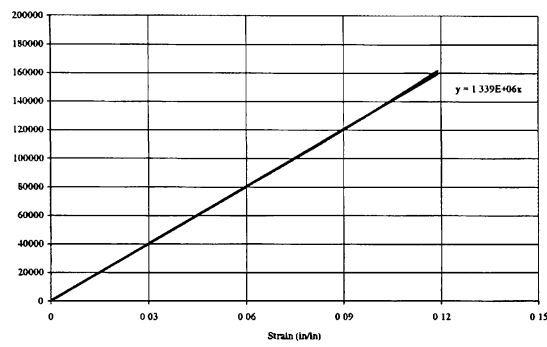
Specimen 1



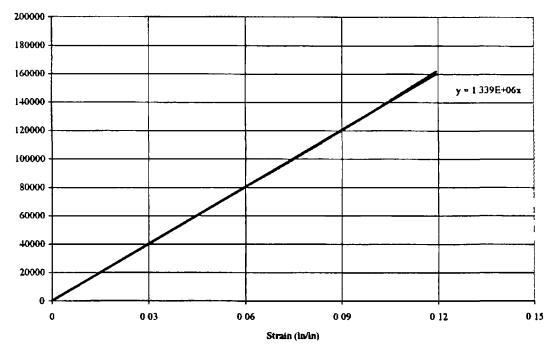
Specimen 2



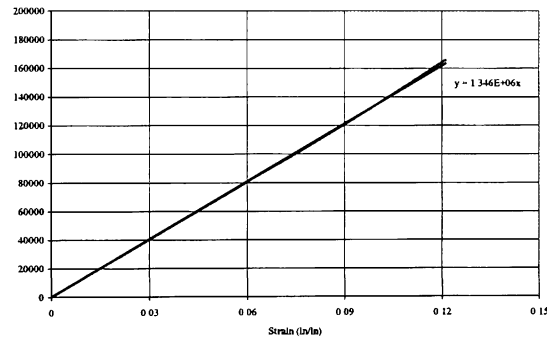
Specimen 3



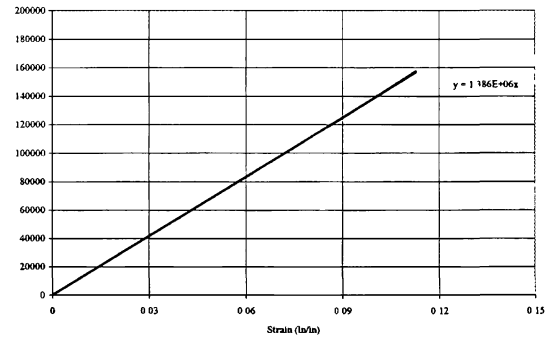
Specimen 4



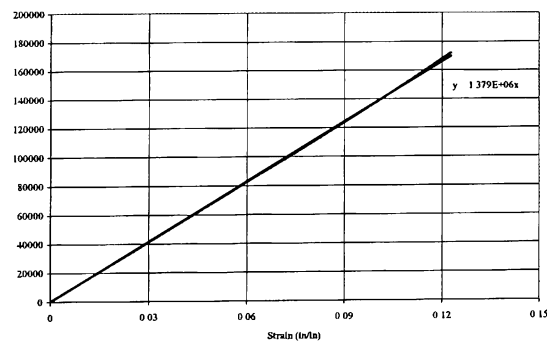
Specimen 5



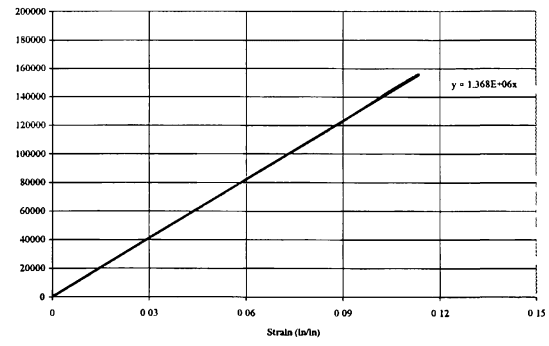
Specimen 6

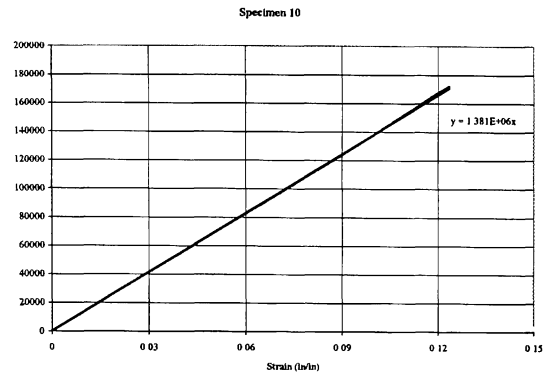
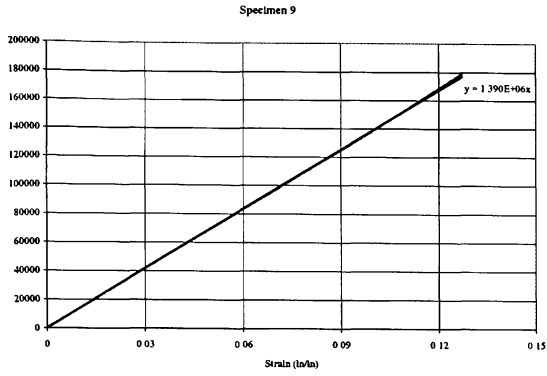


Specimen 7

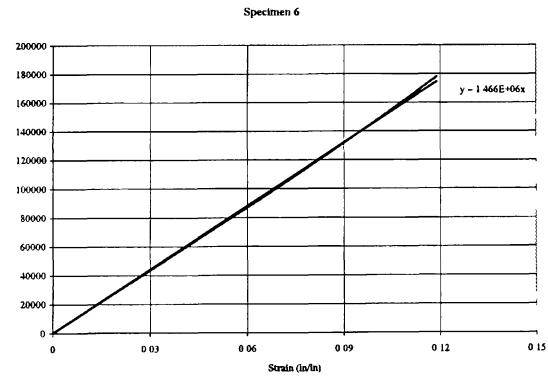
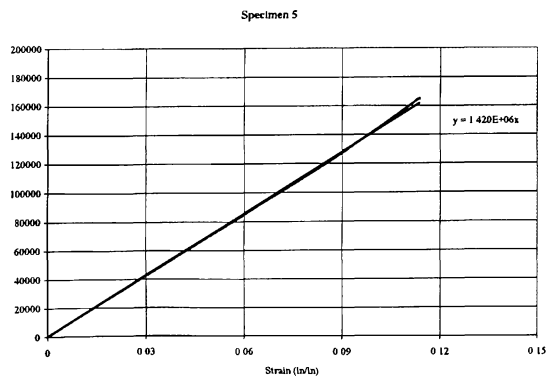
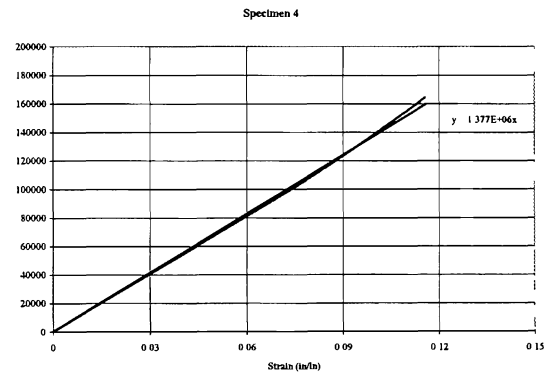
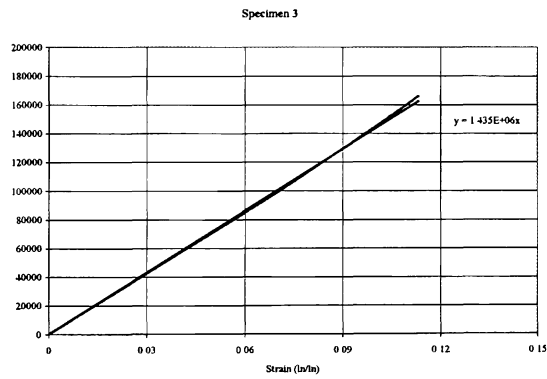
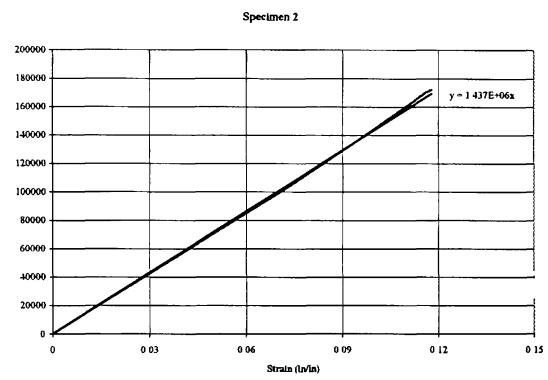
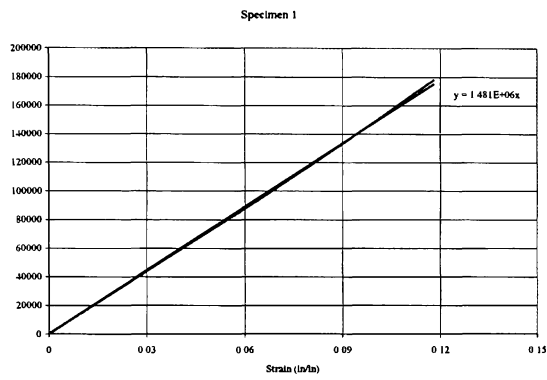


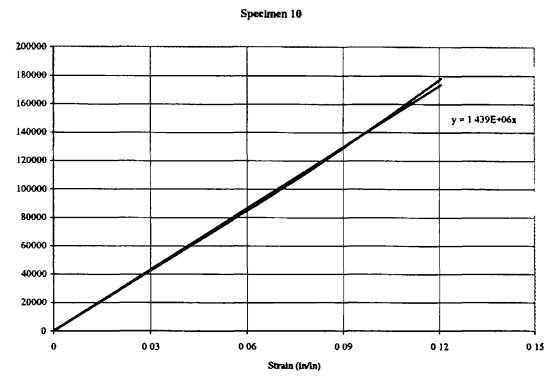
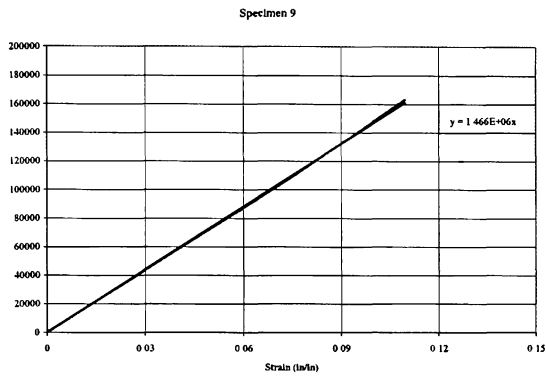
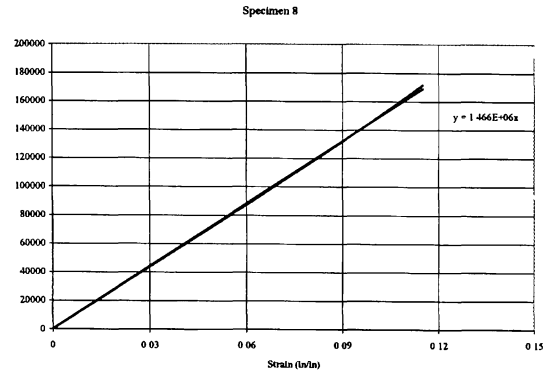
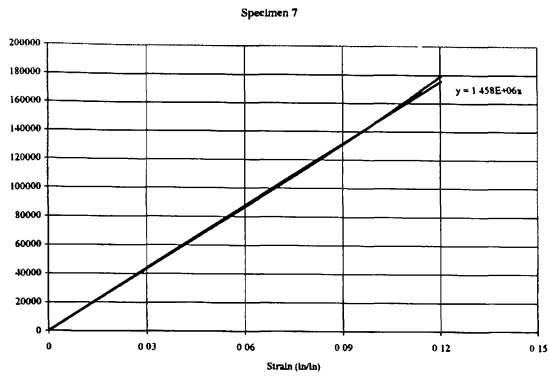
Specimen 8



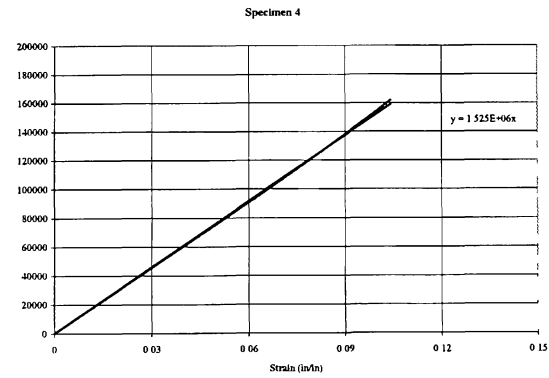
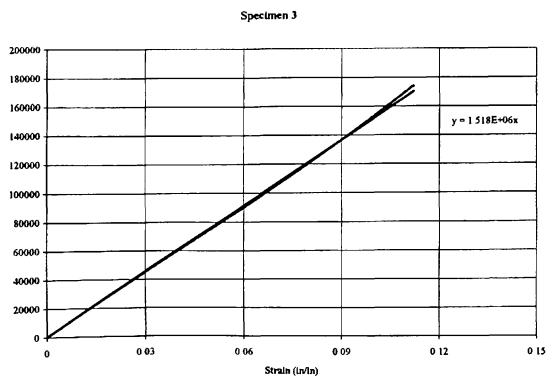
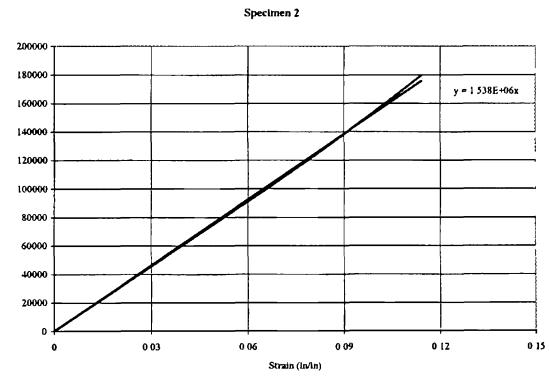
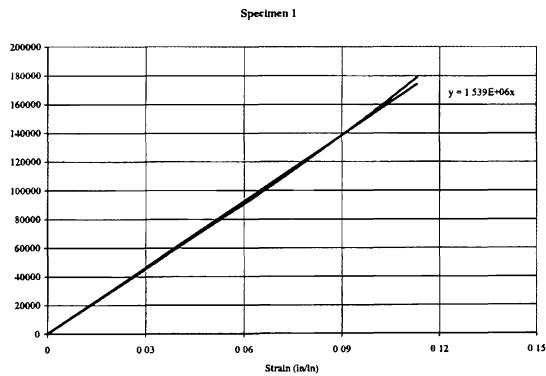


Thiokol [0, ±45, 90]_{4S}

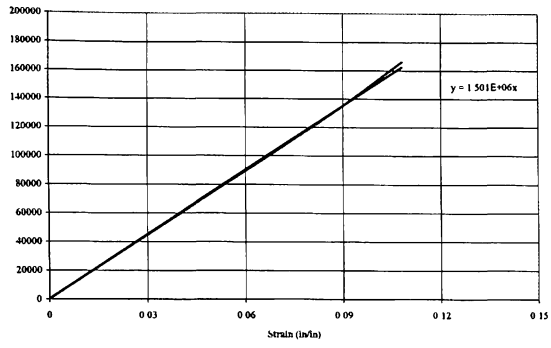




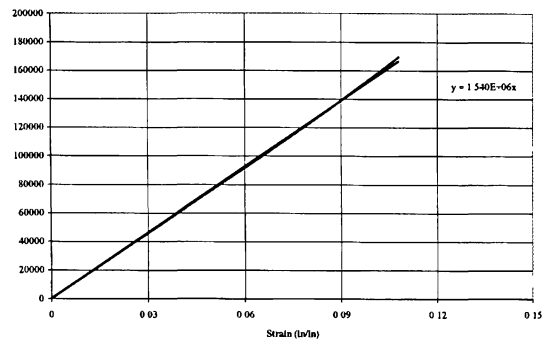
Thiokol [0, ±45, 90]_{SS}



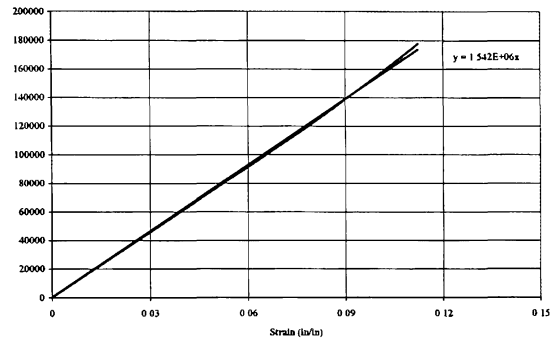
Specimen 5



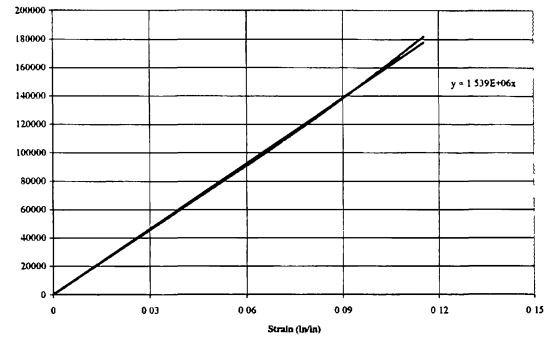
Specimen 6



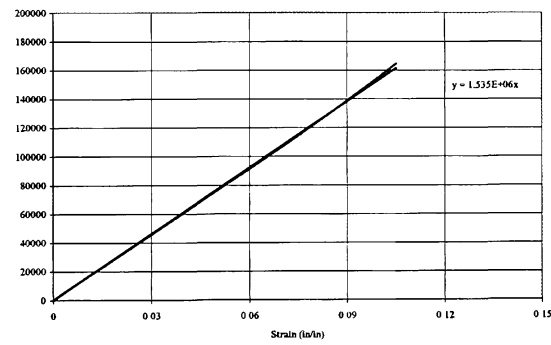
Specimen 7



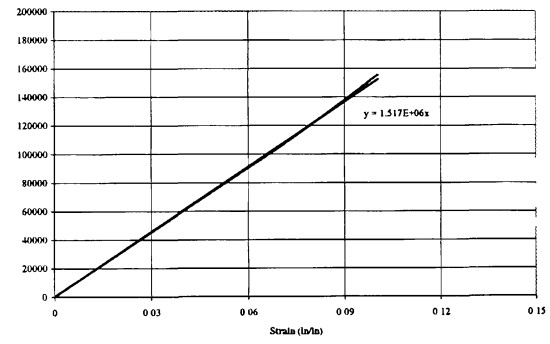
Specimen 8



Specimen 9



Specimen 10

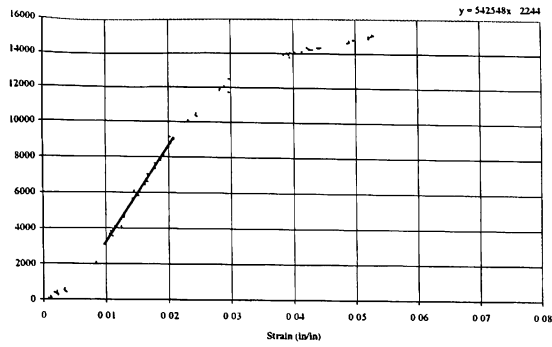


APPENDIX B

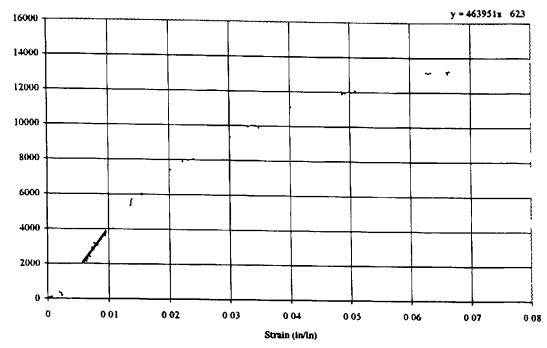
AS4 / 3501-5A TTTC STRESS-STRAIN DATA PLOTS

[0]₃₂

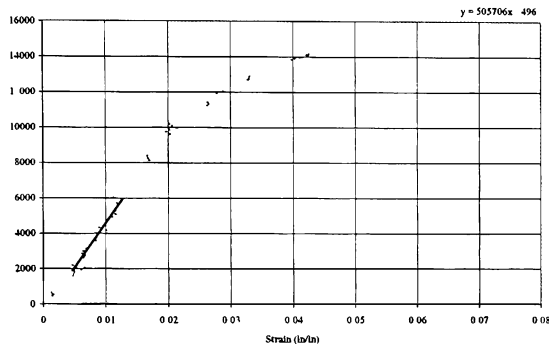
Specimen 1



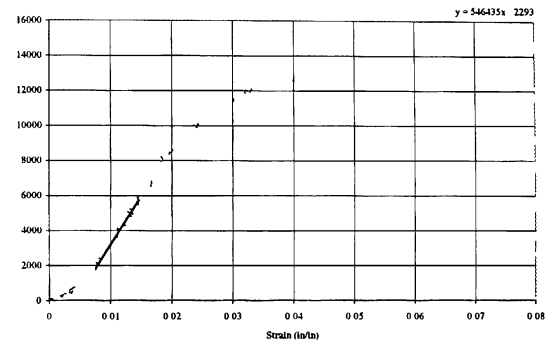
Specimen 2



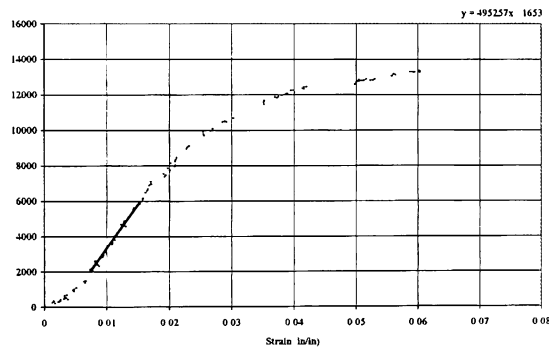
Specimen 3



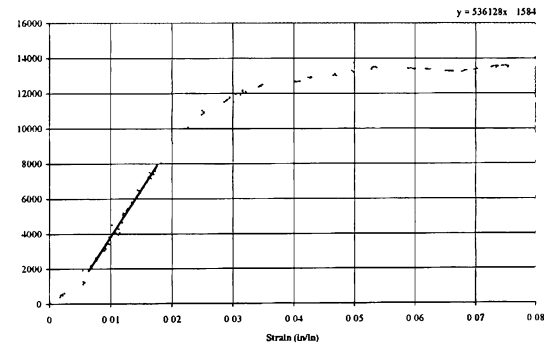
Specimen 4



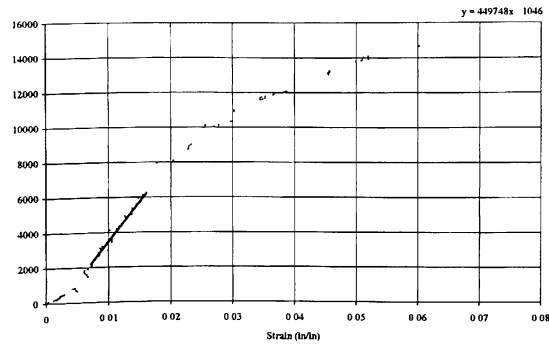
Specimen 5



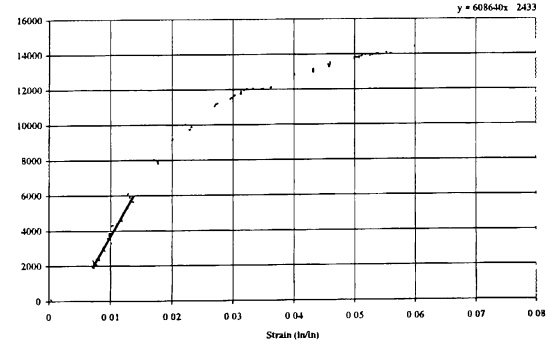
Specimen 6

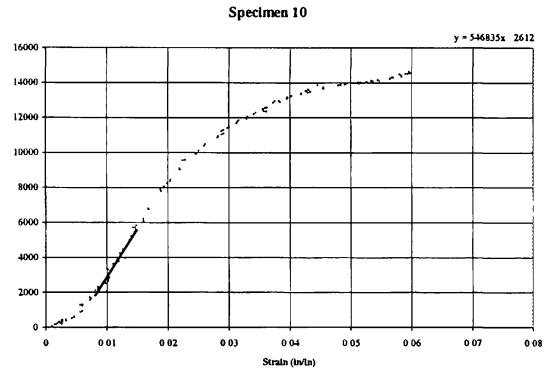
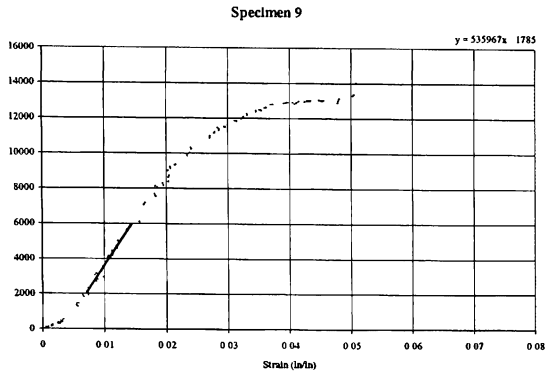


Specimen 7

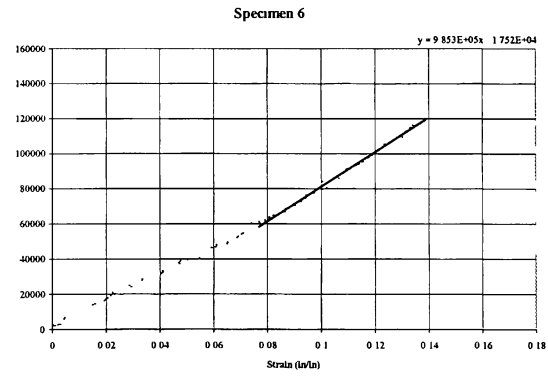
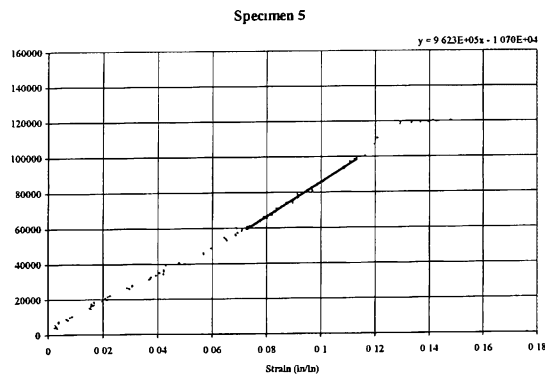
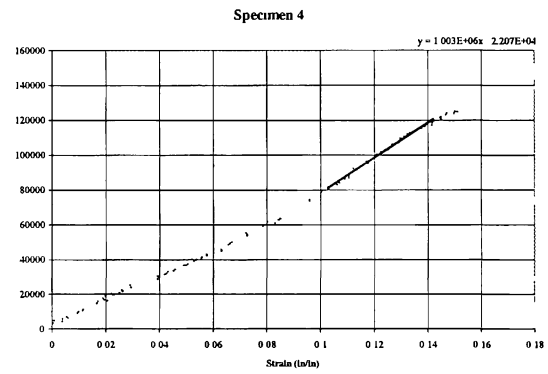
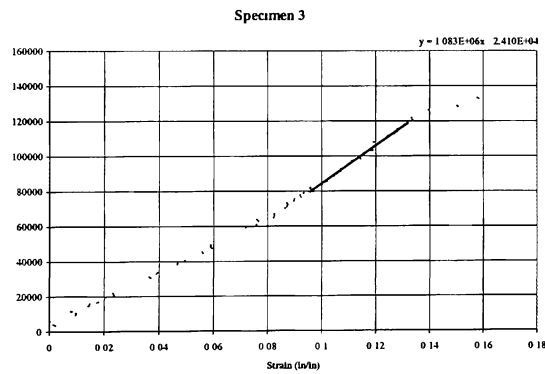
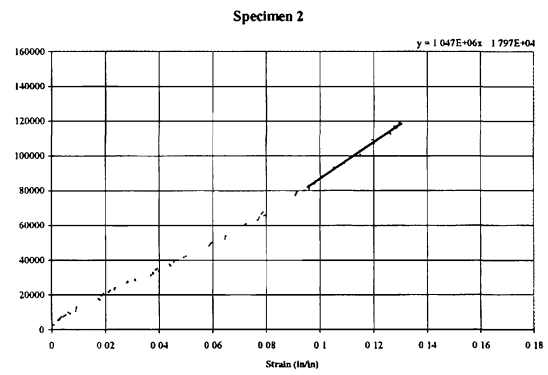
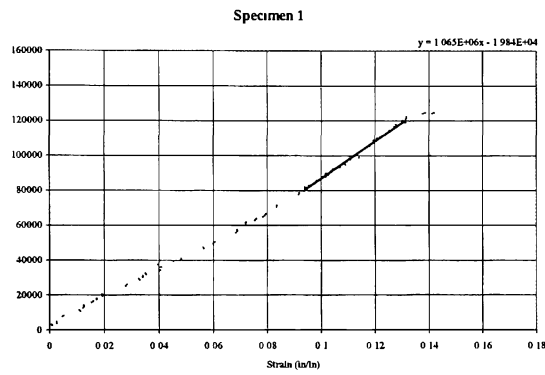


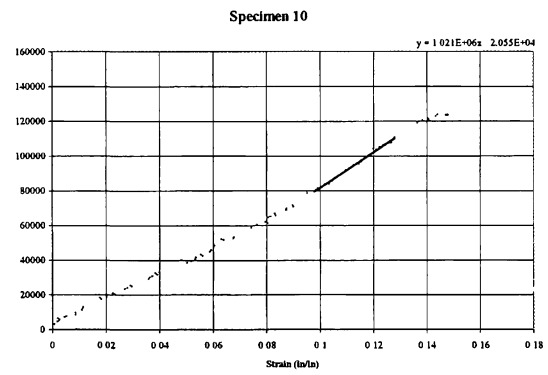
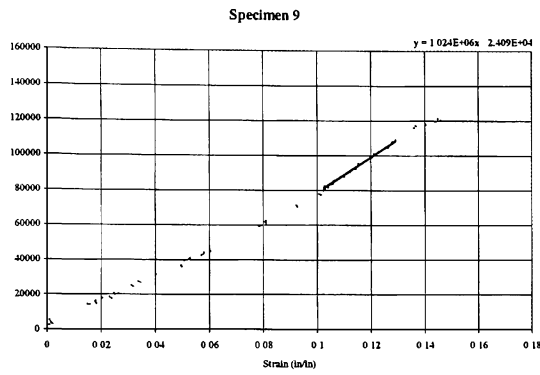
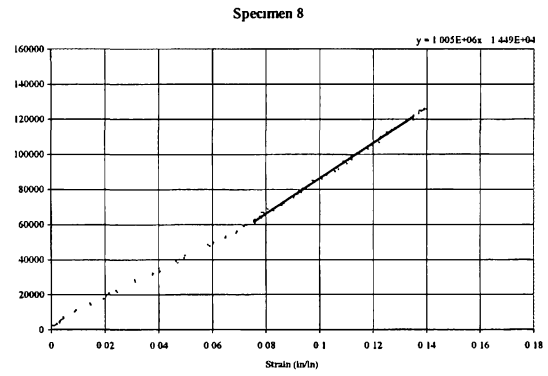
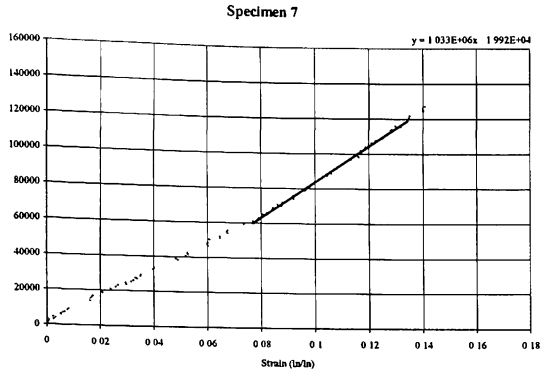
Specimen 8



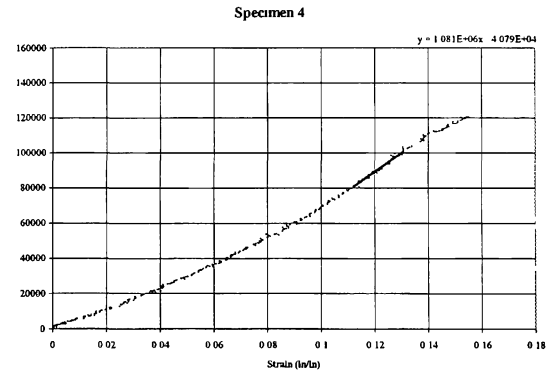
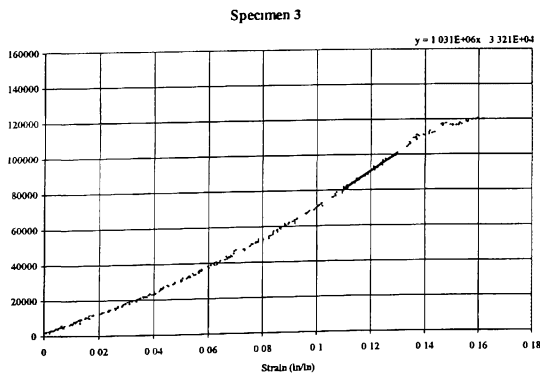
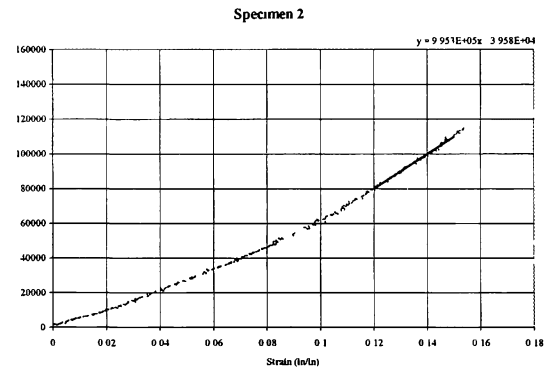
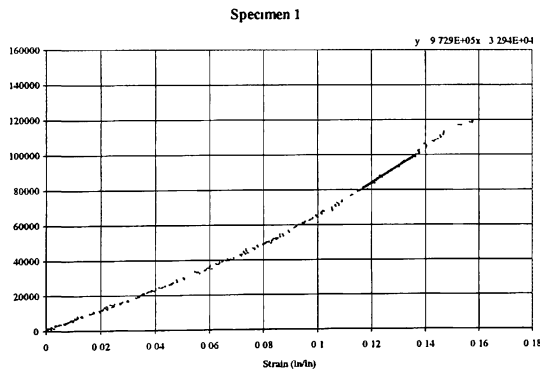


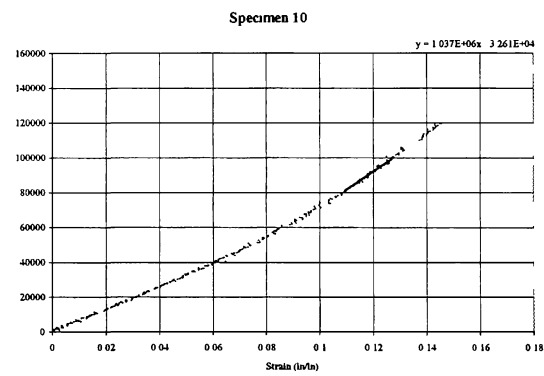
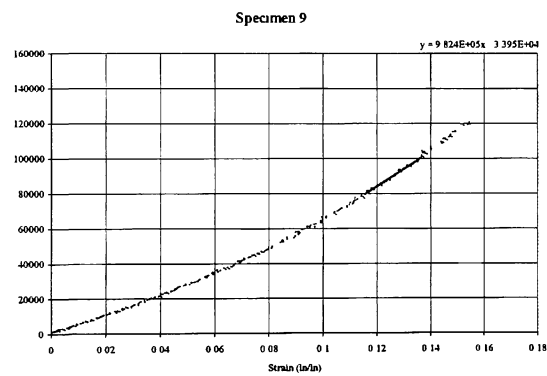
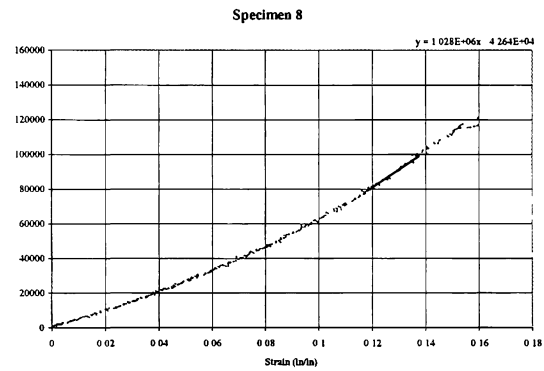
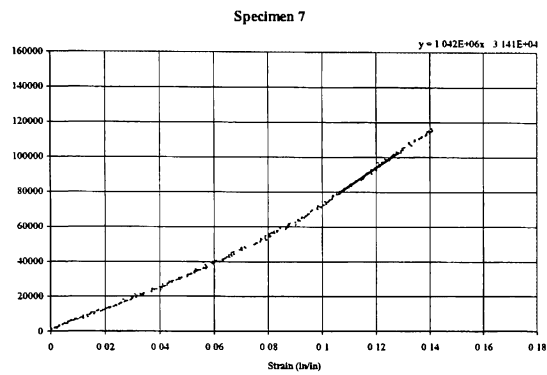
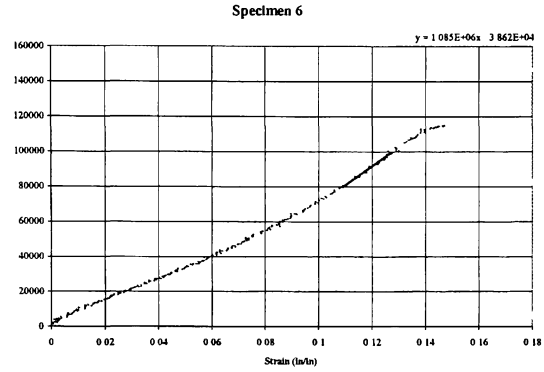
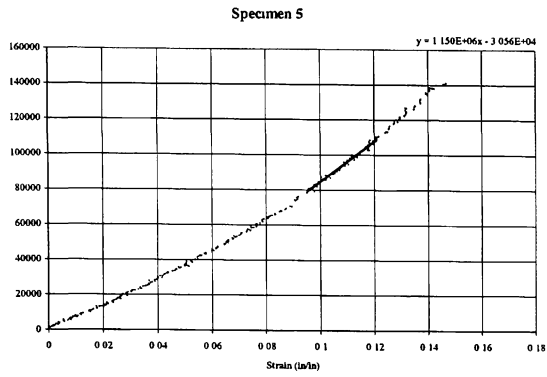
$[0, \pm 45, 90]_{2s}$



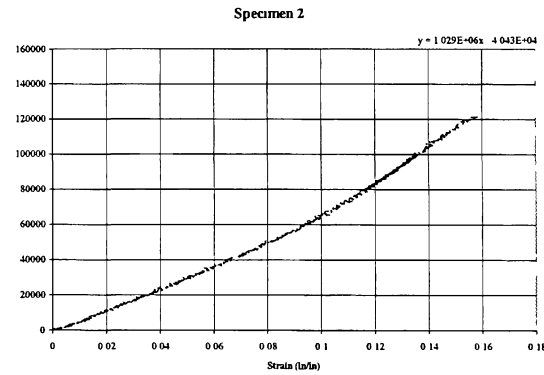
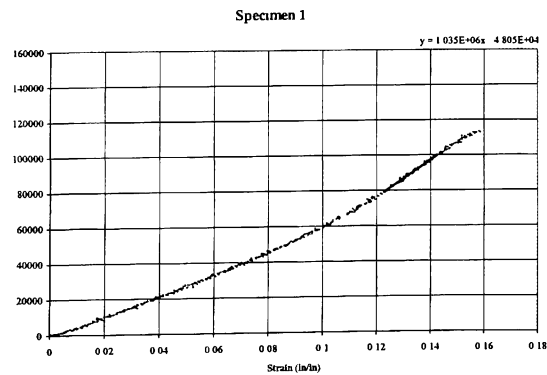


$[0, \pm 45, 90]_{3s}$

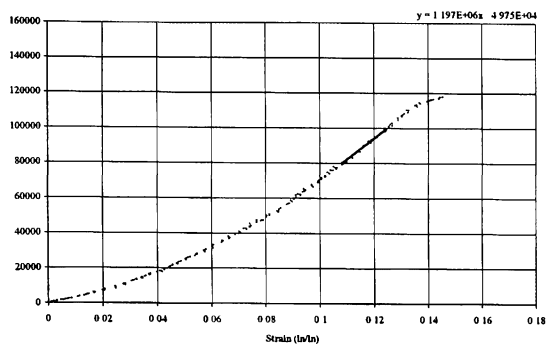




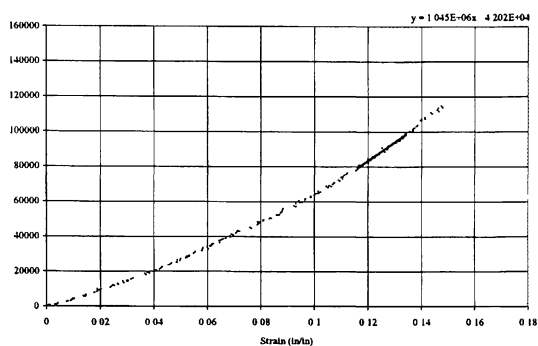
$[0, \pm 45, 90]_{4s}$



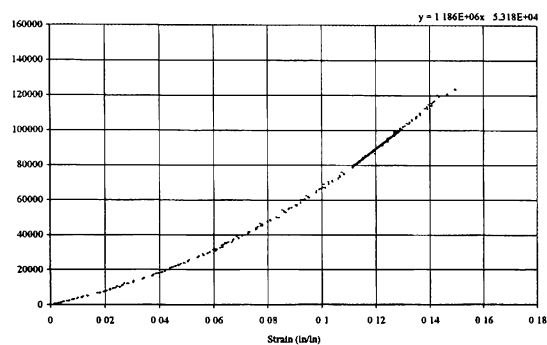
Specimen 3



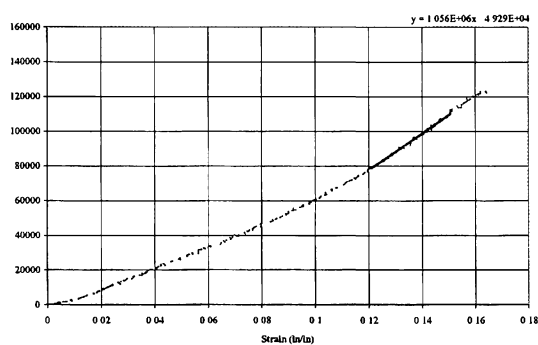
Specimen 4



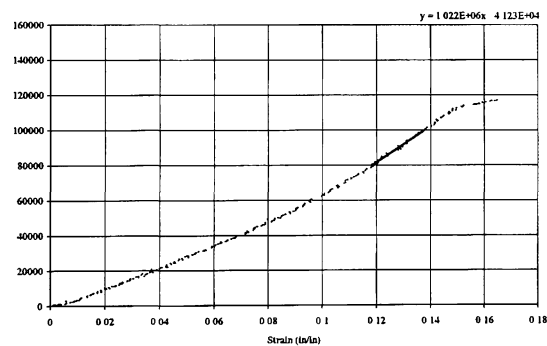
Specimen 5



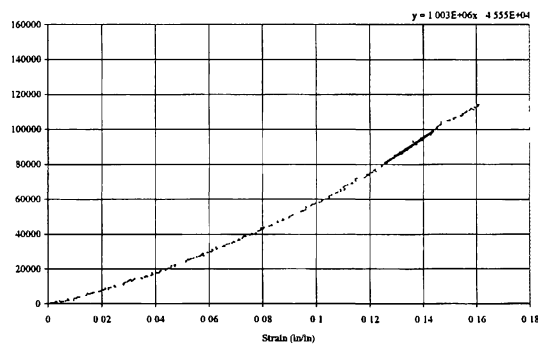
Specimen 6



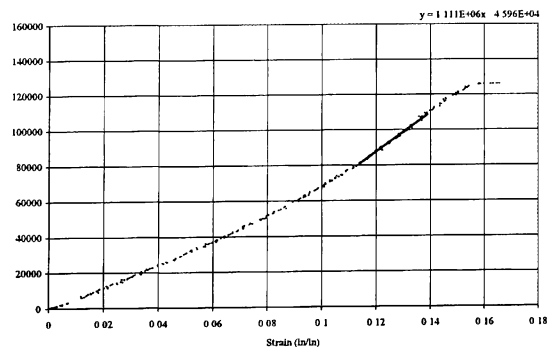
Specimen 7



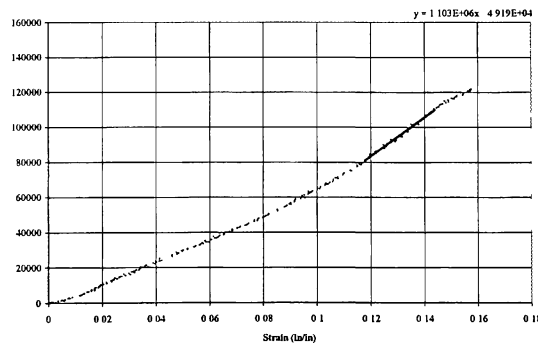
Specimen 8



Specimen 9

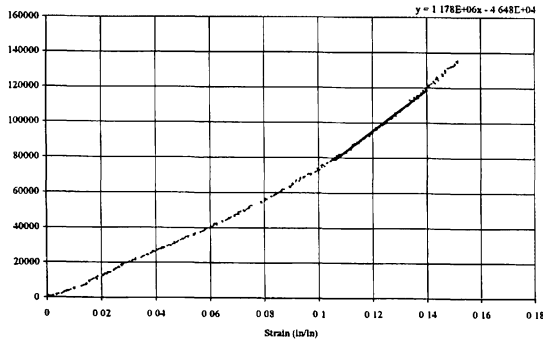


Specimen 10

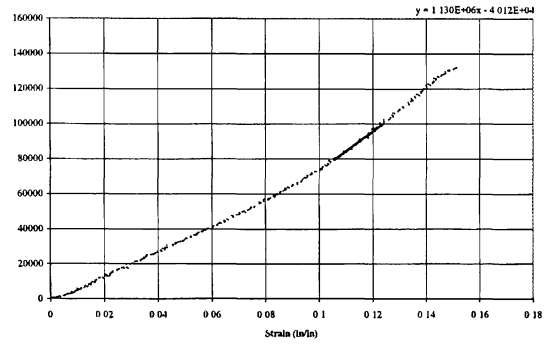


$[0, \pm 45, 90]_{5s}$

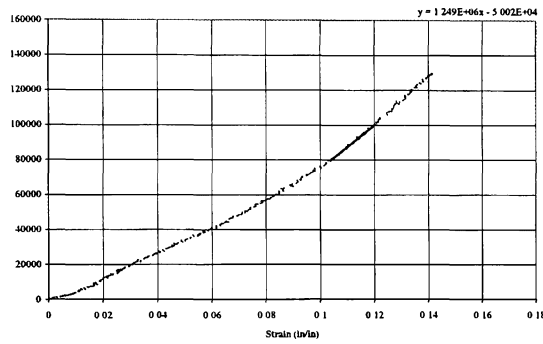
Specimen 1



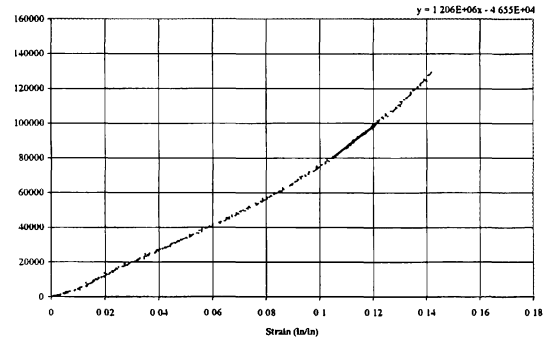
Specimen 2



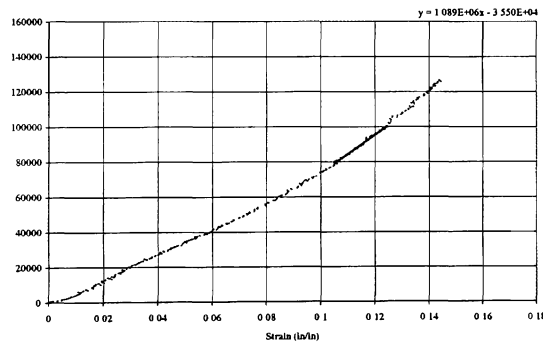
Specimen 3



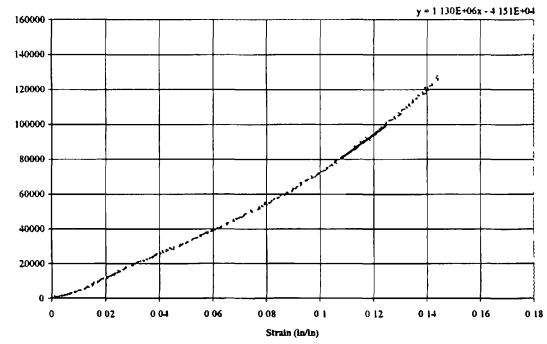
Specimen 4



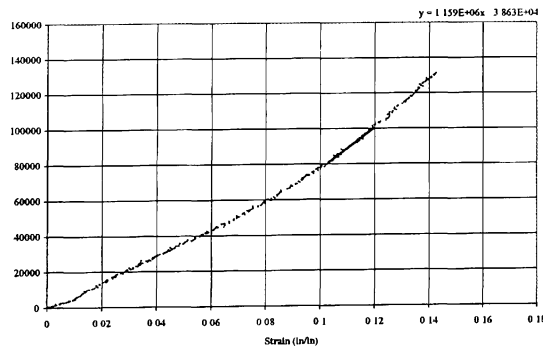
Specimen 5



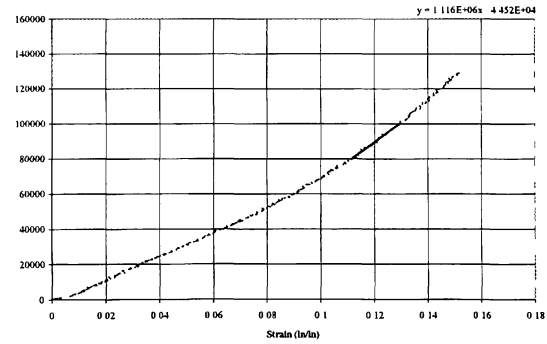
Specimen 6



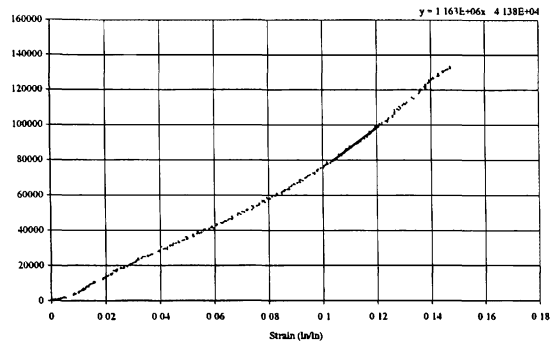
Specimen 7



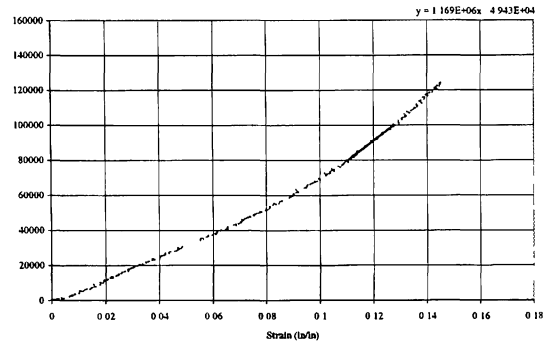
Specimen 8



Specimen 9



Specimen 10

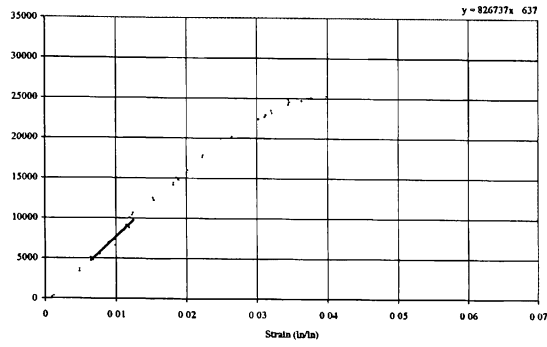


APPENDIX C

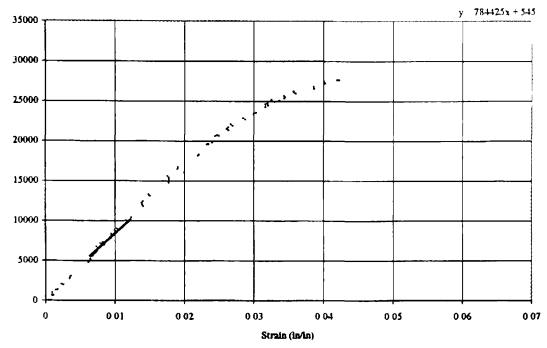
AS4 / 3501-6 TTTC STRESS-STRAIN DATA PLOTS

[0]32

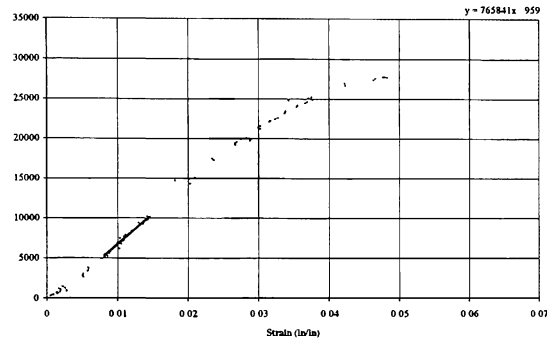
Specimen 1



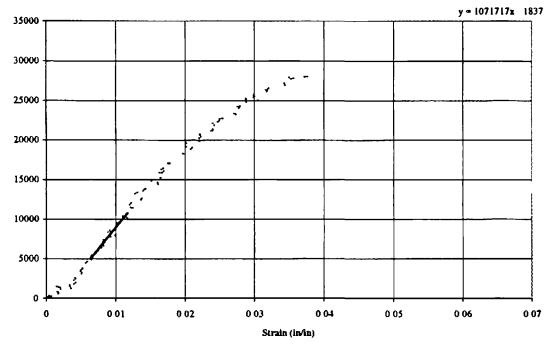
Specimen 2



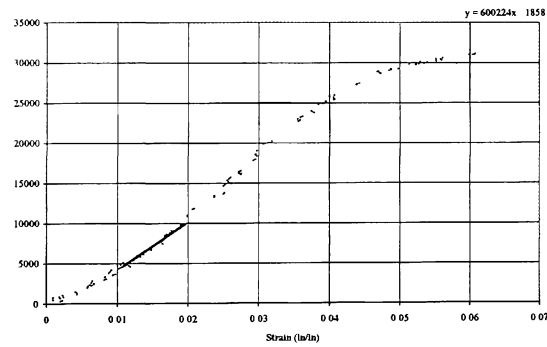
Specimen 3



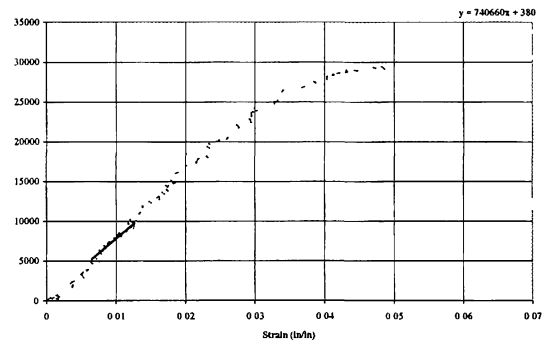
Specimen 4



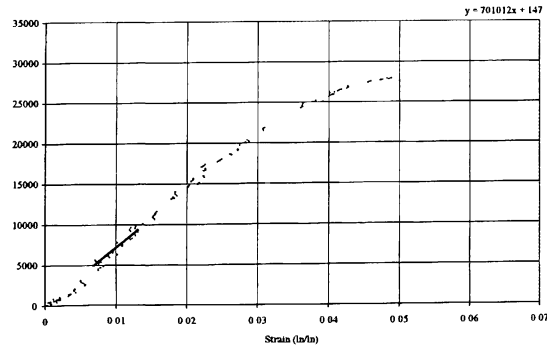
Specimen 5



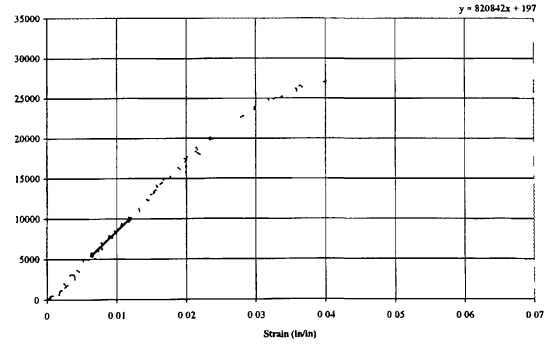
Specimen 6



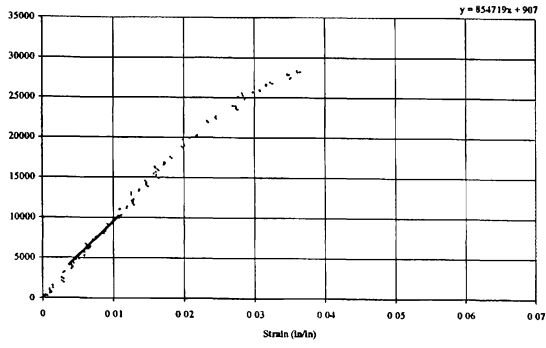
Specimen 7



Specimen 9

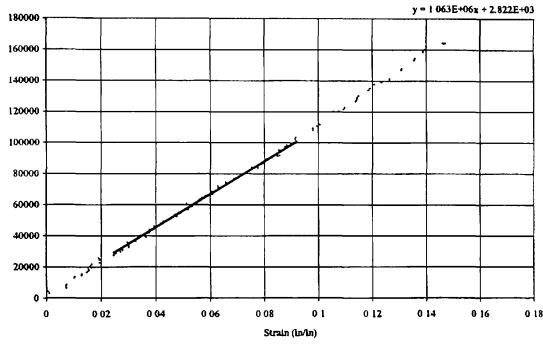


Specimen 10

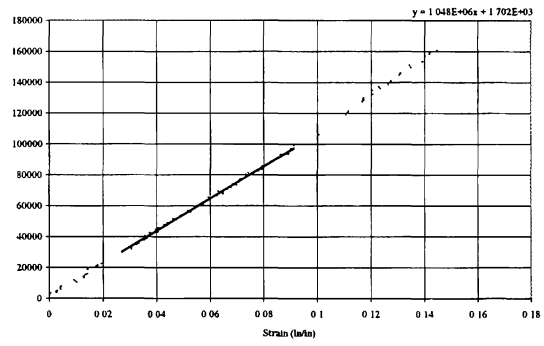


$[0, \pm 45, 90]_{2s}$

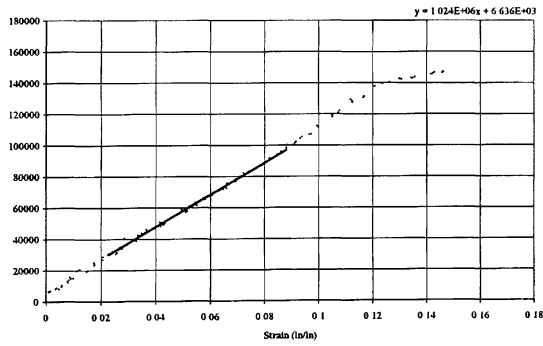
Specimen 1



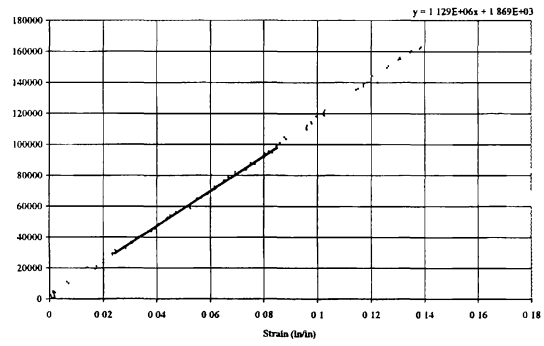
Specimen 2



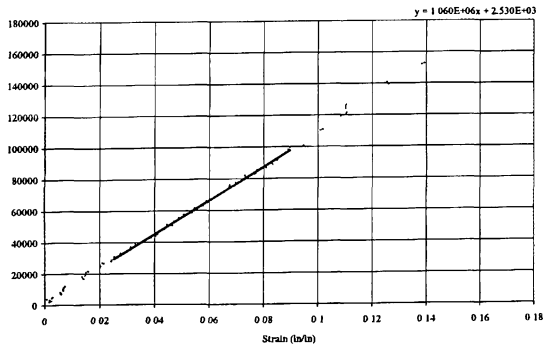
Specimen 3



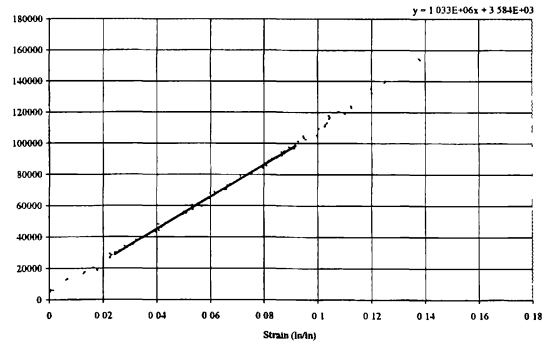
Specimen 4



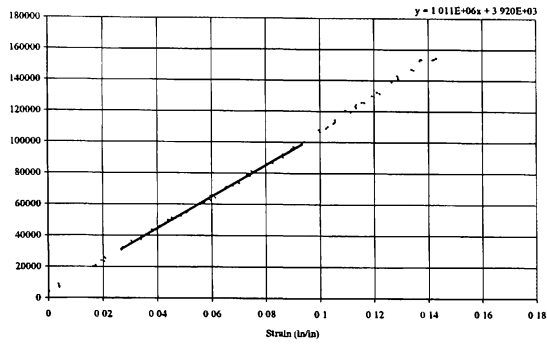
Specimen 5



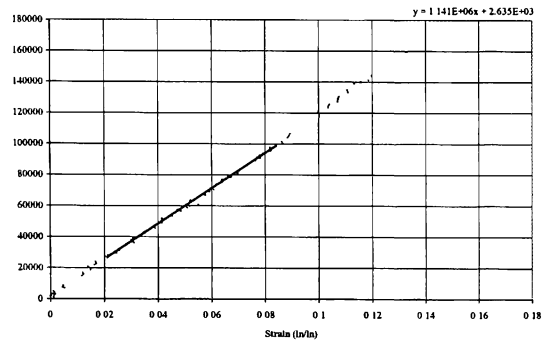
Specimen 6



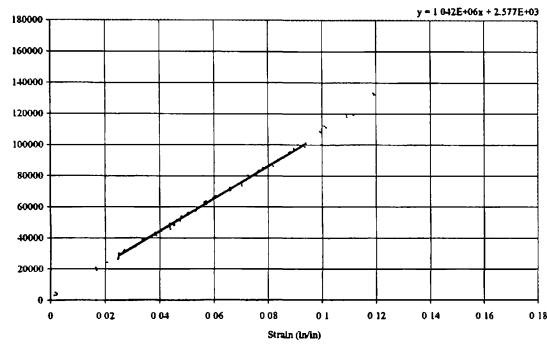
Specimen 7



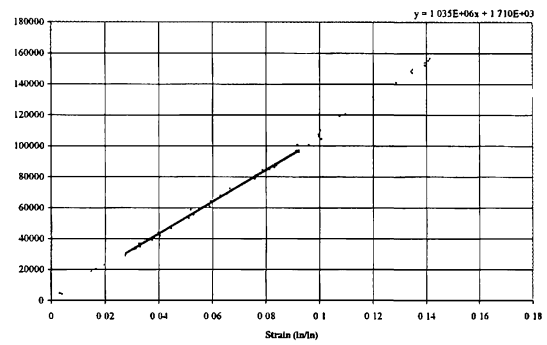
Specimen 8



Specimen 9

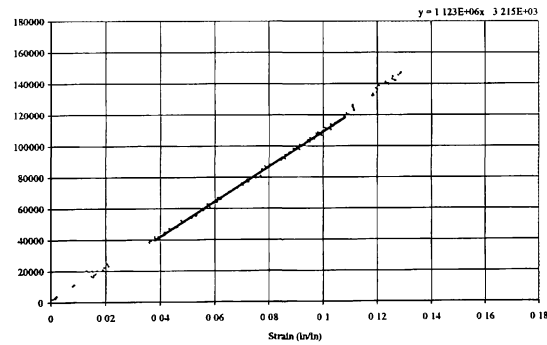


Specimen 10

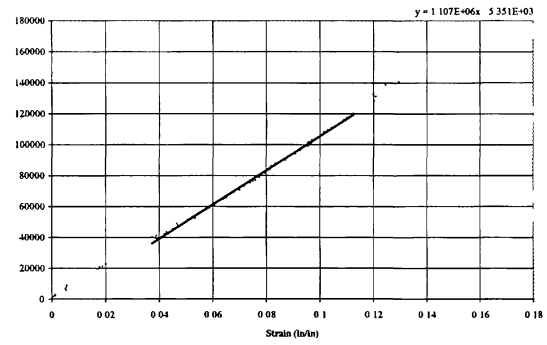


$[0, \pm 45, 90]_{3s}$

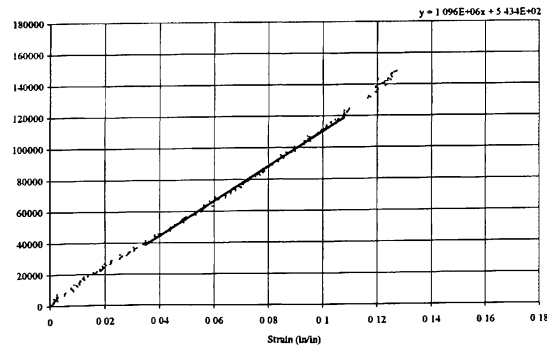
Specimen 1



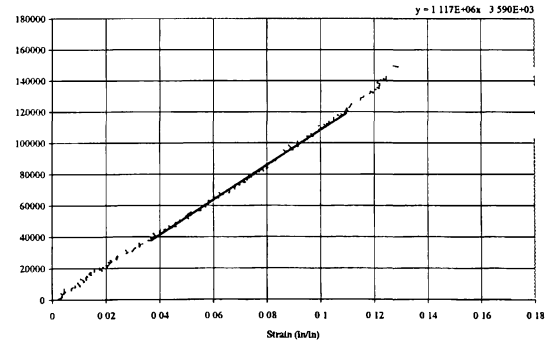
Specimen 2



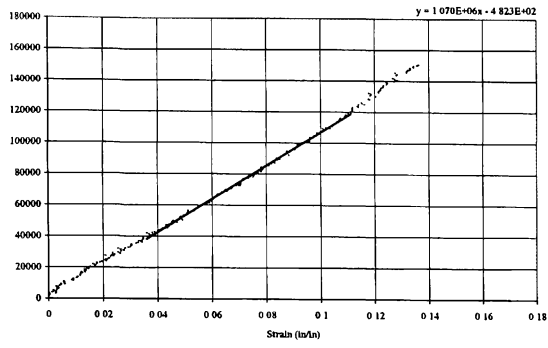
Specimen 3



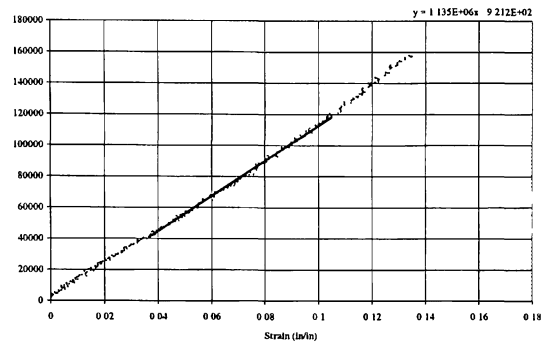
Specimen 4



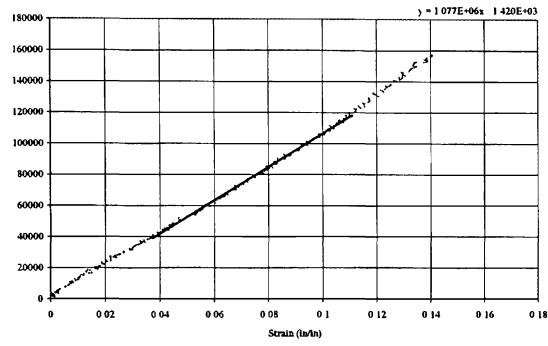
Specimen 5



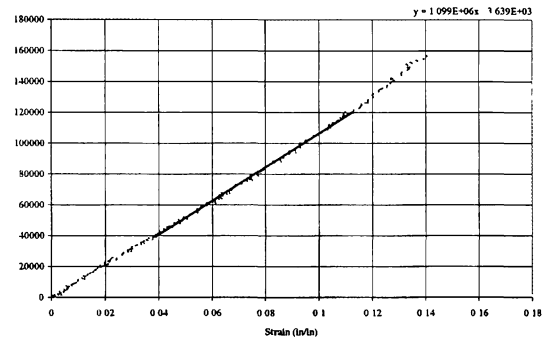
Specimen 6



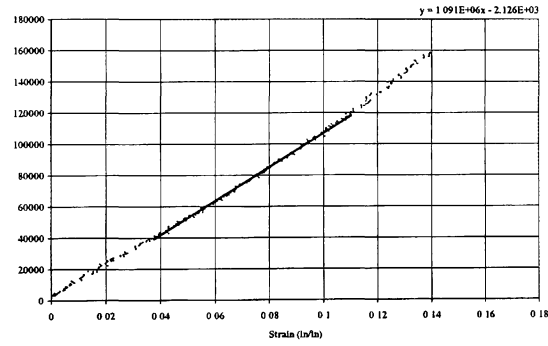
Specimen 7



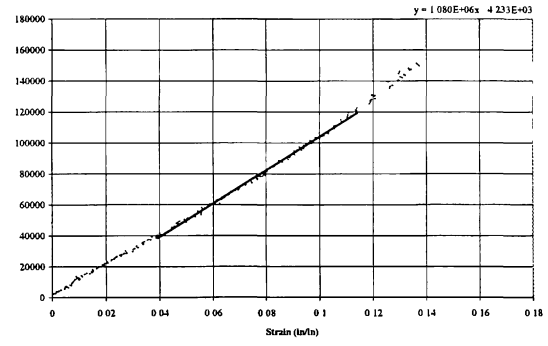
Specimen 8



Specimen 9

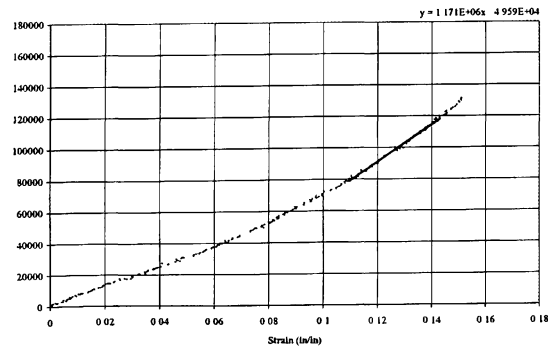


Specimen 10

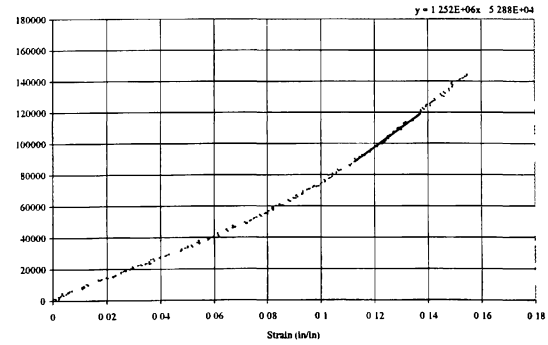


$[0, \pm 45, 90]_4s$

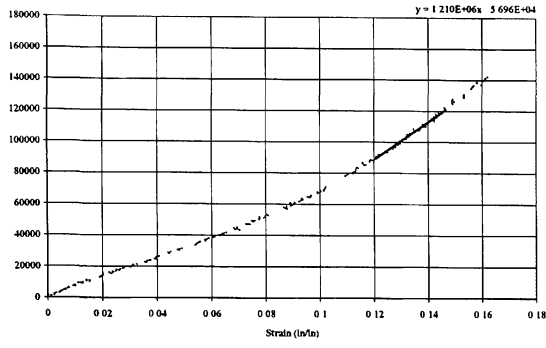
Specimen 1



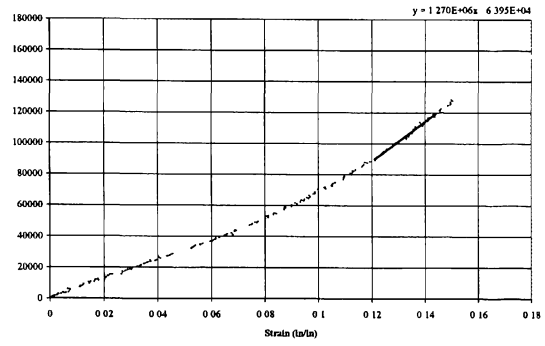
Specimen 2



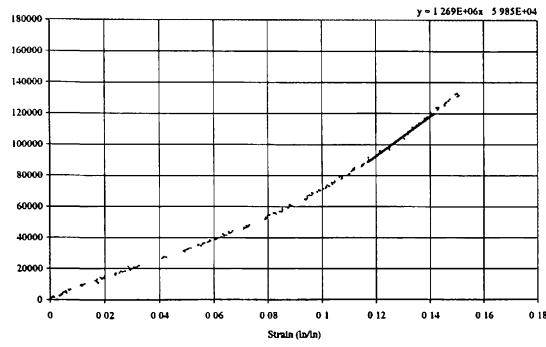
Specimen 3



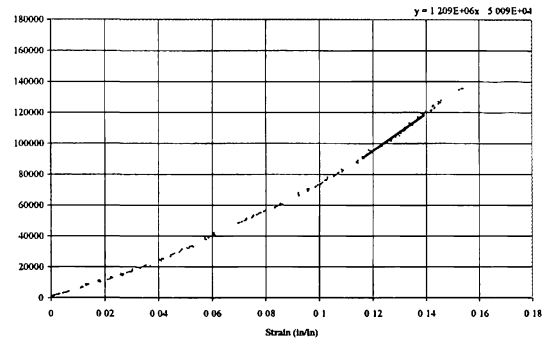
Specimen 5



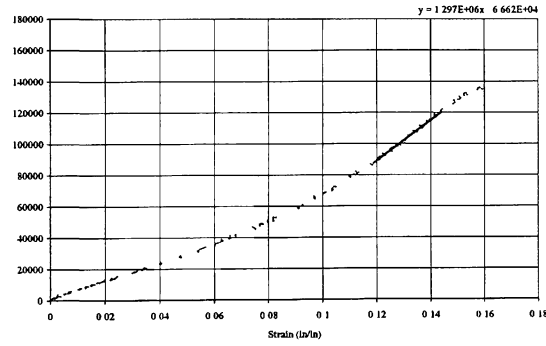
Specimen 6



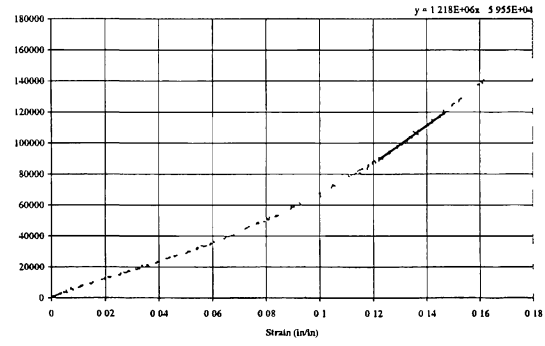
Specimen 7



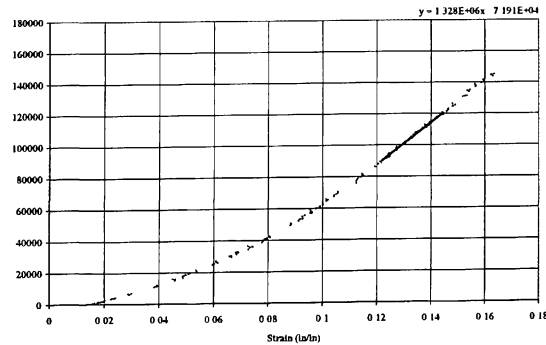
Specimen 8



Specimen 9

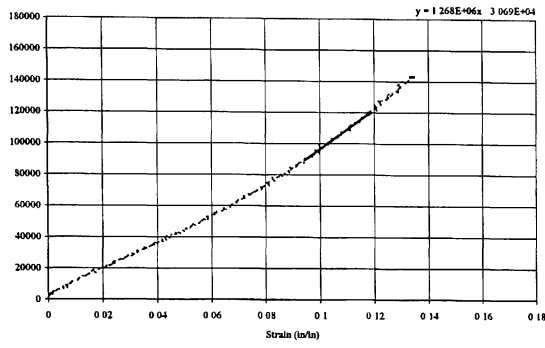


Specimen 10

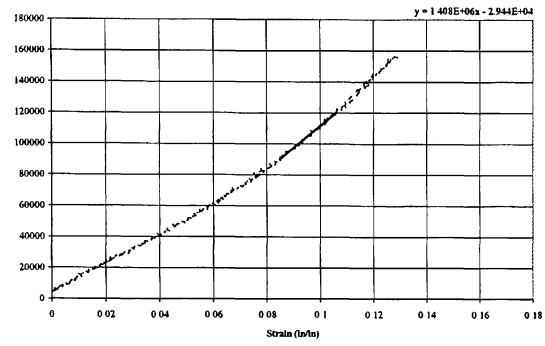


$[0, \pm 45, 90]_s$

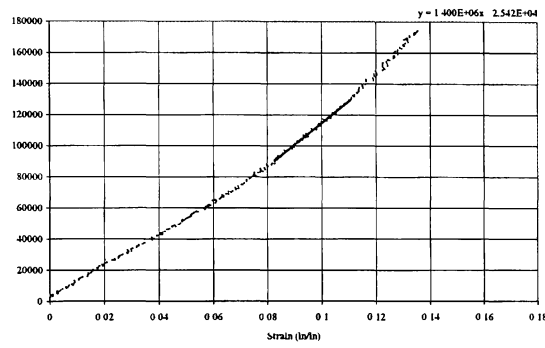
Specimen 1



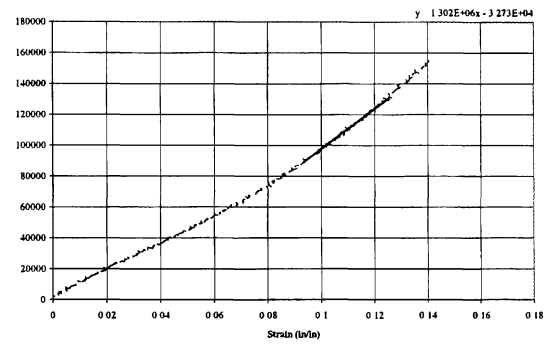
Specimen 2



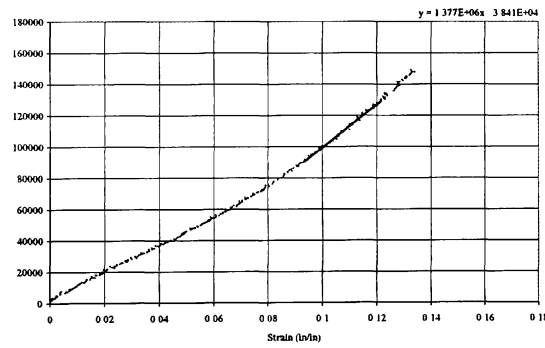
Specimen 3



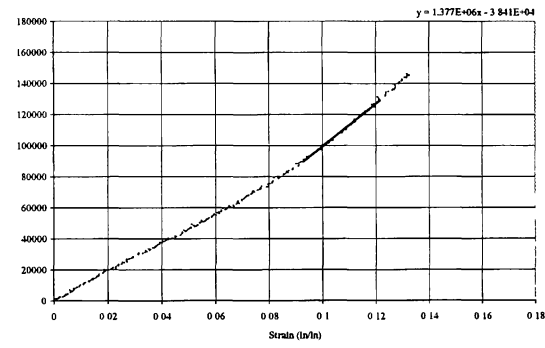
Specimen 4



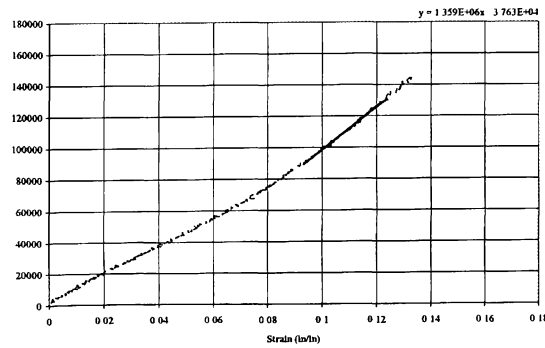
Specimen 5



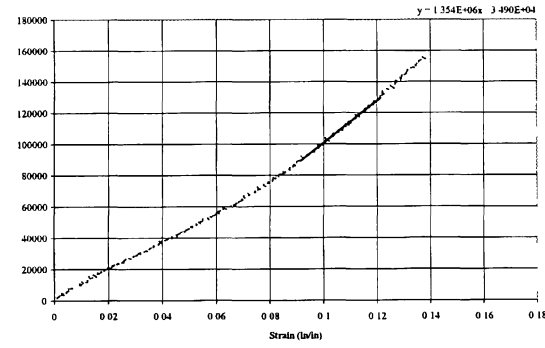
Specimen 6



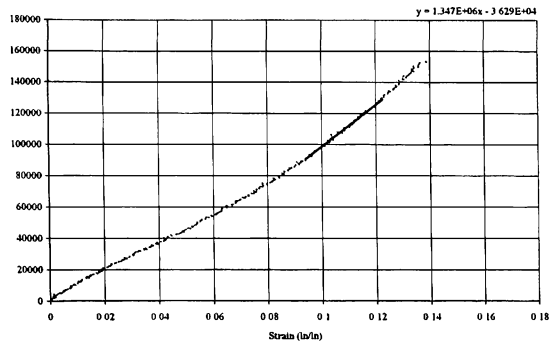
Specimen 7



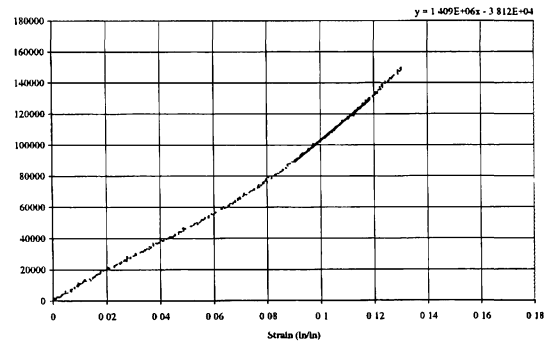
Specimen 8



Specimen 9



Specimen 10

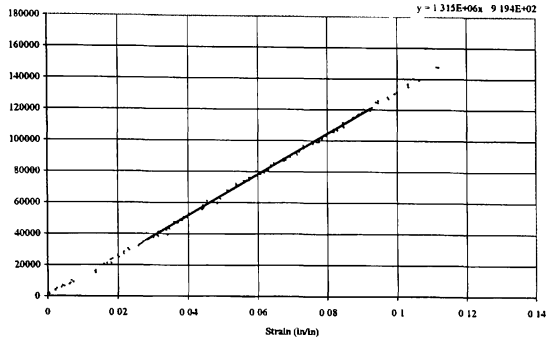


APPENDIX D

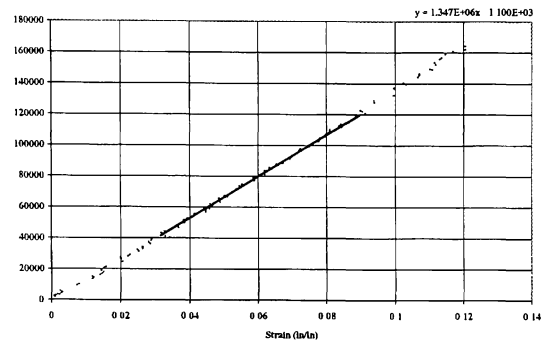
AS4 / 8552 8H FABRIC TTTC STRESS-STRAIN DATA PLOTS

9 Layers

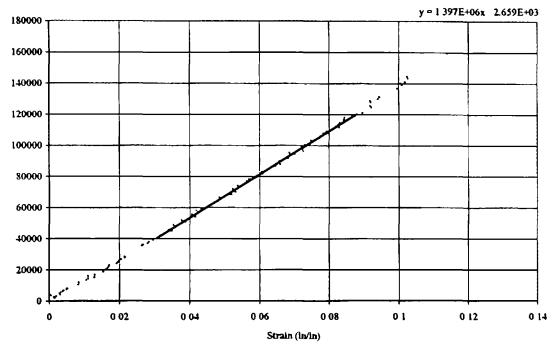
Specimen 1



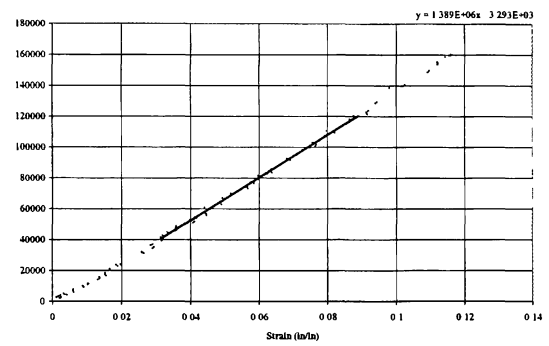
Specimen 2



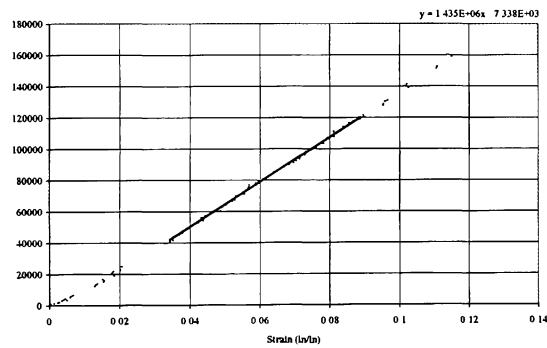
Specimen 3



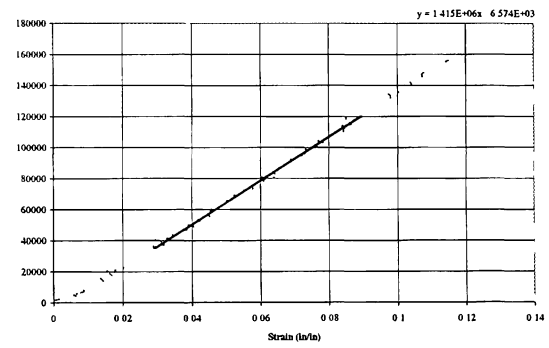
Specimen 4



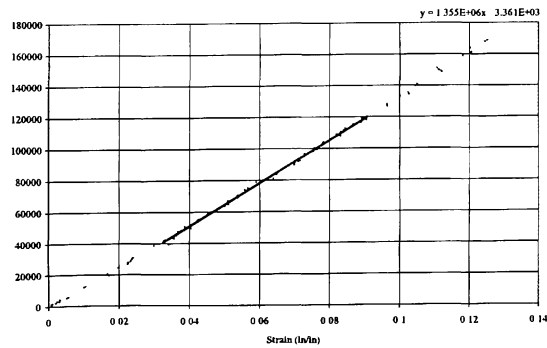
Specimen 5



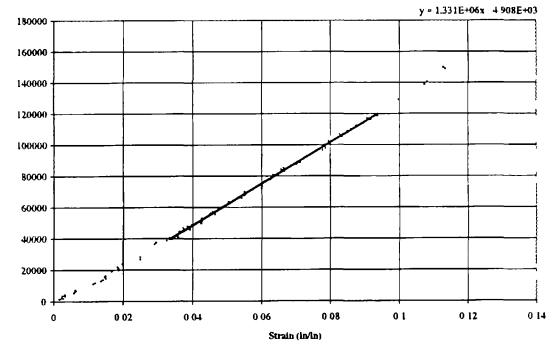
Specimen 6

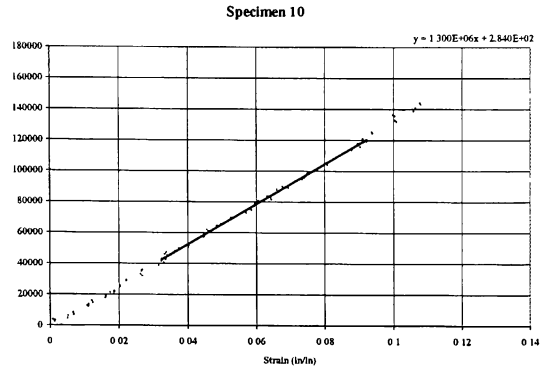
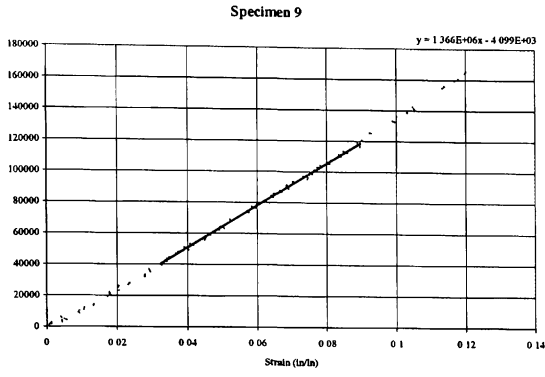


Specimen 7

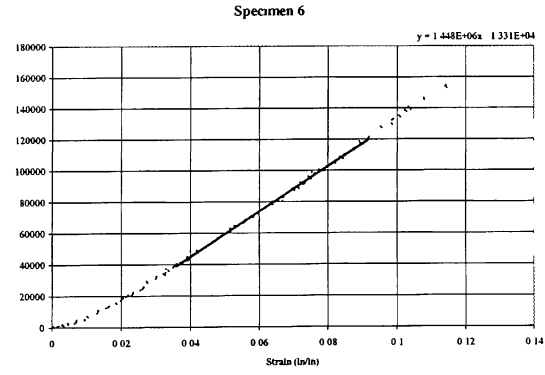
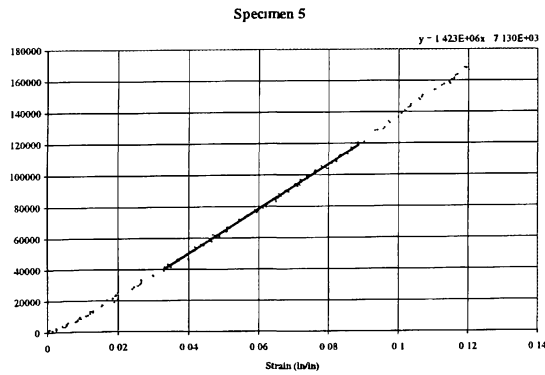
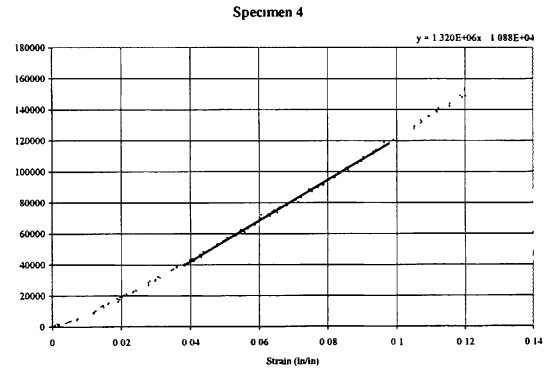
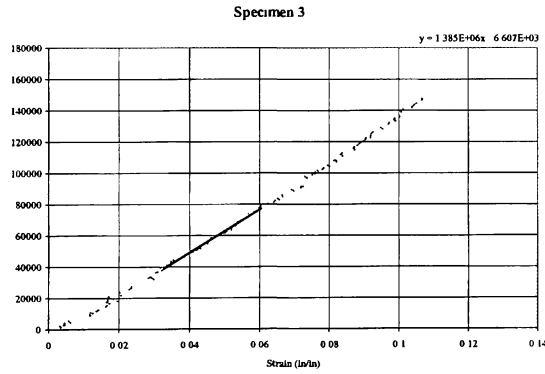
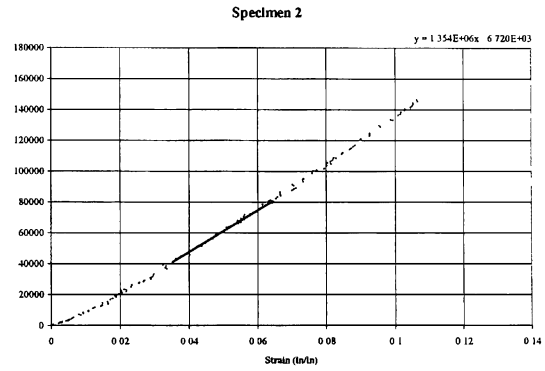
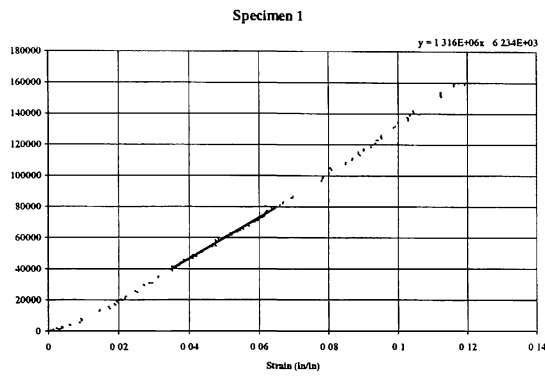


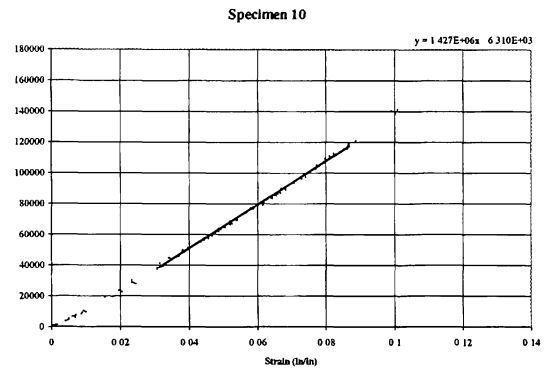
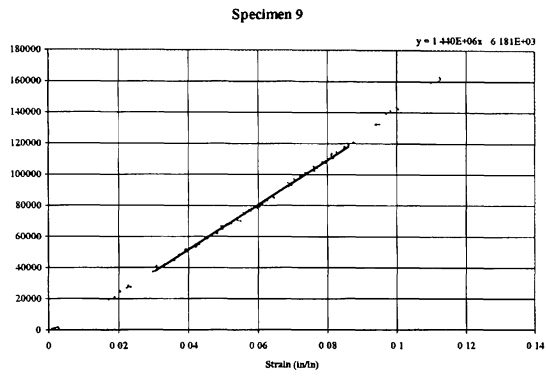
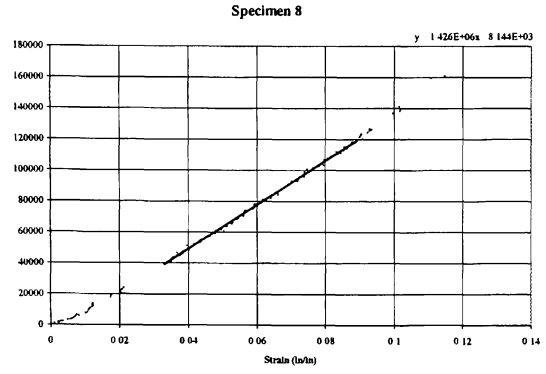
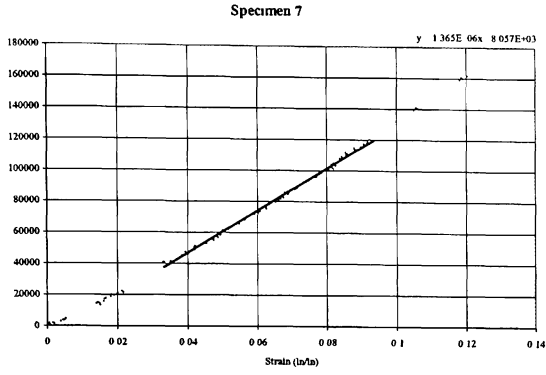
Specimen 8



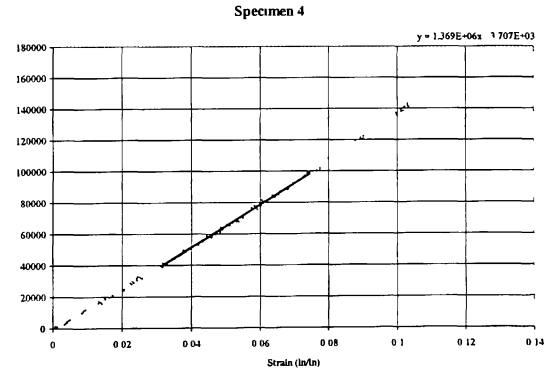
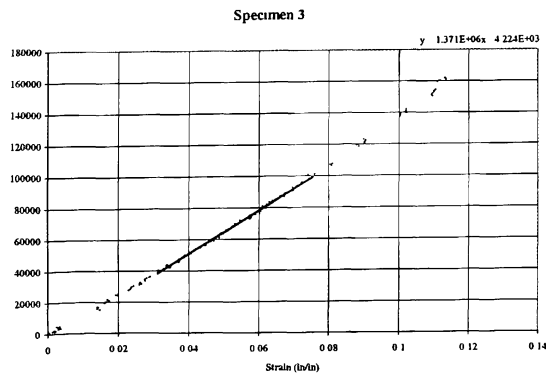
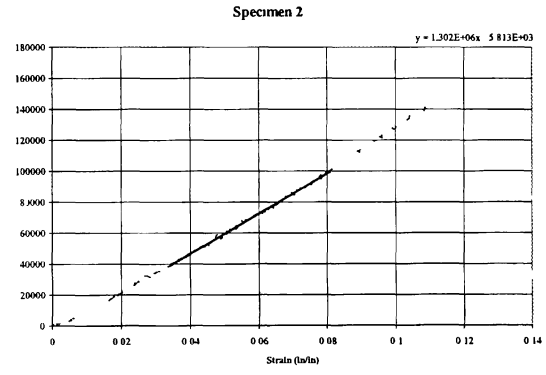
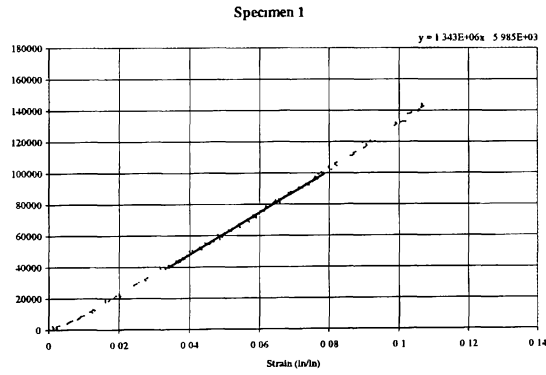


12 Layers

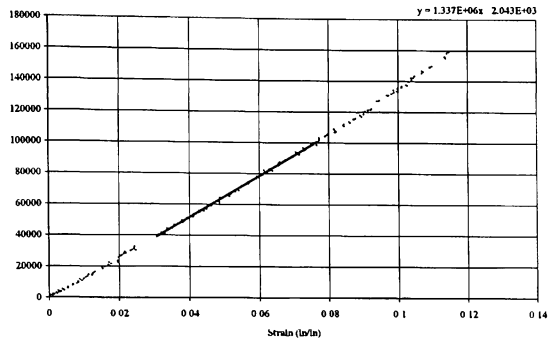




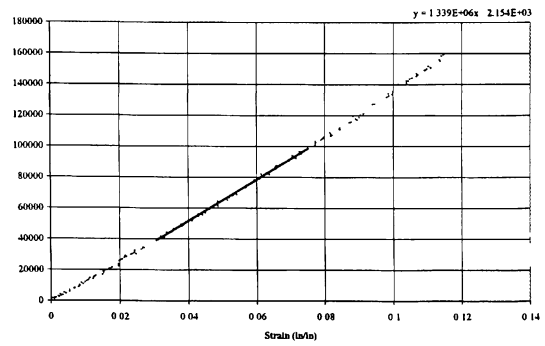
15 Layers



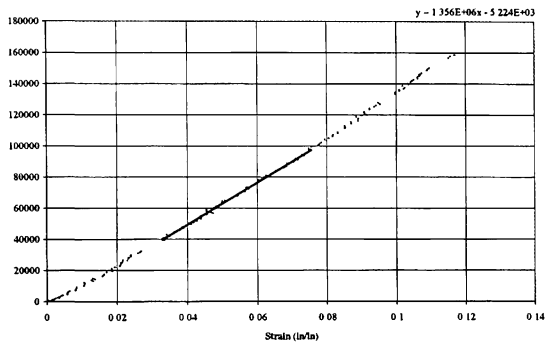
Specimen 5



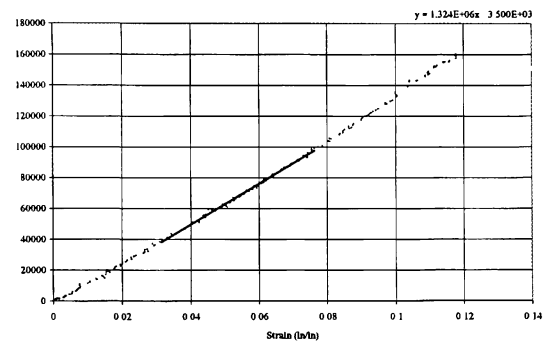
Specimen 6



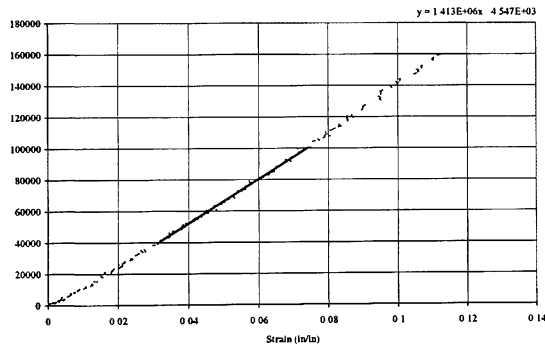
Specimen 7



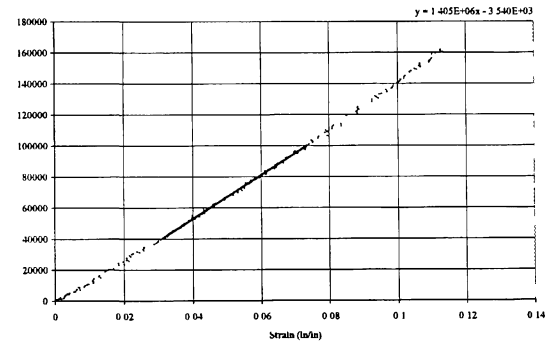
Specimen 8



Specimen 9



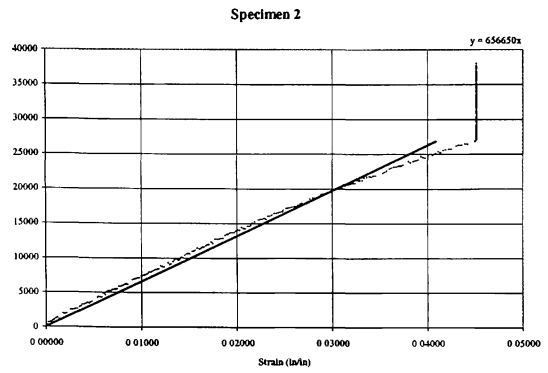
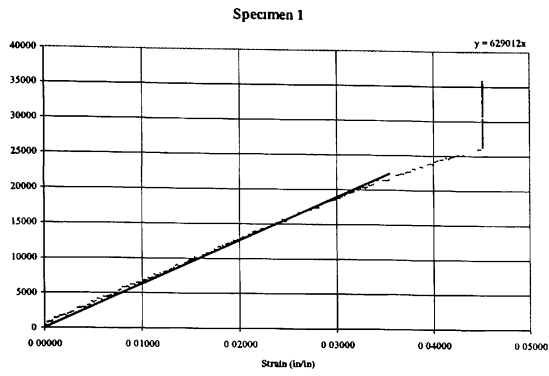
Specimen 10



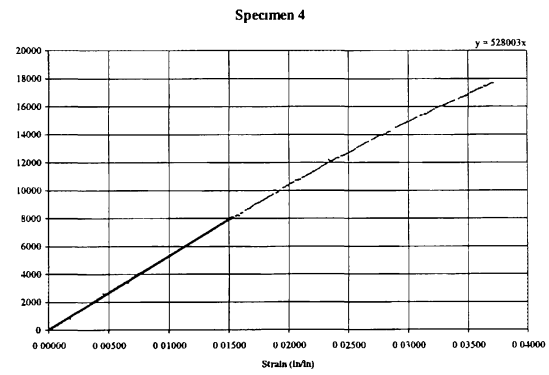
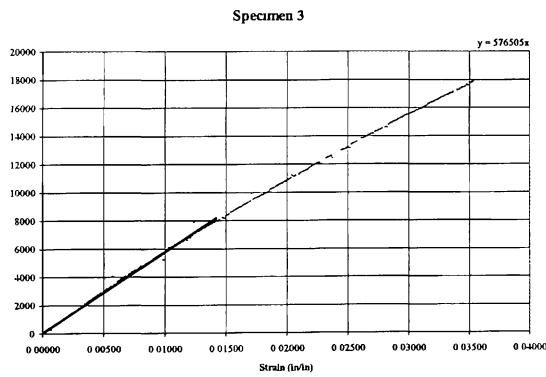
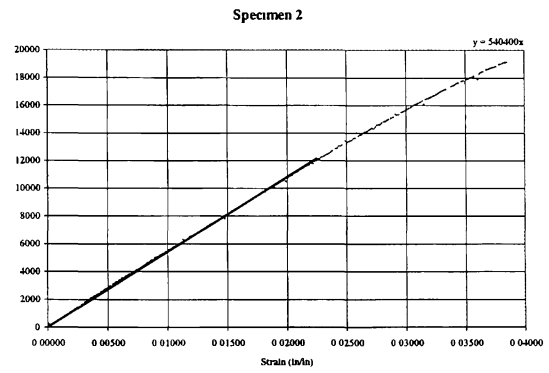
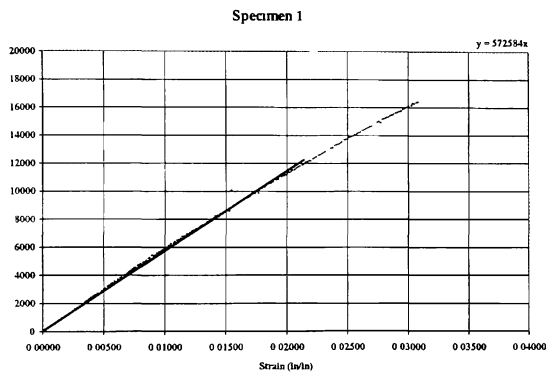
APPENDIX E

D3410-00 (90°) STRESS-STRAIN DATA PLOTS

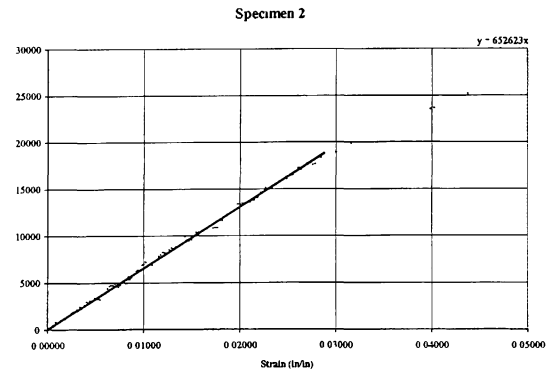
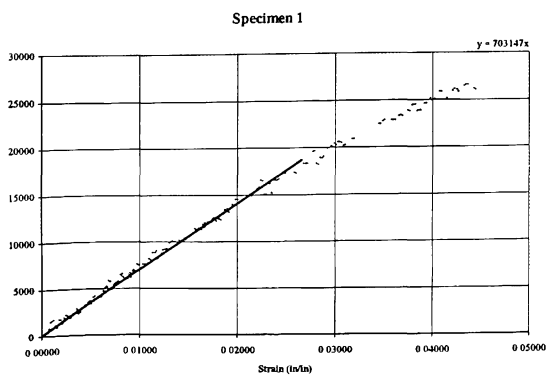
IM7 / 8552



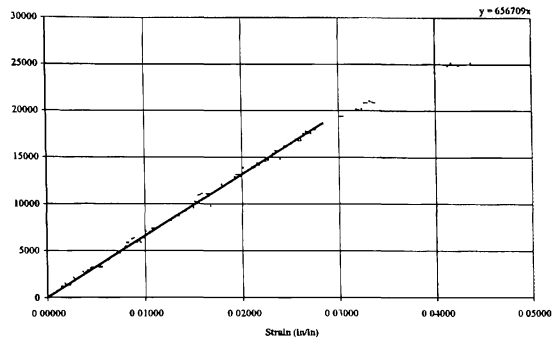
AS4 / 3501-5a



AS4 / 3501-6



Specimen 3



Specimen 4

